Open Research Online

The Open University's repository of research publications
and other research outputs

Morphological Correlates Of Synaptic Plasticity After Long Term Potentiation In The Rat Hippocampus

Thesis

How to cite:

Harrison, Elaine (2001). Morphological Correlates Of Synaptic Plasticity After Long Term Potentiation In The Rat Hippocampus. PhD thesis The Open University.

For guidance on citations see FAQs.

© 2001 The Author

Version: Version of Record

Link(s) to article on publisher's website:
http://dx.doi.org/doi:10.21954/ou.ro.00004be4

Copyright and Moral Rights for the articles on this site are retained by the individual authors and/or other copyright owners. For more information on Open Research Online's data policy on reuse of materials please consult the policies page.

oro.open.ac.uk

UNRESTRICTED

Morphological correlates of synaptic plasticity after Long Term Potentiation in the rat hippocampus.

By Elaine Harrison

A thesis submitted in partial satisfaction for the degree of Doctor of Philosophy

Submitted December 2000

Supervised by
Professor M.G. Stewart,
Department of Biological Sciences,
The Open University,
Walton Hall,
Milton Keynes.
MK7 6AA.

DATE OF AWARD 13 NOV 2001

Acknowledgements

I would like to thank Mike Stewart for his friendship and encouragement over many years and his guidance concerning the presentation of this thesis. This project would have been impossible without the expertise of Dr. Gal Richter-Levin and Mauna Maroun and the assistance of the staff in the University of Haifa, Israel. I am indebted to Heather Davies and Dawn Partner for their invaluable advice and I would like to acknowledge the generosity of the Open University and the Staff Fee Waiver Scheme for assistance during my registration period.

Many colleagues have also encouraged and supported me and I would like to extend an enormous thank-you to Rachel Bourne, Jacki Brown, Heather Holden, Amy Johnston, Chris Lancashire, Verina Waights and Tina Wardhaugh. Thanks too, to the community of postgraduate students in the Department of Biological Sciences, past and present, for their good company at various conferences around the world and all their sympathy while writing up! Special thanks to Claire Kendal, Karine Cambon, Mark Eyre and Mark Bresler.

Finally, I must acknowledge my family, Drew, Jenny and Nicola (who have been subjected to my ill temper for the last few months), and everyone in Northern Ireland, for their love and support.

Contents

List of Figures

List of Tables

Abbreviations

Anatomical

CA1	cornu Ammonis 1
CA3	cornu Ammonis 3
DG	dentate gyrus
EC	entorhinal cortex
GCL	granule cell layer
LEA	lateral entorhinal area
LPP	lateral perforant path
MML	middle molecular layer
MPP	medial perforant path

General

AA	arachidonic acid
ACPD	1-aminocyclopentane-1, 3-dicarboxylic acid
AMPA	α-Amino-3-hydroxy-5-methyl-4-isoxazolepropionate
AP5	2-amino-5-phosphonopentanoate
CaMKII	Ca^{2+}/calmodulin-dependent protein kinase II
CAMP	cyclic AMP
CREB	cAMP response-element-binding protein
E-LTP	early LTP
ERK	extra-cellular signal related-protein kinase
GABA	gamma aminobutyric acid
GluR	ionotropic glutamate receptor
HFS	high frequency stimulation
IML	inner molecular layer
IP3	inositol 1.4.5-triphosphate
L-LTP	late LTP
LTP	long term potentiation
MAPK	mitogen-activated protein kinase
MCPG	S-α-methyl-4-carboxyphenylglycine
MEA	medial entorhinal area

mGluR	metabotropic glutamate receptor
mRNA	messenger RNA
NCAM	neural cell adhesion molecule
NDGA	Nordihydroguaiaretic acid
NMDA	N-methyl-D-aspartate
PKA	protein kinase A
PKC	protein kinase
PLA_2	phospholipase A_2
PP	perforant pathway
PP1	protein phosphatase 1
PSD	postsynaptic density
SNAP	soluble NSF-attachment protein
TBS	theta–burst stimulation

Publications

Abstracts

Harrison, E., G. RichterLevin, G., Stewart, M. G. and Bliss, T. V. P. (1998). Synaptic density is unchanged in the dentate gyrus of the rat 45 min after long-term potentiation of the perforant path. European Journal of Neuroscience 10 (S10): 1404.

Harrison, E., Stewart, M.G., Richter-Levin, G. and Bliss, T.V.P. (1999). Increase in synaptic density in rat dentate gyrus, 24h after induction of long term potentiation. Soc. Neurosci. Abstr., Vol.25 (1):p. 183.2

Full papers

Stewart, M. G., Harrison E., Rusakov, D. A., Richter-Levin, G. and Maroun, M. (2000). Re-structuring of synapses 24 hours after induction of long- term potentiation in the dentate gyrus of the rat hippocampus *in vivo*. Neuroscience 100 (2): 221-227.

Abstract

Changes in synapse and neuronal morphology have been reported in the rat hippocampal formation after the induction of long-term potentiation (LTP) of the perforant path, although few studies have investigated such parameters in the maintenance phase of L-LTP. Moreover, the results of investigations of synaptic and neuronal morphometry changes after LTP have varied and this could be due to the methods of analysis employed, the choice of stimulation protocol and/ or whether an *in vitro* or *in vivo* study.

This *in vivo* investigation applied unbiased stereological methods to examine the morphology and morphometry of perforant path-granule cell synapses, in the dentate gyrus, after the induction of LTP. Two controls were employed, the contralateral hemisphere of each animal and the inner molecular layer, where the medial perforant path has little synaptic input. Many previous studies of the first 60min post tetanisation have used high frequency stimulation (HFS) to induce LTP however, in this study - to determine whether changes in morphology were due to LTP per se - potentiation was induced by theta burst stimulation (TBS).

45min after the induction of LTP there were no significant differences, between hemispheres, in the mean numerical density (*Nv*) of axodendritic or axospinous asymmetric synapses, or the mean number of synapses per neuron in the middle molecular layer (MML) of the dentate gyrus. There were no significant differences, between potentiated and non-potentiated tissue, in the *Nvs* of those asymmetric synapses with perforated or concave profiles. Neither were significant differences following LTP demonstrated in the size of the postsynaptic densities of these synaptic subtypes or the volume density of apposition zone (AZ) area (*Sv*) of individual, or all, asymmetric axospinous synapses. However, there was a trend towards larger perforated synapses in the potentiated hemisphere and, in both hemispheres, concave and perforated synapses were larger than average. In the inner molecular layer (IML), there were no differences except for a significant decrease in the total AZ volume density in the potentiated hemisphere. This would suggest that any morphological modifications taking place in the induction phase of L-LTP may be restricted to a fraction of synapses in the MML, although perforated synapses appear to be involved.

The second part of this study examined morphological correlates 24h after the induction of LTP with TBS and HFS. In the MML after induction of LTP with TBS there were significant increases in the *Nv* of asymmetric axodendritic synapses and the mean number of axodendritic synapses per neuron. There was an increase in the *Nv* of axospinous synapses and in the mean number of axospinous synapses per neuron that was not significant. This was reflected in significant increases in the total AZ *Sv* and in the frequency of macular synapses in the potentiated hemisphere. 24h post tetanisation with HFS, there was a significant difference in the *Nv* of axospinous synapses in the MML of the potentiated compared to the contralateral hemisphere. There were also significant differences in the frequency of synapses with perforated and concave profiles. There were no significant differences in synaptic morphometric parameters, between hemispheres, in the IML after either of the stimulating regimes.

Results from the three animals in each group showing the greatest degree of potentiation, were pooled and demonstrated significant differences in the *Nv* and mean number of axospinous synapses per neuron. There was also a significant difference in the number of synapses with concave profiles but this was replicated in the IML.

The effects of these morphological changes, after LTP induction, on the cellular mechanisms involved and on synaptic efficacy are discussed, and possible reasons for the variable pattern of morphology after different stimulating protocols is considered.

Chapter One Introduction

The account of the long-term potentiation (LTP) of synaptic efficacy reported by Bliss and Lømo in 1973 captured the imagination of neuroscientists and initiated an ever increasing number of investigations to determine whether this was indeed the mechanism underlying learning and the storage of memory. Considerable progress has been made in clarifying the mechanisms underlying LTP induction and expression and LTP in the hippocampus has become the foremost model of activity-dependent synaptic plasticity in the mammalian brain (Bliss and Collingridge, 1993). LTP was seen as an excellent candidate for a memory storage process as it develops quickly, and lasts for a long period, as demonstrated in the hippocampus where LTP lasting for several weeks has been described (Barnes, 1985).

The description of LTP in the hippocampus was fortunate, for had LTP first been identified in a brain region with less of a historical link to memory formation, it might not have received such focused attention. Clinical studies in the late 1950's (Scoville and Milner, 1957), where bilateral surgical resections of the brain induced long-lasting retrograde amnesia, demonstrated that normal memory function depended on the integrity of the medial temporal lobes. It was suspected that the removal of the hippocampal formation was responsible and subsequent animal research has been dedicated to understanding how the hippocampal formation may promote the formation of new memories.

The hippocampus is believed to play a critical role in explicit rather than implicit memory (Cohen *et al*, 1999). However, while LTP has features that

makes it attractive as a memory system it is not clear if this is the mechanism that the hippocampus uses to store declarative memories such as spatial memory (Barnes 1995). LTP is not unique to the hippocampus or to declarative forms of memory and it is more plausible that LTP represents a class of mechanism for changing synaptic strength that might be used for memory storage.

However, the medial temporal lobe is a large region. The dentate gyrus, CA (cornu Ammonis) fields and subicular complex lie in the caudal region but its rostral portion is occupied by the amygdala and both structures are bordered by the entorhinal and perirhinal cortical areas. Therefore, the contribution of the hippocampal and non-hippocampal components of the medial temporal lobe to memory processes is difficult to determine.

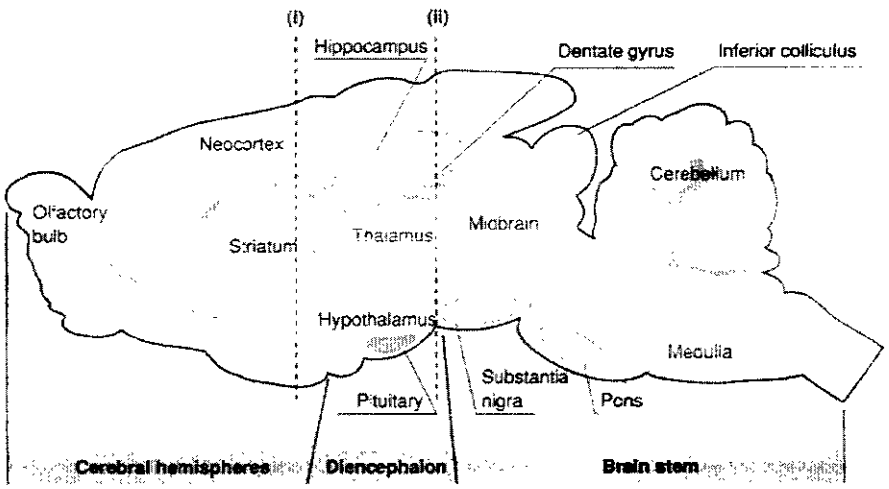

Figure 1.1 The basic neuroanatomy of a rat brain.

The three major divisions of the rat brain are shown in saggital section. The brain stem includes the medulla, midbrain and cerebellum; the diencephalon comprises the thalamus, hypothalamus and pituitary, while the cerebral hemispheres include the striatum, olfactory bulb, neocortex, hippocampus and dentate gyrus. After Nicholls, 1994.

The hypothesis that LTP might serve as a memory storage device or engram is supported by the properties of cooperativity, associatively and input-specificity that characterise LTP. These properties might be expected in a network of neurons designed to associate two distinct pieces of information, and the ability to enhance

one set of inputs is presumably also required for learning and memory (Lynch and Granger, 1992; Gluck and Granger, 1993). LTP also demonstrates the requirement for coincident activation of presynaptic and postsynaptic elements that is the hallmark of the Hebbian postulate (Hebb, 1949). Hebb's postulate, originally formulated to explain the cellular basis of learning and memory, suggested that co-ordinated activity of a presynaptic terminal and a postsynaptic neuron would strengthen the synaptic connection between them. Synaptic terminals strengthened by correlated activity would be retained, or sprout new branches, whereas those that are persistently weakened by uncorrelated activity would eventually forfeit their adherence to the postsynaptic cell.

Although LTP was first observed in the intact experimental animal, progress in understanding its cellular basis has relied on *in vitro* brain slice preparations (Bliss and Collingridge, 1993). The best-characterised form of LTP occurs in the CA1 region of the hippocampus, in which LTP is induced by transient activation of N-methyl-D-aspartate (NMDA) receptors and is expressed as a persistent increase in synaptic transmission through α-Amino-3-hydroxy-5-methyl-4-isoxazolepropionate (AMPA) receptors (Bliss and Collingridge, 1993; Muller *et al.*, 1992). Where, induction of LTP refers to the initial sequence of events that triggers the process of synaptic modification and expression refers to those neurophysiological and biophysical changes that represent the consequence of this modification process. However, *in vivo* quantitative, ultrastructural studies are best facilitated in the hippocampal dentate fascia - where the main afferent path, the perforant path, terminates solely on dendritic spines in restricted zones of the molecular layer (Fifkova, 1975).

The introduction to this thesis will attempt to describe the processes involved in the induction, expression and maintenance of LTP, and review reported morphological changes, after potentiation of the afferents to the hippocampus. Where relevant there will be a brief comment on similarities in morphology between LTP and learning and memory formation. However, it

would be difficult to undertake this exercise without an account of the anatomy of the hippocampus, particularly the dentate gyrus, and its role in memory formation, and some explanation of the morphology of dendritic spines and synapses.

1.1 The Hippocampal Formation

1.1.1 The Hippocampus

In the rat, the hippocampus extends from almost the septum dorsally, to the caudal part of the amygdala ventrally. It consists of Ammon's Horn, the dentate gyrus and the subiculum, and two interlocking cell layers - the granule cell layer of the dentate gyrus (DG) and the pyramidal cell layer of Ammon's Horn. Ammon's Horn is divided into four subfields CA (cornu Ammonis) 1 to CA4, although CA4 generally refers to the polymorphic zone of the dentate gyrus, based on the Golgi preparations of Cajal. (Figure 1.2) From the dentate gyrus to the subiculum, the pyramidal layer of Ammon's Horn contains the CA3 field merging distally with the CA2 field, the proximal part of CA1 joins CA2 and the distal part of CA1 borders the subiculum. The basic architecture of the hippocampal subfields is very similar. They all consist of one single layer, or lamina, of neurons, where the apical dendrites extend into a cell -poor zone - the stratum moleculare in the dentate gyrus and the subiculum, the stratum lacunosum-moleculare and stratum radiatum in Ammon's Horn.

1.1.1.1 Intrinsic circuitry

Anatomical (Blackstad *et al.*, 1970; Hjorth-Simonsen and Jeune, 1972) and electrophysiological (Andersen *et al.*, 1971) data led Andersen to suggest that the hippocampus is organised in a wholly laminar fashion and that each lamella contains a sequence of almost completely unidirectional connections from the dentate gyrus to the subiculum via CA3 and CA1. The mossy fibre axons of the granule cells project to the entire transverse extent of CA3, but fibres that originate in the infrapyramidal and suprapyramidal blades of the DG terminate in

different regions of this field (Claiborne *et al.*, 1986). The pyramidal cells in CA3 give rise to the Schaffer collaterals that synapse in the stratum radiatum and stratum oriens with the dendrites of CA1 pyramidal cells and these cells project to the subiculum.

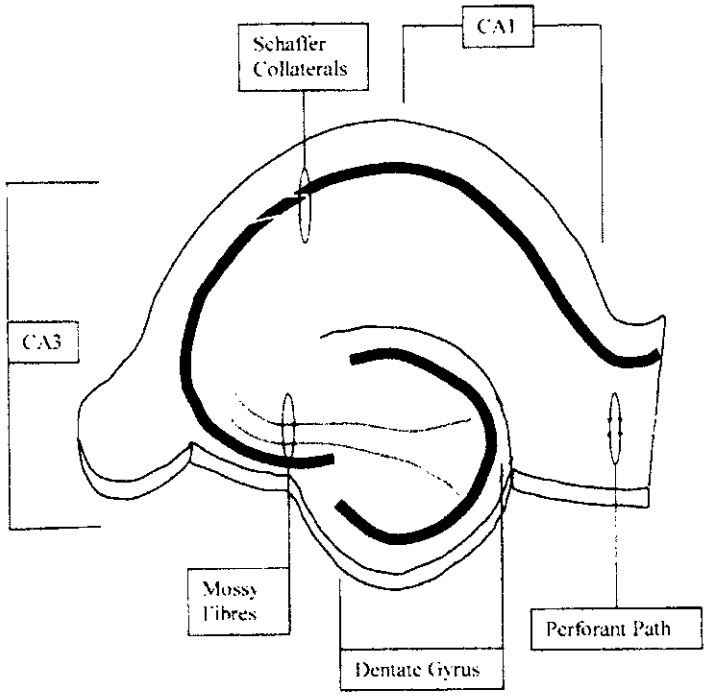

Figure 1.2 Schematic diagram of a section through the rat hippocampus, showing the major excitatory pathways and their synaptic connections.

LTP has been observed in response to stimulation of each of the three pathways shown (the perforant path; the mossy fibre pathway; and the Schaffer collateral pathway). After Purves *et al.*, 1997

However, Amaral and Witter (1989) refuted the idea of non-interaction between these lamella after further neuroanatomical investigations of hippocampal connectivity. They proposed a three-dimensional organisation of hippocampal circuitry where, for example, cells in the entorhinal cortex give rise to axonal projections that distribute for some distance in a transverse direction in the molecular layer of the dentate gyrus. This has implications for the interpretation of research using, *in vitro* slice preparations from the hippocampus,

as slices do not allow for the evaluation of information flow along the transverse and septotemporal axes of the hippocampal system.

1.1.1.2 The Dentate Gyrus

The dentate gyrus (DG) contains three concentric layers. The outermost, the molecular layer (ML), consists primarily of afferent fibres and dendrites and the second, the granule layer (GL), contains the densely packed somata of the granule cells. These two layers are referred to collectively as the fascia dentata (Blackstad, 1958). The third, polymorphic (or infragranular) layer is enclosed within the strong curvature of the granule cell layer in a region known as the hilus. The granule cell layer can be subdivided, in relation to its location to these pyramidal cells, into suprapyramidal and infrapyramidal blades, which merge at the crest of the dentate gyrus.

A number of neuronal forms make up the rodent dentate gyrus but, when classified into groups of similar cells, two types are generally referred to; i.e. projection neurons and local interneurons, although some of these interneurons may possess long range projections (Amaral, 1978). The principal cells of the dentate gyrus are the granule cells. These excitatory neurons have dendrites that extend through the ML and are covered in spines (Scharfman *et al.*, 1990). The synapses their axons make are asymmetric (Claiborne *et al.*, 1990) and have been shown to contain the excitatory, neurotransmitter glutamate (Storm-Matheson *et al.*, 1983). (See Section 1.2.1 Synapses)

Estimates of granule cell number in the rat dentate gyrus vary widely, depending on age and strain as, unlike most neurons, granule cells in the rat may continue to be produced by mitosis well into adulthood. Hippocampal neurogenesis is dependent on proliferation, survival and differentiation and strain differences in granule cell neurogenesis have been identified in mouse (Kempermann *et al*, 1997) and rat (Boss *et al.*, 1985). However, no increase in granule cell number with age has been reported for Sprague-Dawley rats during

the first year of life (approximately $1x10^6$ granule cells per hemisphere at one year old)

The dentate gyrus represents the major input structure of the hippocampus with major afferents emanating from the entorhinal cortex while the subiculum gives rise to most of the hippocampal efferents to subcortical and cortical areas with a contribution from CA1 (Witter *et al.*, 1989; Swanson *et al.*, 1987).

1.1.2 The Entorhinal Cortex and the Perforant Pathway.

The entorhinal cortex (EC), incorporating six cortical layers, is the origin of a massive projection to the hippocampus, the perforant pathway (PP), which has been reported to terminate predominately in the dentate gyrus (Steward, 1976; Wyss, 1981). The dentate gyrus component of the perforant pathway arises primarily from the cells of EC layer II (Ruth *et al.*, 1982; Steward, 1976). Some fibres of the PP cross the molecular layers of the subiculum and CA1 and subsequently traverse the hippocampal fissure, to reach the molecular layer of the dentate gyrus, where they terminate. However, many fibres travel in the molecular layer of Ammon's Horn along its transverse extent and firstly interact with cells in CA3 before reaching the dentate gyrus cells. The EC projects not only to the dentate gyrus and CA3 but also densely to CA1 and the subiculum.

The perforant pathway shows a topological organisation that is related to the organisation of the entorhinal cortex. The lateral entorhinal area (LEA) projection is known as the lateral perforant path (LPP) and that of the medial entorhinal area (MEA) as the medial perforant path (MPP). Anterograde studies (Hjorth-Simonsen, 1972; Hjorth-Simonsen and Jeune, 1972; Steward, 1976; Wyss, 1981) show that MPP fibres distribute preferentially to the middle one third of the molecular layer of the dentate gyrus and CA3 and to the proximal part of CA1 - close to the CA1-CA3 border. The fibres from the LPP project to the outer third of the dentate gyrus and CA3 and distal portions of CA1. The organisation of the LPP is such that a small part of the LEA can interact, not only with a relatively

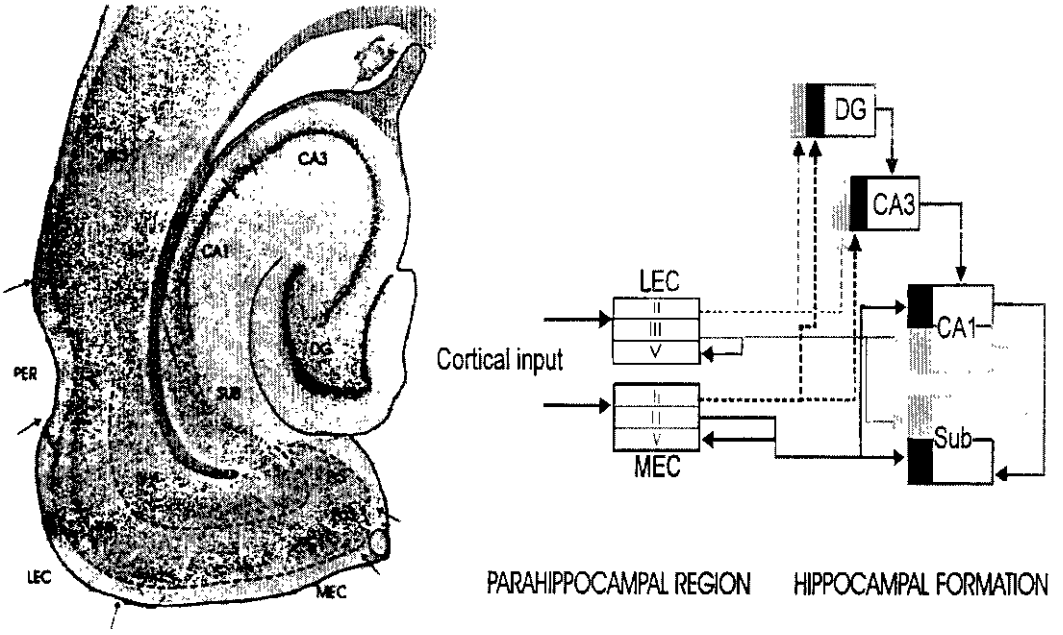

A B

Figure 1.3 The hippocampal formation and parahippocampal region of the rat brain.

(A) Horizontal section through the hippocampal formation and the parahippocampal region, illustrating the various components of the hippocampal formation and parahippocampal region and their laminar organisation. The fields that make up the hippocampal formation i.e. the dentate gyrus, CA fields and the subiculum, are characterised by an overall three-layered appearance. In contrast, at the border between the hippocampal formation and the parahippocampal region, the number of layers abruptly increases. A second, more gradual change in laminar composition takes place at the level of the perirhinal cortex, being replaced by the temporal neocortex with a well-developed inner granular layer IV. (B) Scheme of the connectivity of the hippocampal formation and parahippocampal region. Cells in layer II of the LEC project to the outer one third of the molecular layer of the DG; cells in layer II of the MEC project to the middle one third of the molecular layer of the DG. CA1-3, fields of Ammon's horn; DG, dentate gyrus; SUB, subiculum; LEC, lateral entorhinal cortex; MEC, medial entorhinal cortex; PaS, parasubiculum; PER, perirhinal cortex; PrS, presubiculum. After Witter *et al.*, 2000.

large part of the hippocampus along its longitudinal extent, but also with a large segment of the apical dendrites of the cells of the dentate gyrus and CA3. The MPP exhibits a more restricted distribution, but is responsible for most of the synaptic input onto dendrites in the outer two thirds of the molecular layer of the dentate gyrus (Blackstad, 1958; Matthews *et al.*, 1987). The dentate gyrus also receives sparse input from the contralateral EC and, as with the ipsilateral projection, MPP and LPP terminals are segregated in the ML, with LPP terminals in the outer third and MPP terminals in the middle third (Steward, 1976; Wyss, 1981).

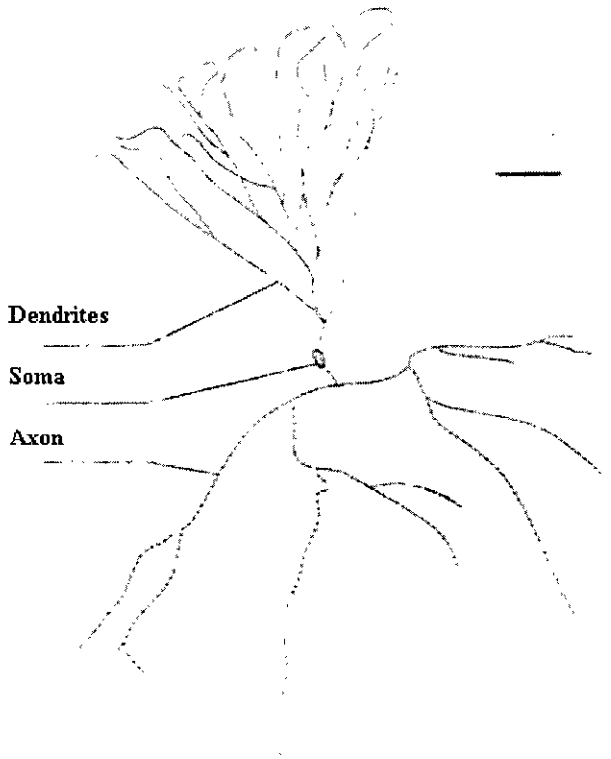

Figure 1.4 Camera lucida drawing of a dentate granule cell in the rat hippocampus.

Camera lucida drawing of a dentate granule cell in the rat hippocampus showing the actual dimensions of the soma, dendritic tree, and axonal arbour of a typical neurone. After Isokawa *et al.*, 1993. Bar 1μm

Dentate gyrus granule cells possess roughly conical dendritic arbours (Figure 1.4) extending into the outer two-thirds of the rat DG molecular layer and are the major recipients of input (Claiborne *et al.*, 1990; Desmond and Levy, 1982). Electrical stimulation of the PP results in direct excitation of granule cells (Lambert, 1990; McNaughton, 1978) and following EC lesions degenerating terminals are seen on the dendritic spines of granule cells (Fifkova, 1975; Matthews *et al.*, 1976); Nafstad, 1967). Each spine generally receives one asymmetric synapse (Patton and McNaughton, 1995) and asymmetric synapses make up 86 ± 2% of all synapses in the outer third of the rat ML and 89± 2% of those in the middle third (Crain *et al.*, 1973). Unilateral removal of rat EC results in the loss of about 86% of all synapses in the outer ¾ of the ML (Matthews *et al.*, 1976).

1.1.2.1 EC connectivity

The EC plays a central role in the communication between the hippocampal formation and the neocortex. Much of the cortical sensory information that enters the hippocampus does so through the entorhinal cortex e.g. there is substantial input from olfactory structures including olfactory bulb, anterior olfactory nucleus and piriform cortex. This is spread over much of the surface of the entorhinal cortex (Amaral, 1993) although some olfactory terminals also occur in layers II and III. A second major input is from the perirhinal cortex that receives information from auditory, visual, polysensory, autonomic and limbic association cortices (Witter *et al.*, 1989) and terminates preferentially in layers I-III. The communication is reciprocal as projections to the neocortex originate in the EC, particularly those that go by way of the subiculum.

Therefore, inputs to certain mediolateral portions of the entorhinal cortex will be relayed almost exclusively to certain septotemporal portions of the dentate gyrus. (Dolorfo and Amaral, 1998). For example, projections conveying information from the neocortex terminate preferentially in the MEA (Insausti *et*

al., 1987) or the parts of the EC that send projections to the dentate gyrus. In contrast, subcortical structures such as the amygdala, which express information concerning the affective significance of stimuli, terminate primarily in the LEA (Krettek and Price, 1977) or the part of the EC that sends projections to the temporal levels of the dentate gyrus. If there is a topographic organisation to the inputs to the EC then this implies that septal and temporal hippocampus may receive different kinds of information through the perforant path inputs.

Rats with lesions restricted to the septal portions of the hippocampal formation exhibit longer escape latencies in the Morris water maze than rats with lesions restricted to temporal portions of the hippocampus (Moser *et al.*, 1993). Furthermore, electrophysiological studies have reported difficulties in recording place fields in neurons in the ventral hippocampus (Jung *et al.*, 1994). These studies would suggest that the septal portion of the hippocampus receives greater direct sensory information from the neocortex and is responsible for carrying out spatial information processing.

1.2 Morphology

1.2.1 Synapses

Chemical synapses in the nervous system can be described as asymmetric or symmetric, depending on the prominence of the cytoplasmic densities, on each side of the synaptic junction (Gray, 1959). Asymmetric synapses (Gray's type I synapses), with a prominent postsynaptic density (PSD), are usually excitatory and have clear, spherical synaptic vesicles that contain glutamate. Inhibitory synapses (Gray's type II synapses) tend to be symmetric and their smaller, oval synaptic vesicles contain gamma aminobutyric acid (GABA) or glycine. Axons may form synapses onto the dendritic shaft or onto small protrusions of the dendrite called spines and can therefore be further characterised according to their contact i.e. axospinous or axodendritic. (Figures 1.5 and 1.6)

The presynaptic element and the apposed postsynaptic element surround the synaptic cleft, which is an intercellular space between 20 and 30nm wide. The synaptic junction, which incorporates the plasma membranes of the pre- and postsynaptic elements, closely binds one neuron with another and cell adhesion molecules (CAMs) help to maintain the structural integrity of the synapse (Peters and Palay, 1996).

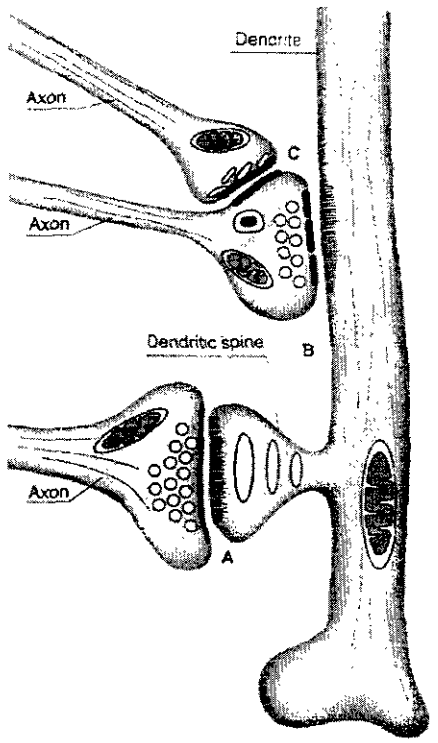

Figure 1.5. Schematic diagram of chemical synapses.

(A) An excitatory axospinous synapse between a terminal, containing clear, spherical synaptic vesicles, and a dendrite containing spine apparatus (Ca^{2+} -sequestering compartments). (B) An excitatory axodendritic synapse containing small synaptic vesicles synapsing directly onto a dendrite, and regulated by an inhibitory axo-axonal synapse (C) which contains oval synaptic vesicles. After Nicholls, 1994.

Of particular interest are neural cell adhesion molecules (NCAMs) - cell surface glycoproteins that belong to the immunoglobulin superfamily and have various closely related isoforms. There are three major isoforms with molecular weights of 120 (NCAM120), 140 (NCAM140) and 180 (NCAM 180) kDa that are

characterised by identical extracellular domains containing five immunoglobulin-like domains and two fibronectin type III homologous repeats. The NCAM 140 molecule has membrane spanning and cytoplasmic domains similar to the NCAM180 molecule although it has an additional intracellular domain. The prevalence of the isoforms differs during neural development and NCAM180 seems to be exclusively expressed on neurons (Kramer *et al.*, 1997) and has been shown to accumulate in the postsynaptic density (Persohn *et al.*, 1989). Cells expressing polysialylated forms of NCAM have a marked increased capacity for structural plasticity (Muller *et al.*, 1996) and sialic acid is strongly expressed during neural development. Sialic acid expression remains prominent in the hippocampus although generally down regulated in other brain regions in the adult rat (Seki and Arai, 1993).

Application of function blocking antibodies to NCAM have been found to inhibit LTP induction in hippocampal region CA1 (Luthi *et al.*, 1994). The induction of LTP can also be inhibited by the addition of peptides that block the function of cadherins (Tang *et al.*, 1998) and integrins (Xaio *et al.*, 1991). These CAMs appear to be required in the very early stage of LTP stabilisation, as delaying the application of peptide for 30min had no effect on established LTP.

The release of transmitter from a presynaptic terminal is regulated by the exocytic fusion of secretory vesicles with the plasma membrane and is strongly dependent on Ca^{2+} concentration. In the presynaptic terminal synapsin and actin filaments link vesicles together and regulate the numbers of synaptic vesicles available to release neurotransmitter into the synaptic cleft (Peters and Palay, 1996). When a terminal is depolarised and calcium enters, synapsin I becomes phosphorylated by Ca^{2+}/calmodulin-dependent protein kinase II (CaMKII) and phosphorylation frees the vesicles from cytoskeletal constraint allowing them to move into the active zone.

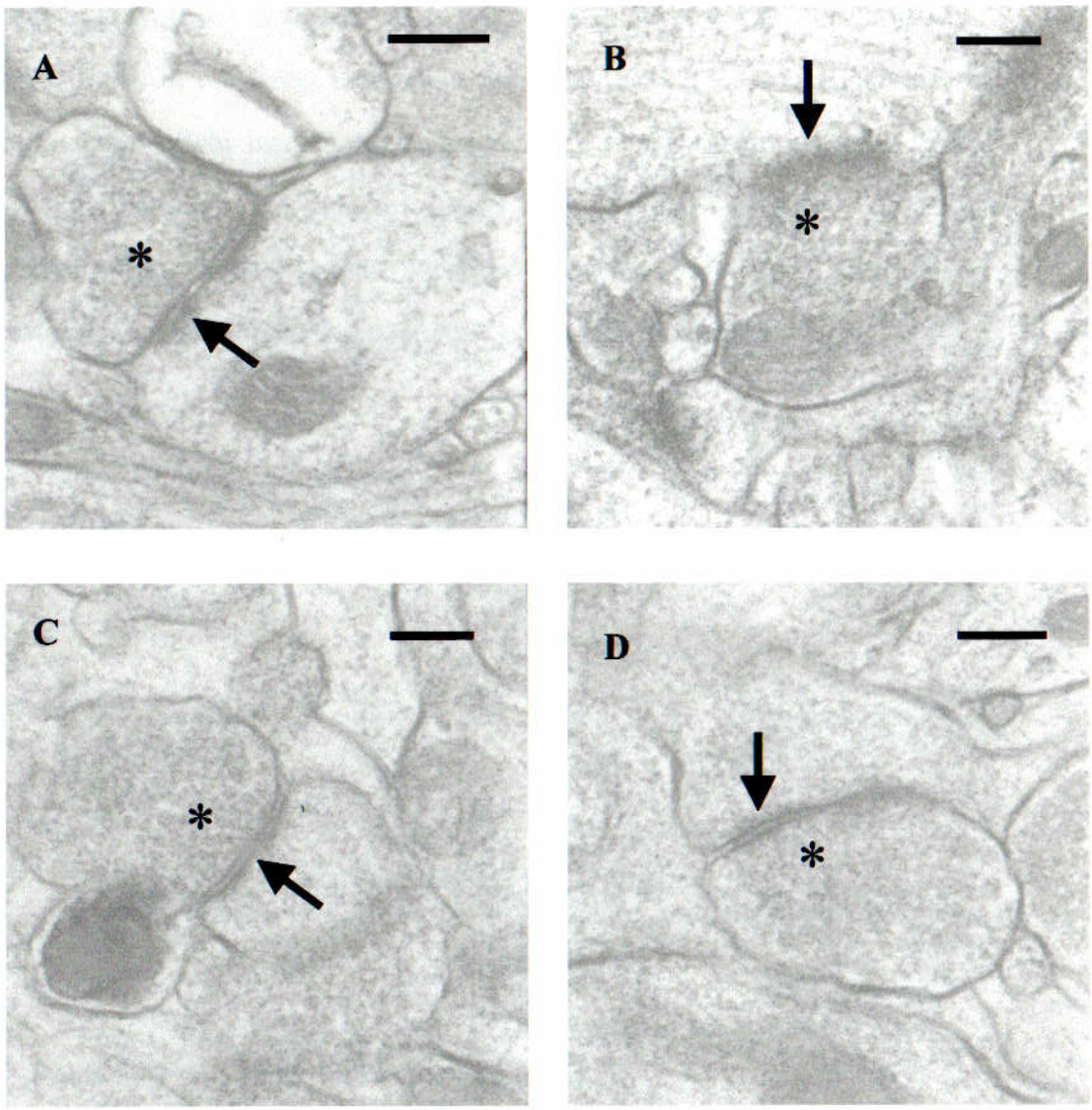

Figure 1.6 Electron micrographs of asymmetric synapses

(A, B) Axodendritic asymmetric synapses. (C,D) Axospinous asymmetric synapses. The postsynaptic densities are indicated by arrows and the presynaptic boutons, containing round vesicles, by *. Magnification x40k, bar =200nm

Specific integral proteins e.g. synaptobrevin and synaptotagmin (Gerst, 1999; Sugimori *et al.*, 1998) in the vesicle membrane bind to specific receptor proteins e.g. syntaxin (Bennett *et al.*, 1992) and soluble NSF-attachment protein – 25 (SNAP-25) in the target membrane (Lledo *et al.*, 1998). It is suggested that synaptotagmin might insert into the presynaptic membrane in response to Ca^{2+} influx thus serving as a calcium sensor for exocytosis (Sudhof, 1995). The neurotransmitter released at these localised sites, by exocytosis, rapidly reaches the postsynaptic membrane that contains the receptor molecules.

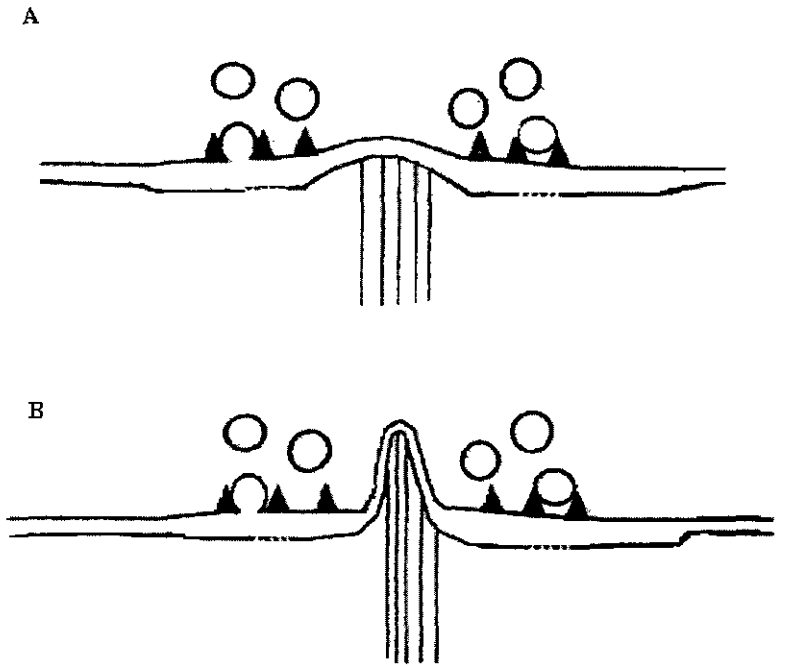

Figure 1.7 Schematic diagram of a perforated synapse.

(A) The presynaptic grid splits with some spillover of transmitter between them and, (B) a spinule may invaginate the presynaptic terminal and completely separate active zones are formed. After Edwards, 1995.

NMDA and AMPA receptors are localised in the postsynaptic membrane with its adjacent PSD. This is an electron-dense area formed by a planar array of spherical sub-units of 18nm in diameter (Kennedy, 1997) and contains many proteins, including CaMKII, and signalling molecules that modulate synaptic transmission (Kennedy, 1998). The PSD influences the shape of the terminal by controlling the size and orientation of filaments linking it to the surrounding

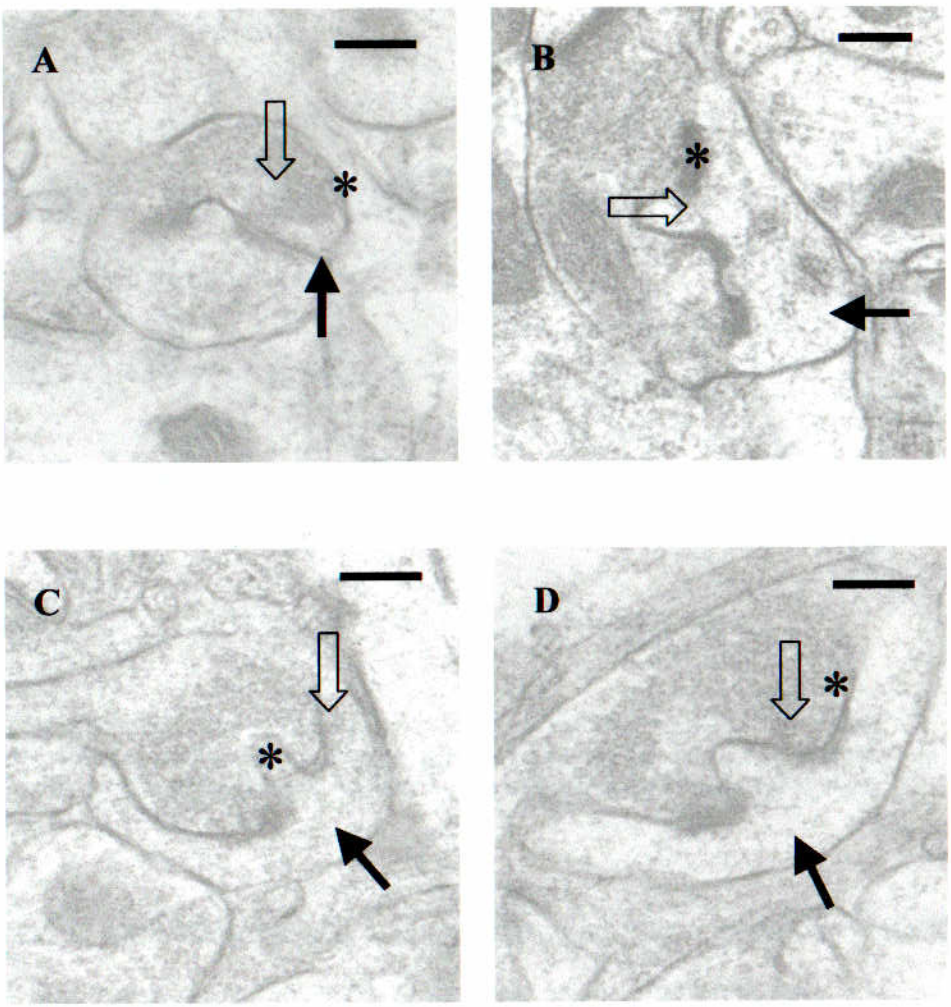

Figure 1.8 Electron micrographs of perforated, or segmented, synapses.

Synapses with perforated or segmented postsynaptic densities. The postsynaptic densities are indicated by black arrows and the presynaptic boutons by *. The open arrows indicate spinules from the postsynaptic membrane. Magnification x40k, bar = 200nm

cytoplasm (Siekevitz, 1985). Synapses can become segmented and presynaptic stimulation may cause a spinule to appear in the postsynaptic density and the spinule may develop to invaginate the presynaptic terminal leading to the formation of two release sites (Carlin and Siekevitz, 1983). (Figures 1.7 and 1.8)

1.2.2 Dendritic Spines

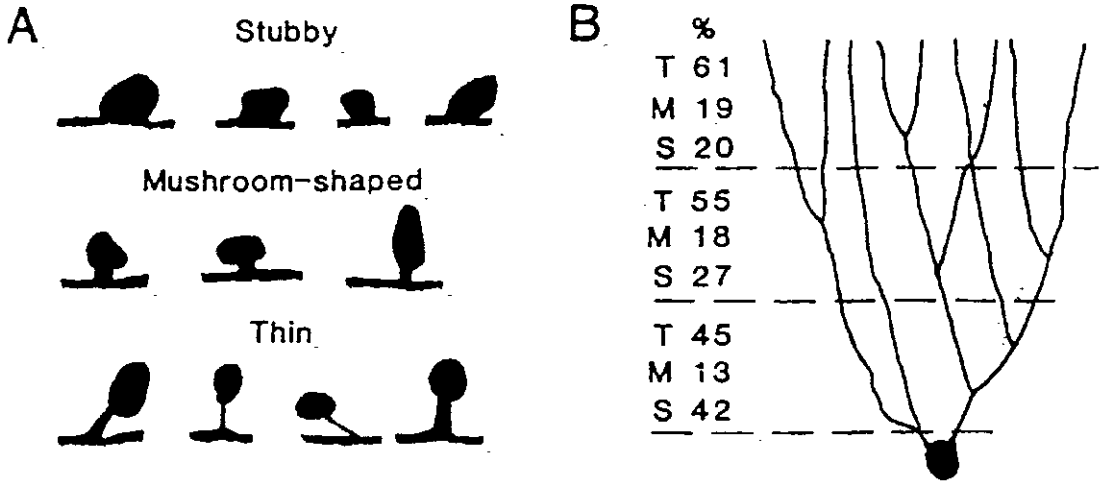

Figure 1.9 Spine morphology in the molecular layer of the dentate gyrus.

(A) Camera lucida drawings of the morphology of dendritic spines in the dentate gyrus. (B) Incidence of stubby (S), mushroom-shaped (M) and thin (T) spines on the inner, middle and outer regions of the dendritic arbour of a granule cell in the dentate gyrus. After Desmond and Levy, 1985.

Dendritic spines may be long or short, stumpy- or thin- necked and with or without a mushroom-shaped head (Desmond and Levy, 1985). (Figures 1.10 and 1.11) They are thought to localise the Ca^{2+} signal and compartmentalise biochemical changes occurring inside them, therefore restricting the diffusion of Ca^{2+} (Guthrie *et al.*, 1991; Segal *et al.*, 2000). The entrance of Ca^{2+}, following removal of the Mg^{2+} block, during LTP induction (see section 1.3.1 LTP induction) is believed to trigger a series of reactions involving modifications of cytoskeletal proteins and thus modification of spine shape (Kim and Lisman, 1999). Actin (Crick, 1982), myosin (Morales and Fifkova, 1989) microtubule - associated protein (Aoki and Siekevitz, 1985) and calpain (Lynch and Baudry, 1987) have all been implicated in the change in spine shape and total spine area

occurring during LTP. This may limit plastic changes only to those spines that have detected release of neurotransmitter from the presynaptic terminal (Halpain *et al.*, 1998).

Spines are dynamic structures that can undergo fast morphological modification. These morphological effects can alter the biophysics of the spine producing a larger synaptic current for a given amount of released transmitter (Lynch and Baudry, 1984). Widening of the spine neck could decrease its longitudinal resistance and modelling studies indicate that this would have a greater impact on fast rather than slow currents i.e. facilitate AMPA receptor currents without changing those associated with NMDA receptors. Conversely, an increase in the neck resistance, by decreasing the diameter or increasing the length of the neck could cause a decrease in synaptic efficacy (Jung *et al.*, 1991; Korkotian and Segal, 1998; Korkotian and Segal, 1999). However, studies have suggested that LTP expression is not due to changes in spine resistance (Jung *et al.*, 1991; Larson and Lynch, 1991).

1.3 Long Term Potentiation

LTP is expressed as " a persistent increase in the size of the synaptic component of the evoked response recorded from individual cells or from populations of neurons" (Bliss and Collingridge, 1993) and can last for 3-8 hours in slices and weeks *in vivo.*

An early phase of LTP (E-LTP), lasting less than 3 hours, can be dissociated from late-phase LTP and does not depend on protein synthesis. Protein phosphorylation is crucial in the first few hours of LTP development (Colley and Routtenberg, 1993; Reymann *et al.*, 1988) but later protein synthesis and gene expression are necessary as demonstrated by experiments using protein synthesis inhibitors (Fazeli *et al.*, 1993). The duration of LTP can be restricted to 3 hours if anisomycin, which prevents the translation of proteins from messenger RNA, is

Figure 1. 10 Electron micrographs of dendritic spines

Electron micrographs of dendritic spines in the molecular layer of the dentate gyrus (A) stubby spine, (B) mushroom-headed spine and (C) thin spine.The postsynaptic densities are indicated by arrows and the presynaptic boutons by *. Magnification x40k, bar = 200nm

present at the time of tetanisation but this duration is not affected by actinomycin, which blocks the transcription of mRNA from DNA (Matthies, 1989). Therefore, the early maintenance of LTP seems to require the synthesis of protein from pre-existing mRNA and does not depend on gene transcription. More persistent late LTP (L-LTP), or the protein synthesis-dependent phase of LTP maintenance, lasts for at least 24h and requires transcription and translation (the cAMP-PKA-MAPK-CREB signalling pathway) (Krug *et al.*, 1984; Otani and Abraham, 1989; Otani *et al.*, 1989; Nguyen and Kandel, 1996) and the generation of diffusable retrograde messengers (Williams, 1996),

If activity-dependent synaptic plasticity, such as LTP, in the hippocampus plays a critical role in certain kinds of memory, then saturation of hippocampal LTP may impair spatial learning. Repeated tetanisation at a single site in the perforant path has been reported to block spatial learning when leading to LTP in the dentate gyrus (McNaughton *et al.*, 1986; Castro et al., 1989) but this has not been successfully repeated (Korol *et al.*, 1993; Jeffrey *et al.*, 1993). However, (Moser *et al.*, 1998) have been able to disrupt spatial learning in animals with no residual LTP but not in animals that were capable of further potentiation.

The intense interest in the phenomenon of LTP and the research into all aspects of the mechanisms involved in the induction, expression and maintenance of LTP have provided a vast literature. Many studies have concentrated on the induction and expression of LTP due, in part, to the relative ease of monitoring experiments for a few hours. However, the maintenance and late phase of LTP, especially morphological changes, are less well studied. This introduction will give a general overview of the mechanisms believed to be involved.

1.3.1 The induction and expression of LTP

The threshold for inducing LTP is a complex function of the intensity and pattern of tetanic stimulation. Delivering a tetanus to the pathway of interest can

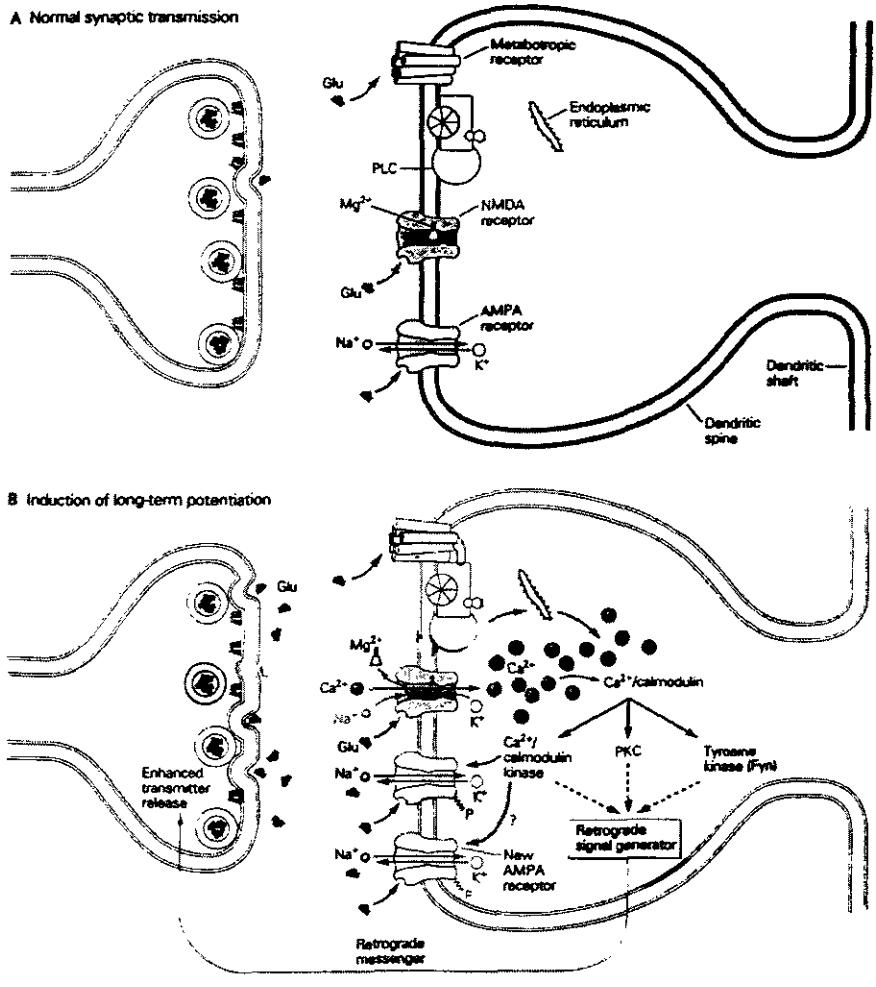

Figure 1.11 A model for the induction of LTP.

(A) During normal, low frequency synaptic transmission, glutamate (Glu) is released from the presynaptic terminal and acts on both the NMDA and non-NMDA receptors (the AMPA type are shown here). Na^+ and K^+ flow through the non-NMDA but not the NMDA channels owing to Mg^{2+} blockage of this channel at the resting membrane potential. (B) When the postsynaptic membrane is depolarised by the actions of the non-NMDA receptor channels, as occurs during a high frequency tetanus that induces LTP, the depolarisation relieves the Mg^{2+} blockage of the NMDA channel. This allows Ca^{2+} to flow through the NMDA channel. The resulting rise in Ca^{2+} in the dendritic spine triggers calcium-dependent kinases (CaMKII and PKC) and tyrosine kinase that together induce LTP. The CaMKII phosphorylates non-NMDA receptors and increases their sensitivity to glutamate thereby also activating some otherwise silent receptor channels. Once LTP is induced, the postsynaptic cell is thought to release a set of retrograde messengers e.g. nitric oxide (NO) that act on protein kinases in the presynaptic terminal to initiate an enhancement of transmitter release that contributes to LTP. After Kandel *et al.* Principles of Neural Science.

induce LTP and, while this may vary considerably, the tetanus usually consists of a train of 50-100 stimuli at 100Hz or greater. LTP can also be induced in the hippocampus by stimulation patterns that occur physiologically which mimics hippocampal theta rhythm (Larson and Lynch, 1986, 1988) - the firing pattern of hippocampal neurons recorded during exploratory behaviour in intact awake animals (Izquierdo, 1973; Oddie and Bland, 1998). Despite the potential behavioural importance of theta frequency - generated LTP most studies have focused on LTP induced more artificially by high frequency tetanisation and it has generally been assumed that since both are dependent on NMDA receptor activation the molecular mechanisms of LTP are the same.

The induction of LTP in hippocampal region CA1 and the dentate gyrus depends on four postsynaptic factors; (i) activation of NMDA receptors, (ii) postsynaptic depolarisation (iii) influx of calcium and (iv) activation of several second messenger systems in the postsynaptic cell by the rise in calcium concentration. (Figure. 1.11)

1.3.2 The N-methyl-D-aspartate (NMDA) receptor channel

The NMDA receptor channel is responsible for the events leading to the postsynaptic depolarisation required to trigger the induction of LTP and its properties of cooperativity, associativity and input-specificity. Under normal circumstances, the NMDA group of receptors contributes little to transmission because its associated ion channel is blocked in a voltage-dependent manner by magnesium (Nowak *et al.*, 1984). Therefore, the postsynaptic membrane must be sufficiently depolarised to expel Mg^{2+} from NMDA channels, at the same time that L-glutamate has promoted their opening, by binding to NMDA receptors (Collingridge and Bliss, 1995). The requirement of the presynaptic terminal to provide a sufficient concentration of L-glutamate to activate NMDA receptors has been demonstrated by experiments with the NMDA antagonist 2-amino-5-

phosphonopentanoate (AP5) (Collingridge *et al.*, 1983) and the NMDA channel blocker MK801 (Coan *et al.*, 1987).

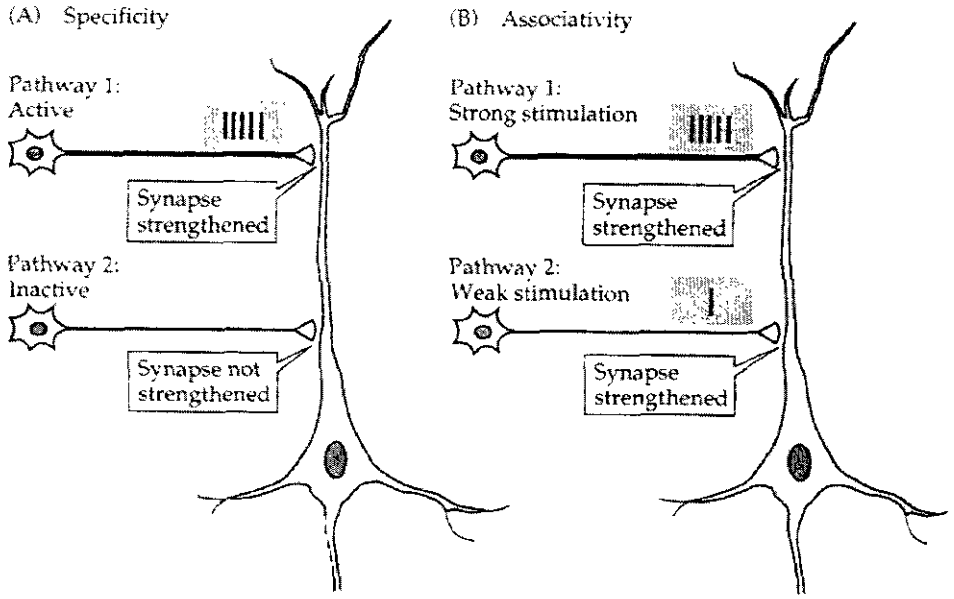

Figure 1.12 The properties of specificity and associativity of LTP in the hippocampus.

The cells represent CA1 pyramidal neurons receiving synaptic inputs from two independent sets of axons. (A) Strong synaptic activity initiates LTP at active synapses (pathway 1) without initiating LTP at nearby inactive synapses (pathway 2) (B) weak stimulation of pathway 2 alone does not trigger LTP. However, when the same weak stimulus to pathway 2 is activated together with strong stimulation of pathway 1, both sets of synapses are strengthened. After Purves et al., 1997.

The frequency-dependence of the induction of LTP is due to the slow time course, and voltage-dependence, of the NMDA receptor-mediated conductance that is susceptible to the hyperpolarising influence of synaptic inhibition (Collingridge *et al.*, 1988). 'Weak' stimuli activating relatively few afferent fibres do not trigger LTP (McNaughton *et al.*, 1978) because they fail to depolarise the membrane rather than as a result of insufficient glutamate. However, LTP is associative, in that weak stimulation of a pathway will not by itself trigger LTP but, if a neighbouring pathway is strongly activated at the same time, the weak pathway can be activated in a Hebbian like manner (McNaughton et al., 1978; Levy and Steward, 1979) i.e. the membrane is sufficiently depolarised. (Figure

1.13) LTP is also specific to activated synapses rather than to all synapses on a given cell (Andersen *et al.*, 1977; Lynch *et al.*, 1977). When LTP is induced by the stimulation of one pathway, it does not occur in other, inactive inputs that contact the same neuron.

1.3.3 Calcium influx

LTP is induced through NMDA receptor activation and calcium entry into post-synaptic spines (Lynch *et al.*, 1983; Nicoll and Malenka, 1995) and this rise in Ca^{2+} may be enhanced by the release of Ca^{2+} from intracellular stores (Alford and Collingridge, 1992). The increase in Ca^{2+} concentration activates different cascades of events, including phosphorylation mechanisms, which ultimately modify the functioning synapse by modifications in the structure of the synapses (Geinisman *et al.*, 1993) and eventually changes in synaptic connectivity. However, LTP expression must, in its initial stages, be related to modifications that can be established quite rapidly and that can be reversed since not all E-LTP may develop into a long-lasting increase in synaptic expression.

It seems reasonable to assume that if the triggering mechanism is located post-synaptically then the processes that express the effect are located proximal to the events that induce it (Bliss and Collingridge, 1993), although whether the locus of stable synaptic changes responsible for LTP expression is pre- or postsynaptic is a matter of debate. Imaging experiments (Connor *et al.*, 1994; Segal, 1995) have shown that tetanic stimulation elevates concentrations of Ca^{2+} transiently within dendrites and spines, and this activates enzymes to initiate the cascade that leads to the expression of LTP by the potentiation of the AMPA-receptor-mediated current.

1.3.4 Protein kinases

Although many protein kinases, e.g. CaMKII, protein kinase C (PKC), protein kinase A (PKA), mitogen-activated protein kinase (MAPK) and tyrosine kinases, (Mackler *et al.*, 1992) are involved in the induction and expression of

LTP, the current evidence suggests a central role for Ca^{2+}/calmodulin-dependent protein kinase II (CaMKII) (Fukunaga and Miyamoto, 2000). CaMKII, an oligomeric protein that consists of 10-12 subunits, is a major constituent of the postsynaptic density. In its basal state, CaMKII is inactive owing to the presence of an auto inhibitory domain that blocks intrasubunit substrate binding. Binding of Ca^{2+}- calmodulin (Ca^{2+}- CaM) adjacent to the auto inhibitory domain, alters its conformation and disrupts its inhibitory interaction, thereby causing activation of the kinase. The activated kinase undergoes rapid autophosphorylation that promotes the association of CaMKII with the PSD, partly through an interaction with the NMDA receptor. This places CaMKII not only proximal to a major source of Ca^{2+} influx, but also close to AMPA-type glutamate receptors, which become phosphorylated upon stimulation of NMDA receptors (Leonard et al., 1999).

The autophosphorylation also generates active CaMKII that can slowly phosphorylate exogenous substrates as well as catalysing additional autophosphorylation on other sites. Therefore, an elevation of Ca^{2+} concentration in a dendritic spine can produce a prolonged kinase activity that persists in the absence of Ca^{2+} levels. For example, the induction of LTP in hippocampal slices results in activation of CaMKII within one minute and this activity is stable for at least one hour (Fukanaga *et al.*, 1993; Barria *et al.*, 1997b) in contrast with a transient increase in MAPK activity (Liu *et al.*, 1999). The appropriate protein phosphatase - probably protein phosphatase 1 (PP1) which is also found at high levels in the PSD - dephosphorylates Thr286 and inactivates CaMKII (Strack *et al.*, 1997). Transgenic mice in which the autophosphorylation site Thr286 in CaMKII is mutated to Ala have normal basal synaptic transmission but do not exhibit LTP (Giese *et al.*, 1998).

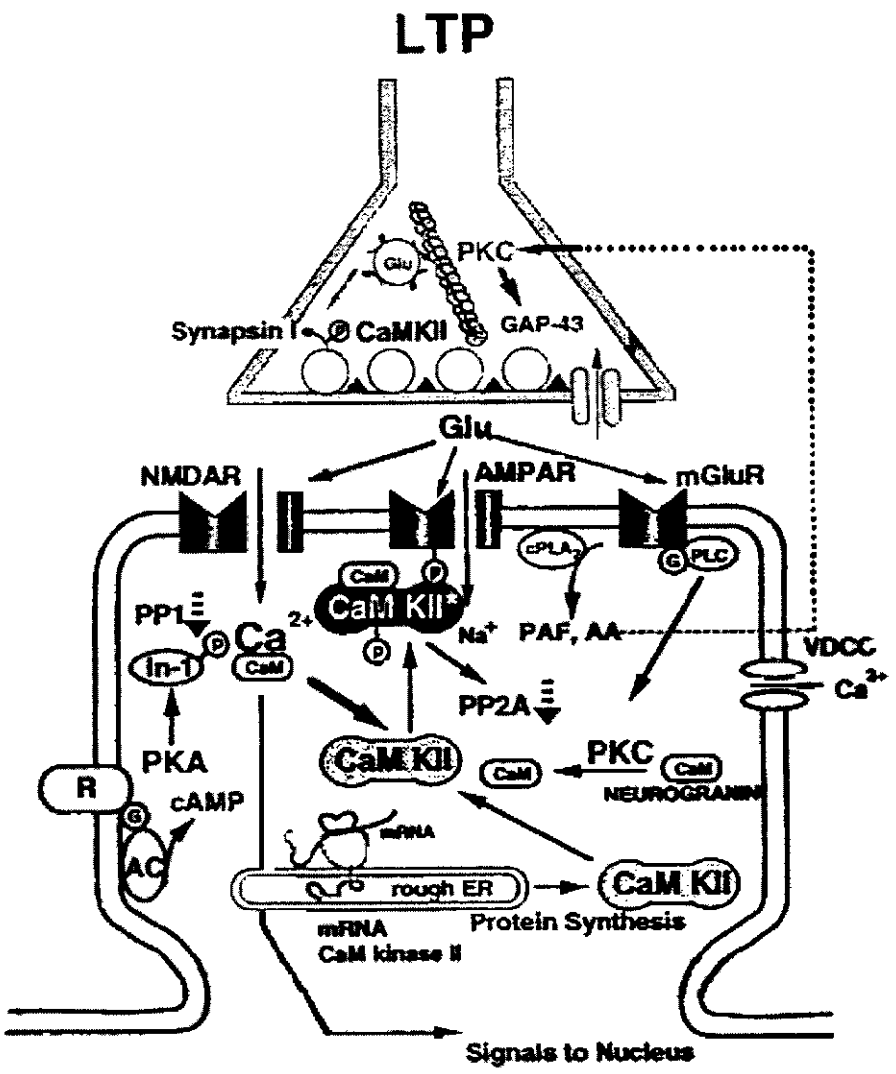

Figure 1.13 The role of protein kinases in the induction of LTP.

The rise in Ca^{2+} in the postsynaptic cell resulting from the influx through the NMDA receptors leads to generation of the Ca^{2+}- independent form of CaMKII. Activation of the NMDA receptors and mGluRs are linked to activation of PKA through adenylate cyclase (AC) and activation of PKC, respectively. Inhibition of protein phosphatase 2A (PP2A) activity by CaMKII and of protein phosphatase 1 (PP1) by PKA through phosphorylation of inhibitor 1 (In-1) may maintain autonomous kinase activity. Newly synthesised CaMKII translated from pre-existing mRNA may account for an increase in CaMKII activity. The long-lasting enhancement of CaMKII activity increases the sensitivity of AMPA receptors in postsynaptic sites. The increased phosphorylation of neurogranin and Gap 43 by PKC in the postsynaptic and presynaptic sites, respectively could increase free Cam concentrations and thereby potentiate CaM-dependent signalling, including CaMKII in both sites. Large increase in Ca^{2+} and cAMP in turn activate PKA to stimulate gene expression in the nucleus. After Fukunaga and Miyamoto, 1999.

NMDA receptor-dependent LTP is also associated with an increase in PKC activity (Akers *et al.*, 1986; Klann *et al.*, 1991; Klann *et al.*, 1993) and the application of PKC inhibitors can block the expression of LTP (Malinow *et al.*, 1988; Wang and Feng, 1992). The degree of phosphorylation of PKC substrate protein can be correlated with the degree of potentiation produced by tetanic stimulation of the perforant path *in vivo* (Routtenberg *et al.*, 1985; Lovinger et al., 1986). Indeed, in chronically implanted animals the phosphorylation still matched that of LTP when measured 3 days after induction (Lovinger *et al.*, 1985). Computer modelling of the three - dimensional structure of the PKC molecule has proposed that the conformation of PKC regulates accessibility of the phosphates to phosphatase (Sweatt *et al.*, 1998). This and other data has suggested that PKC is not part of the molecular machinery that produces LTP but is an important regulatory component. (Abeliovich *et al.*, 1993). Numerous PKC substrates are present postsynaptically but principally they are the AMPA and NMDA subtypes of glutamate receptors (Raymond *et al.*, 1993) (discussed later) and neurogranin.

The phosphorylation state of neurogranin is increased during the maintenance of LTP (Ramakers *et al.*, 1995). Neurogranin binds to calmodulin in the absence of Ca^{2+} and the affinity of calmodulin for neurogranin is lowered when the Ca^{2+} concentration is elevated. Phosphorylation of neurogranin by PKC lowers the affinity of neurogranin for calmodulin and this could lead to a postsynaptic elevation of calmodulin (Gerendasy *et al.*, 1995; Gerendasy *et al.*, 1994). Therefore, a persistent increase in the phosphorylation of neurogranin may provide a sustained increase in local Ca^{2+} and calmodulin concentrations that might result in altered Ca^{2+} / CaMKII activity (Chen *et al.*, 1997).

While NMDA receptors can induce LTP, the expression of the potentiation effect is accomplished by the AMPA receptors (Muller *et al.*, 1988). The simplest assumption is that calcium-dependent protein kinases directly phosphorylate ion channels e.g. phosphorylation of the AMPA receptor by CaMKII results in potentiation of the AMPA-receptor mediated current and requires 15-30 min to

develop (Mammen *et al.*, 1997). This is supported by evidence that the induction of LTP is associated with an increase in single-channel conductance of AMPA receptors, in 60% of potentiated cells (Benke *et al.*, 1998).

Experiments with transgenic mice have indicated that phosphorylation of the GluR1 subunit is particularly important for LTP expression. LTP can be induced in GluR2 subunit knockout mice (Jia *et al.*, 1996) but while the adult GluR1 subunit knockout mouse shows normal basal synaptic transmission, LTP cannot be induced (Zamanillo et al., 1999). The GluR1 subunit is regulated by protein phosphorylation at two sites on its carboxy terminal Serine 831, phosphorylated by CaMKII and PKC, and Serine 85 phosphorylated by PKA (Roche *et al.*, 1996; Barria *et al.*, 1997a; Mammen *et al.*, 1997). GluR1 can adopt multiple conductance states and phosphorylation has been shown to stabilise the higher conductances (Derkach *et al.*, 1999).

If phosphorylation of the AMPA receptors is required for insertion into synaptic membranes only dendritic spines having active CaMKII could express functional AMPA receptors. Translation of pre-existing CaMKII mRNA can occur within 15-30min of tetanisation and following this local up-regulation of translation, cAMP and / or Ca^{2+} signals can trigger transcription of synaptic elements including AMPA receptors (Fukunaga and Miyamoto, 1999). Therefore in early LTP maintenance, newly synthesised CaMKII could account for stabilisation of synaptic plasticity in specified dendrites that have received tetanic stimulation.

In summary, within one minute of LTP induction there is activation of CaMKII, which is stable for at least one hour and allows translocation of CaMKII to the PSD. This Ca^{2+} independent activity of CaMKII slowly phosphorylates the GluR1 subunit of the AMPA receptor, resulting in potentiation of the AMPA-receptor-mediated current, because of an increase in single-channel conductance.

1.3.5 Silent synapses

LTP has little effect on the NMDA receptor current but instead selectively increases the currents produced by the AMPA receptor (Muller and Lynch, 1988a; Muller *et al.*, 1988). This is not consistent with an increase in release of neurotransmitter, from a constant population of terminals (Stevens, 1993). If an increased number of effective synapses was responsible for explaining the selective nature of LTP, then they would need to lack NMDA receptors which seems unlikely. However, changes in the shape of existing spines could modify the surface geometry of the synaptic region and thereby expose previously inaccessible AMPA receptors. Alternatively, modification may affect the biophysics of the dendritic spine so as to facilitate AMPA receptor currents without markedly changing those associated with NMDA receptors. Facilitation of AMPA receptor-mediated transmission in slices of hippocampus is known to reduce the amount of afferent stimulation needed to induce a maximal degree of LTP (Arai and Lynch, 1992). Enhancement of AMPA receptors with drugs that prolong the opening time of AMPA receptors has been shown to improve spatial learning in a water maze task (Staubli *et al.*, 1994) and interference with the expression of AMPA receptors at the time of testing in rats hinders retrieval of memory for a few weeks (Bianchin *et al.*, 1993; Izquierdo *et al.*, 1997).

The insertion of AMPA receptor protein into the postsynaptic membrane of previously silent synapses may contribute to LTP. The fact that not all potentiated neurons show an increase in AMPA-receptor channel conductance suggests that other mechanisms as well as phosphorylation of AMPA receptors by CaMKII may be in operation. Reports have suggested that synapses expressing only NMDA receptors before potentiation are prompted by LTP to express functional AMPA receptors; these silent synapses are effectively non-functional at normal resting potentials but acquire AMPA-type responses after LTP induction (Liao, 1995). Specifically, induction of LTP has been shown to induce redistribution of transiently expressed GluR1 within 30 minutes in hippocampal slices from

intracellular sites in the dendritic shaft of dendritic spine apical dendrites (Shi *et al.*, 1999).

1.3.6 Metabotropic glutamate receptors (mGluRs)

Eight sub-types of mGluRs have been cloned and divided into three groups according to their sequence homology, pharmacological characteristics and coupling to second messenger pathways. Activation of group I mGluRs (mGluR1, 5) gives rise to the hydrolysis of phosphatidylinositol 4,5-biphosphate into inositol 1.4.5-triphosphate (IP3) and diacylglycerol, which are required for intracellular Ca^{2+} release and activation of PKC, respectively (Nakanishi, 1994). mGluRs of group II (mGluR2, 3) and group III (mGluR4, 6, 7, 8) are negatively coupled to adenylyl cyclase (Conn and Pin, 1997).

mGluRs have been implicated in LTP and learning and memory formation but the involvement of different receptor groups in particular functions is still controversial. The mGluR group I/II agonist 1-aminocyclopentane-1, 3-dicarboxylic acid (ACPD), plus the addition of NMDA, can induce LTP after sub-threshold or low frequency stimulation (McGuinness *et al.*, 1991). An inhibition of LTP by the class I/II specific antagonist S-α-methyl-4-carboxyphenylglycine (MCPG) has been described (Bashir *et al.*, 1993; Richter-Levin *et al.*, 1994) however, in other studies this could not be repeated (Manzoni *et al.*, 1994; Martin, 1997).

Bortolotto *et al.*, 1994 have suggested that the activation of mGluRs before LTP sets an input-specific molecular switch that then negates the necessity of further mGluR-activation during LTP induction, but again others have failed to find evidence of this molecular switch (Martin, 1997; Selig *et al.*, 1995). Results are similarly inconclusive regarding the function of mGluRs in learning and the group I mGluRs may be involved in the fine tuning of hippocampal synaptic plasticity. The impact of mGluRs appears to depend on the type and strength of

the stimulus supplied and the particular properties of the spatial learning paradigm employed (Balschun *et al.*, 1999).

mGluRs have been shown to modulate the facilitation of LTP within a distinct time window of less than 30mins following stimulation and support an important role for mGluRs in the events that immediately follow NMDA receptor activation (Manahan-Vaughan and Reymann, 1996). This facilitation by mGluRs of LTP may be mediated by mGluR-induced activation of PKC and the triggering of subsequent second messenger processes that are involved in the maintenance of the late phase of LTP.

Since the characteristics of the enduring form of LTP imply that the mechanism probably involves a signal transduction event at the activated synapse it has been suggested that LTP may initiate the creation of a short lasting (less than 3 hours) protein-synthesis-independent 'synaptic tag' at the potentiated synapse that isolates the relevant proteins to establish late LTP (Frey and Morris, 1997). mGluRs may be important in this process as they are believed to couple to nearby protein synthesis machinery in the postsynaptic cell to homosynaptically regulate an intermediate phase of LTP dependent on new proteins made from pre-existing mRNA. (Raymond *et al.*, 2000). (See Section 1.4.2 protein synthesis)

1.3.7 Retrograde messengers

If the maintenance of LTP involves a presynaptic enhancement of neurotransmitter release then some message must be sent from postsynaptic to presynaptic neurons. Similarly, the associative property of LTP suggests the requirement for a signalling molecule that could percolate to adjacent activated pathways. Since dendritic spines do not have the conventional machinery for the release of neurotransmitter, the putative retrograde messenger may be membrane permeable and reach the presynaptic terminals by free diffusion. There is some evidence for several candidates including the soluble gases nitric oxide (Zhuo, 1999), and carbon monoxide (Stevens and Wang, 1993) as well as arachidonic

acid (Williams and Bliss, 1989), platelet activating factor (Wieraszko *et al.*, 1993) and several neurotrophins (Kang, 1995; Korte *et al.*, 1996).

Nitric oxide (NO) is a gas, generated by the enzyme NO synthase (NOS) from the amino acid l-arginine. Synthesis of the neuronal type I isoform of NOS is triggered by increased Ca^{2+} /calmodulin in the postsynaptic terminal (O'Dell *et al.*, 1991). This soluble gas diffuses back to the presynaptic terminal, activates guanylyl-cyclase and cGMP-dependent protein kinases (Zhuo *et al.*, 1994), and leads to an activity-dependent increase in transmitter release (Hawkins, 1996). An inherent problem with the retrograde messenger theory was guaranteeing the maintenance of the pathway specificity of LTP. However, when NO was applied to hippocampal slices, paired with weak tetanic stimulation of the presynaptic fibres, the EPSP was rapidly enhanced and remained enhanced for at least one hour (Hawkins *et al.*, 1998). Weak tetanisation, or the application of NO alone, had no effect (Zhuo *et al.*, 1993), indicating that NO is only effective at recently activated presynaptic terminals.

Inhibitors of the type I NOS isoform have been shown to block the induction of LTP in hippocampal slices especially when injected into the postsynaptic cell (O'Dell *et al.*, 1991) suggesting that the production of NO is postsynaptic. However, some subsequent studies failed to confirm these results (O'Dell *et al.*, 1994; Cummings *et al.*, 1994). Crucially, LTP was found to be normal in mice with a mutation of the isoform suggesting that other isoforms contribute to the production of NO during the induction of LTP (O'Dell *et al.*, 1994).

Alternatively, other retrograde messengers may have a role e.g. arachidonic acid (AA). This is an unsaturated fatty acid, and is produced by the hydrolysis of phospholipids by phospholipases, particularly phospholipase A_2 (PLA_2). Nordihydroguaiaretic acid (NDGA), an inhibitor of lipoxygenase, the enzyme which metabolises AA and PLA2, blocks the induction of LTP in vivo and in vitro (Lynch et al., 1988; Williams and Bliss, 1988,1989). AA has been shown to

produce an input specific and NMDA receptor independent form of potentiation when paired with weak afferent activity (Williams and Bliss, 1989). Yet, the slow onset, the loss of input specificity at lower concentrations of AA and disagreement over the sensitivity of this form of potentiation to NMDA receptor antagonists (O'Dell *et al.*, 1991), raised doubts over the role of AA as a retrograde messenger. However, when the application of AA is combined with the activation of metabotropic glutamate receptors, biochemical and electrophysiological changes are produced that are consistent with a role in producing synaptic potentiation (McGahon and Lynch, 1994; Collins and Davies, 1993).

Unfortunately, there is no compelling evidence to support the candidacy of any of these proposed molecules as putative retrograde messengers. Indeed, the absolute requirement for a retrograde messenger is still speculative, as there is no confirmation, although it cannot be excluded, that the maintenance of LTP is at least, in part, presynaptic. Rather than a diffusable messenger there may be some signalling event involving neuron and glial cell communication (Attwell, 1994).

1.3.8 Morphological modifications

Electron microscopic studies have identified changes in spines and synapses that accompany LTP and there is increased interest in determining the functional consequences of such structural alterations. Morphological modifications, especially alterations in synaptic size and shape, have been observed in the first hour after tetanisation. (Table 1.1) This can involve perforation of the postsynaptic density (Geinisman *et al.*, 1993; Buchs and Muller, 1996) modification of presynaptic active zones (Desmond and Levy, 1986b; Schuster *et al.*, 1990; Geinisman *et al.*, 1992b), or redistribution of vesicles at the axon terminal (Applegate and Landfield, 1988). These early mechanisms, including the redistribution of postsynaptic receptors, are likely to be a dynamic feature and, as synaptic efficacy may be finely regulated at each individual synapse by activity, subtle changes in synaptic profiles are difficult to detect.

However, there has been insufficient morphological information from the maintenance phase of LTP, and results can be difficult to interpret, due to the different stimulation paradigms and time points used (Geinisman, 1996; Weeks *et al.*, 1998). Data from continued studies of synaptic morphology, at time points beyond 3 hours after induction, could provide important information contributing to an understanding of the late phase of LTP.

Cleavage of adhesive connections could be an early step in the formation of new synaptic configurations. Neuronal activity has been shown to regulate the expression of PSA-NCAM at the synapse and this expression may be required for the induction of synaptic plasticity (Muller *et al.*, 1996). In rats, the level of PSA on NCAM increases after a passive avoidance task (Doyle *et al.*, 1992b). Stimulation of hippocampal NMDA receptors results in the extracellular proteolysis of NCAM (Hoffman et al, 1998) and peptides and antibodies that disrupt the extracellular interactions of CAMs cause stable LTP to quickly decay over several minutes (Luthi *et al.*, 1994). Elevated concentrations of adhesion molecules, have been demonstrated 90min after the induction of LTP in the dentate gyrus (Fazeli *et al.*, 1994).

In addition to their involvement in synaptic remodelling accompanying LTP induction, these molecules may contribute to the persistence of potentiation by stabilising synapses at later time points. 24h after high frequency stimulation of the perforant path, there is a two-fold increase in the number of spine synapses, in the molecular layer of the dentate gyrus, expressing NCAM180 (Schuster *et al.*, 1998). Studies using NCAM antibodies have been shown to disrupt consolidation of a passive avoidance response in rats when administered 6-8hrs after task acquisition (Doyle *et al.*, 1992a). This group have also shown a transient elevation in the sialylation state of NCAM 12 to 24 hrs following training (Doyle *et al.*, 1992b).

Similarly, for memories persisting more than a few weeks, in whose retrieval cortical structures other than the hippocampus play a role, activity-

dependent synaptic adhesion changes followed by morphological changes may be important. This would require a mechanism to sustain activity-dependent cell adhesion changes for long periods until synaptic morphological changes have been established - perhaps by a replay of learning related activity by hippocampal cells that project to those synapses. Interestingly, a replay of correlated neuronal firing patterns acquired during spatial learning by groups of hippocampal pyramidal cells has been reported to occur in rats during sleep (Skaggs and McNaughton, 1996).

1.3.8.1 Dendritic spines

Investigations of spine morphological modifications in the initial hour after LTP induction have produced many contradictory results. Increases in the mean area of spines, in the width of the spine head and spine neck, have been shown after high-frequency stimulation of the perforant path to the dentate gyrus (Van Harreveld and Fifkova, 1975). In addition, similar studies have reported a decrease in the length of the spine neck (Fifkova and Anderson, 1981). These modifications would produce a reduction in the linear resistance of the spine and have a greater affect on fast synaptic currents i.e. AMPA - produced responses rather than slow NMDA receptor-generated responses (Wilson, 1984).

However, when CA1 pyramidal neurons were potentiated, there was no change in the width of dendritic spine neck or the area of dendritic spines (Lee *et al.*, 1980). Another study in the CA1 region showed an increase in the number of short and stumpy spines (Chang and Greenough, 1984). The morphological differences between areas CA1 and dentate gyrus, might be explained by the different protocols used to induce LTP in the two areas (Chang and Greenough, 1984). Alternatively, the anatomical correlates of LTP may be different in the two systems.

While it is technically difficult to visualise individual synapses in the hippocampus during potentiation it is possible to image spines in slices. Using

these confocal microscopy techniques (Hosokawa *et al.*, 1995) observed the growth of a sub-population of small spines, as well as angular displacement of spines, 3.5 hours after chemical induction of potentiation. A decrease in the numbers of spines was described 24hrs after tetanisation of the perforant path (Rusakov *et al.*, 1997b). Passive avoidance training in one-day old chicks has been shown to cause an increase in spine density and spine head diameter, and a decrease in spine neck length, 24hrs after passive avoidance learning in the day-old chick (Lowndes and Stewart, 1994).

1.3.8.2 Postsynaptic density

Morphological changes may not be a consequence of potentiation but a necessary prerequisite and anatomical change could be a phenomenon required for LTP expression. The distribution of receptors at the postsynaptic membrane may provide evidence for this hypothesis as changes in shape and size of the PSD would alter the ratio of receptor groups. AMPA type-receptors are concentrated in the membrane opposite the transmitter release site. However, the type 1 and 5 mGluRs are concentrated in an annulus, around the synapse, surrounding the ionotropic receptors, followed by a wider band of receptors that decrease in density (Lujan, 1996). Larger spines generally have larger PSDs (Harris, 1989; Lisman and Harris, 1993) and more receptors and ion channels. In studies on the hippocampal, dentate gyrus (Desmond and Levy, 1983; Desmond and Levy, 1986a; Desmond and Levy, 1988) found that there was an increase in the number of synapses with large postsynaptic densities following LTP induction. However, two hours after LTP induction in hippocampal area CA1 *in vitro*, there was no increase in synapse size (Sorra and Harris, 1998). They also reported no significant difference in total synapse number, on the distribution of different types of synapses, on the frequency neither of shaft synapses nor on the relative proportion of single or multiple synapse axonal boutons.

It has been reported that perforated axospinous synapses are twice as likely as non-perforated ones to express detectable levels of AMPA receptor subunits, whereas no significant differences in NMDA receptor expression were observed (Desmond and Weinberg, 1998). As already discussed, the insertion of AMPA receptor protein may render perforated synapses especially potent and increasingly studies may concentrate on 'activated' synapses when investigating ultrastructural modifications (Buchs, 1996), and use confocal microscopy techniques.

The curvature of the membrane above the PSD may also vary during LTP. In the dentate gyrus, an increase in the number of concave spine synapses with large postsynaptic densities was observed (Desmond and Levy, 1983, 1986b, 1988). This increase was accompanied by a decrease in the number of convex synapses and persisted for 60min after stimulation, suggesting a possible interconversion from non-concave to concave synapses during LTP.

1.3.8.3 Presynaptic glutamate release.

Modification of postsynaptic morphology has functional implications for the presynaptic terminal and can influence neurotransmitter release from activated synapses. Increased probability of release would result from spine growth, if it lead to perforation of the PSD, (Greenough *et al.*, 1978) and/or synchronous changes in the presynaptic bouton (Desmond and Levy, 1986b; Schuster *et al.*, 1990; Geinisman *et al.*, 1992b; Lisman and Harris, 1993). The number of synaptic vesicles attached to the active zone membrane is significantly increased, together with the percentage of vesicles adjacent to the active zone, during LTP induction of CA1 (Applegate *et al.*, 1987). Alternatively, spine growth or displacement could permit receptor-bearing membranes to come into close contact with pre-existing release sites allowing receptor access to previously ineffectual transmitter release sites. (Hosokawa *et al.*, 1995).

Protein kinase activation by presynaptic depolarisation and a rise in calcium concentration may influence the dynamics of the presynaptic terminal. (Figure 1.13) e.g. Persistently activated PKC may be found in the presynaptic compartment (Chen *et al.*, 1997) as demonstrated by increased phosphorylation of neuromodulin / GAP 43, reported in LTP (Wang and Feng, 1992; Ramakers *et al.*, 1997).

Investigations of LTP induction suggest an increased probability of release although the mechanism for the expression of LTP may also involve an increase in quantal size (Isaac *et al.*, 1996). However, a recent study of the late phase of LTP, on synapses of CA1 neurons, demonstrated an increase in the number of quanta released, and suggested an increase in the number of sites of synaptic transmission (Bolshakov *et al.*, 1997).

1.4 The Maintenance of LTP

1.4.1 Protein kinase A

Changes in the abundance of mRNAs for a number of protein kinase proteins have been identified 30 min to 3 hours after tetanisation (Mackler *et al.*, 1992) suggesting that protein kinases may play a role in the maintenance stages of LTP in addition to their contribution during the early phase, e.g. AMPA-receptor channels can be rapidly modulated by PKA activators (Greengard *et al.*, 1991). Studies have suggested that as well as PKC the synergistic activation of PKA is necessary for the maintenance of LTP (Matthies and Reymann, 1993; Frey *et al.*, 1993). In experiments with transgenic mice, with reduced PKA activity in their hippocampus, L-LTP was significantly decreased in region CA1, without affecting basal synaptic transmission or the early phase of LTP (Abel *et al.*, 1997).

The catalytic subunit of PKA recruits another second messenger kinase MAPK (Martin *et al.*, 1997; Impey *et al.*, 1998) commonly associated with cellular growth Doherty *et al.*, 2000, and together the two kinases translocate to the nucleus where they activate a genetic switch. (Figure 1.15) The catalytic

subunit phosphorylates, and thereby activates, a transcription factor called CREB 1 (cAMP response element binding protein). This phosphorylated transcriptional activator binds to a promoter element called CRE (cAMP response element). By means of the MAPK, the catalytic subunit of PKA also acts to relieve the inhibitory actions of CREB 2 – an inhibitor of transcription.

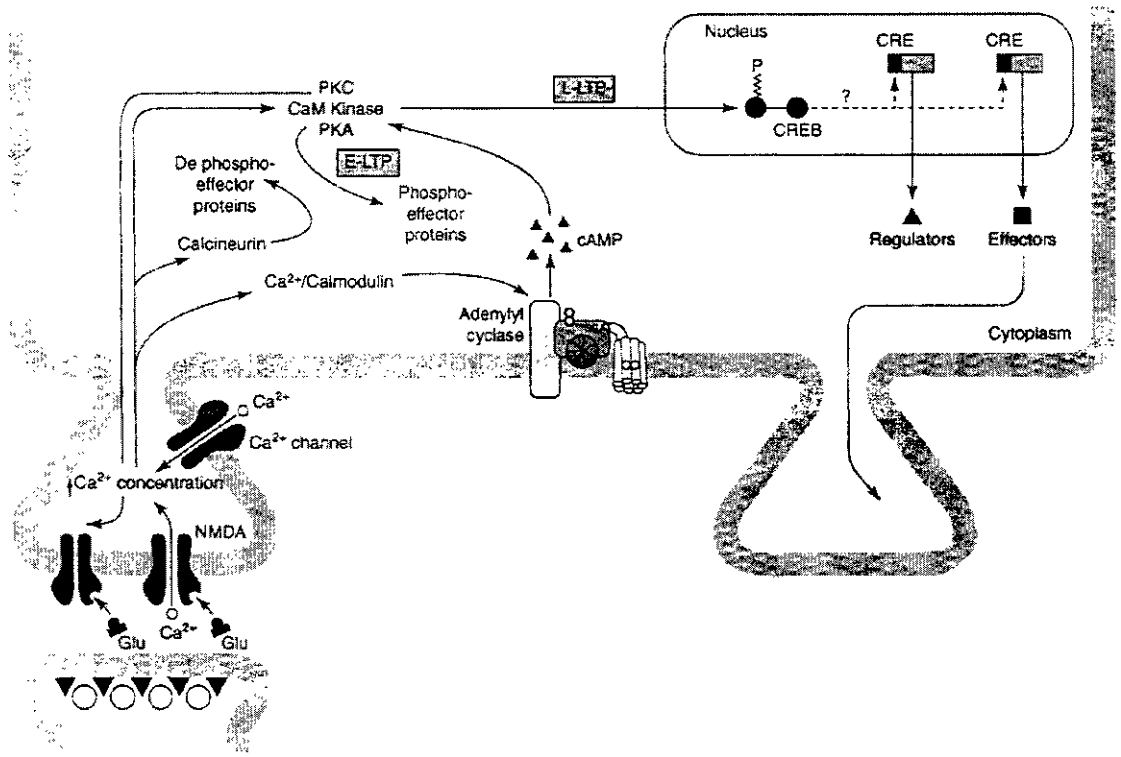

Figure 1.14 A model for the early and late phase of LTP

A single train of action potentials leads to early LTP by activating NMDA receptors, Ca^{2+} influx and into the postsynaptic cell and a set of second messengers. With repeated trains the Ca^{2+} influx also recruits an adenylyl cyclase, which activates the cAMP-dependent protein kinases. The catalytic subunit of PKA recruits another second messenger kinase MAPK and together the two kinases translocate to the nucleus where they phosphorylate the CREB protein. This phosphorylated transcriptional activator binds to a promoter element called CRE (cAMP response element) and activates targets that are thought to lead to structural changes. After Purves *et al.*, 1997

The presence of a repressor and an activator of transcription suggest that the mechanism is highly regulated but CREB activation leads to a cascade of gene activation that can lead to growth of new synaptic connections. Inhibitors of PKA block L-LTP and associated increases in CRE-mediated gene expression (Impey

et al., 1996). Proteolytic processes that lead to the degradation of the regulatory subunits of PKA allow the catalytic subunits to continue phosphorylating proteins long after the second messenger cAMP has returned to basal levels and can make PKA persistently active for up to 24h without requiring a continuous signal.

There is evidence of increased *de novo* gene expression after LTP. In the first few hours after LTP induction there is an increase in *Zif/268* (an immediate early gene (IEG) induced by stimuli that produce LTP (Cole *et al.*, 1989; Roberts *et al.*, 1996), CaMKII, PKC (Thomas *et al.*, 1994) and MAP2 mRNA levels (Roberts *et al.*, 1998a). Increased expression of dendritic CaMKII mRNA and microtubule-associated protein 2 (MAP2) mRNA is suggested to be a general feature of hippocampal plasticity, since it occurs following LTP induction in both the dentate gyrus and the CA1 region. Long lasting increases in CaMKII activity has been closely associated with stable phosphorylation of the GluR1 receptor, synapsin 1 and MAP2 during LTP maintenance (Fukanaga *et al.*, 1995). Increased extracellular signal-regulated kinase 2 (ERK2)/MAP kinase and raf-B mRNA levels are observed by 24 h (Thomas *et al.*, 1994).

Growth factors e.g. brain-derived neurotrophic factor (BDNF) acutely modify synaptic transmission (Figurov *et al.*, 1996) and are required for the establishment of LTP (Patterson et al 1996). Synapse-specific effects of growth factors may be provided by localised presynaptic release. Synaptosomes prepared from the hippocampus of BDNF knockout mice exhibited synaptic fatigue and a marked decrease in the levels of synaptophysin as well as synaptobrevin (Pozzo-Miller *et al.*, 1999). Treatment of the mutant slices with BDNF reversed the electrophysiological and biochemical deficits in the hippocampal synapses. These results suggest a role for BDNF in the mobilisation and/or docking of synaptic vesicles to presynaptic active zones.

In vivo studies of the messenger RNAs (mRNAs) encoding proteins of the exocytic machinery have been measured at different times following the induction of long-term potentiation in the dentate gyrus. *In situ* hybridisation has revealed

increased levels of mRNAs encoding both synapsin I and syntaxin 1B in the dentate gyrus 2h and 5h following the induction of long- term potentiation (Hicks *et al.*, 1997). An increase in the protein levels of syntaxin 1B and, to a lesser extent, the synapsin I, was observed 5h after the induction of LTP, associated with an increase in depolarisation-induced release of glutamate within these terminals (Helme-Guizon *et al.*, 1998). Increases in both the protein levels and glutamate release were not observed when dentate gyrus LTP was blocked by an NMDA receptor antagonist. Increased mRNA levels of SNAP-25 are reported 2 h after the induction of LTP in granule cells of the dentate gyrus following high frequency stimulation of the perforant path *in vivo* (Roberts *et al.*, 1998b). The persistent long-term potentiation- induced postsynaptic increase in mRNAs encoding these presynaptic proteins has important implications for the propagation of signals downstream from the site of long-term potentiation induction in hippocampal neural networks.

1.4.2 Protein synthesis

It has already been established that the late phase of LTP requires the synthesis of new proteins (Fazeli *et al.*, 1993), and these may play a structural role in the modification of existing synapses or the *de novo* synthesis of new synapses. If LTP does incorporate the formation of new synapses, and therefore co-ordinated changes on both sides of the synapse, LTP would display pre- and postsynaptic effects.

This process necessitates the delivery of mRNAs to particular intracellular locations that allow a local synthesis of macromolecules, with particular intracellular domains. In neurons, protein synthetic machinery made up of polyribosomes and associated cisterns, are selectively localised beneath individual postsynaptic sites (Steward *et al.*, 1996). These polyribosomes may be found at the intersection between the spine neck and the main dendritic shaft or beneath synapses on dendritic shafts (Steward and Ribak, 1986). They are particularly

prominent during periods of synapse growth, during development (Steward and Falk, 1986) and when neurons are reinnervated following injury (Steward, 1983).

Immediate early genes (IEGs) are rapidly induced and exert their effect by regulating downstream genes. Late response genes are induced over periods of hours to days and frequently encode genes of direct physiological function such as growth factors and their receptors, enzymes and proteins. In neurons there are perhaps 30-40 IEGs (Lanahan and Worley, 1998), 10-15 are transcriptional factors and a subset are transcriptionally induced at the cell body (Steward 1994) remote from the synapses yet are anticipated to directly modify synaptic function.

This would require a signalling process to modulate gene expression in the postsynaptic neuron and synthesis of particular gene products to the individual synapses that are to be modified. This must be co-ordinated so that modifications occur selectively at the activated synapses. e.g. *in situ* hybridisation techniques have shown that the mRNA encoding the α-subunit of CAM kinase II is present at high levels throughout the molecular layer of the dentate gyrus (Steward and Wallace, 1995).

Several of the mRNAs that are present in dendrites have been identified and appear to provide evidence for this mechanism of synapse specific gene expression (Steward *et al.*, 1998) where particular mRNAs are translated locally at postsynaptic sites on dendrites. The transcript of an immediate early genes (IEG) named *Arc (*activity-regulated cytoskeleton) - associated protein (Lyford *et al.*, 1995) is rapidly and transiently induced after LTP (Wallace *et al.*, 1998) and delivered into dendrites (Lyford *et al.*, 1995) within 1 hour. Stimulation of the medial perforant path to produce a band of activated synapses in the molecular layer showed that high frequency stimulation (HFS) induces *arc* expression and causes newly synthesised mRNA to localise in the synaptically activated dendritic lamina.

The elevation of mRNA levels in a restricted region close to the afferent synapses would allow a localised enhancement of the synthesis of the

corresponding proteins, therefore providing a mechanism for a high degree of anatomical specificity and satisfy some of the characteristics of a synaptic tag (Frey and Morris, 1997). Evidence of possible candidates and mechanisms reinforce this hypothesis.

Homer, a small (186 amino acid) soluble cytosolic protein, is strongly induced in neurons of the hippocampus after LTP and may be involved in the structural changes that occur at metabotropic glutamatergic synapses during the maintenance phase of LTP (Kato *et al.*, 1998). *Homer* protein binds to the C terminus of metabotropic receptors and appears to rapidly target excitatory synapses and dendritic spines (Brakeman *et al.*, 1997). Neuronal activity can modify the affinity of the interaction between *homer* and mGluR5 and, if it occurs at individual synapses, could underlie the synapse specific effects of *homer* (Lanahan and Worley, 1998)

Rheb a GTP-binding protein (Yamagata *et al.*, 1994) interacts with Raf kinase and appears to activate subsequent signalling events (Yee and Worley, 1997). *Rheb* signalling requires the coincident activation of PKA, and therefore localised response to growth factors, since signalling would be restricted to regions of the neuron with activated PKA. These signalling properties of *rheb* may afford synapses specific effects of the IEG even in the absence of specific targeting of *rheb* protein.

1.4.3 Synapse number

New synapse formation may involve an intermediate stage, such as the perforation of synapses (Nieto-Sampedro, 1982). Alternatively, spine branching may occur to either increase or decrease spine density as demonstrated in dentate gyrus-granule cell synapses (Trommald *et al.*, 1990; Rusakov *et al.*, 1997b). (Figure 1.16)

Later studies in area CA1 of hippocampal slices in young adult rats suggested that branched spines are unlikely to be transient intermediates in the

process of dividing from perforated synapses (Sorra, 1998). These results reported that different branches of the same spine never synapsed with the same presynaptic bouton and that division of a presynaptic bouton is not part of synapse splitting to generate new unbranched spines.

Perforated synapses appear to be functionally related to synaptic plasticity (Greenough *et al.*, 1978) and result from splitting of PSDs. PSDs might increase in size before breaking down into several fragments, which may or may not give rise to a new simple synapse (Hoff and Cotman, 1982). Jones (1993) has suggested that perforated and non-perforated synapses constitute separate populations that are formed early in development and each represents complementary forms of plasticity.

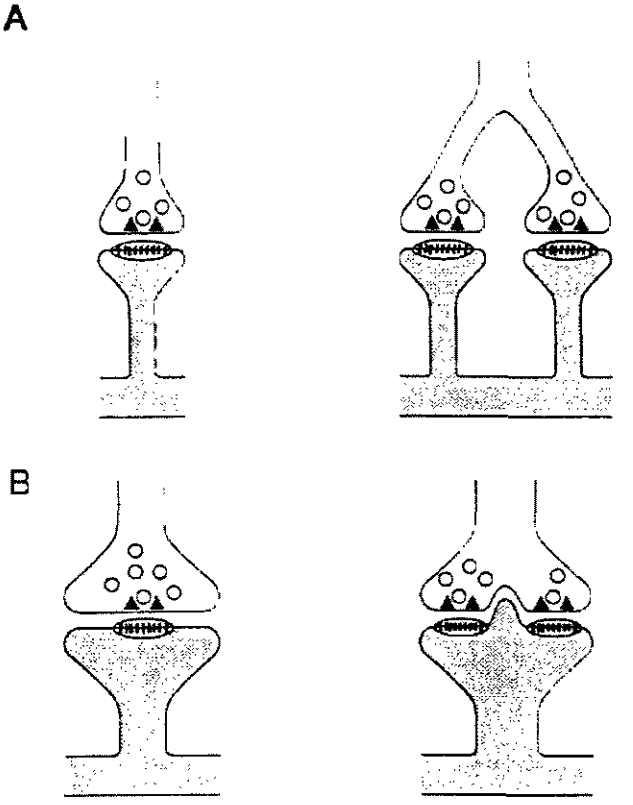

Figure 1.15 Schematic diagram of models of synapse formation

LTP may involve the formation of new synapses. Two possible models of synapse formation involve; (A) the sprouting of a new branch from an exiting terminal or; (B) a spinule in the postsynaptic membrane protrudes into the presynaptic terminal to form a new synapse. After Agnihotri *et al.*, 1998

High frequency stimulation of the Schaffer-collateral commissural pathway in the hippocampus causes an early increase in the number of perforated synapses (Geinisman *et al.*, 1991). A similar study on slices was able to demonstrate that the increase in perforated synapses occurred at synapses that had been potentiated (Buchs and Muller, 1996). At these synapses, the apposition zones between pre- and postsynaptic structures were also larger, PSDs were longer, and spine profiles were enlarged (Buchs and Muller, 1996). After high frequency stimulation of the perforant path in young rats the number of perforated synapses with a segmented PSD was increased and this increase was confined to the area where LTP had occurred (Geinisman *et al.*, 1991). 24hrs after the induction of LTP *in vivo* an increase in the number of perforated concave synapses was found which exceeded the overall increase in concave synapses (Weeks *et al.*, 1999).

Behavioural studies have supported a relationship between the numbers of perforated synapse and learning and memory. Aged rats that exhibit a deficit in spatial memory showed a reduction in the number of perforated synapses in the dentate gyrus in comparison with either young adults or aged rats with good memory (Geinisman *et al.*, 1986).

There is evidence that LTP is associated with the formation of new, mature and functional spine synapses, at least, contacting the same presynaptic terminals. (Toni *et al.*, 1999) have reported an increase in the proportion of multiple spine boutons detected 45-60min after potentiation induced by theta burst stimulation (TBS) in slices. An increase in the number of axodendritic synapses has been reported 15mins after potentiation (Lee *et al.*, 1980). There is a considerable degree of variation in the level of potentiation induced in different animals following the induction of LTP. Although, reporting no significant increase in synaptic density, Weeks *et al* (1998) have reported a positive correlation between the degree of LTP and the number of synapses per neuron. At later time points, an increase in the number of axodendritic synapses was detected 13 days after the induction of LTP (Geinisman *et al.*, 1996). During passive avoidance learning in

the chick an increase in synapse number in the lobus parolfactorius was detected (Stewart *et al.*, 1984, 1987; Patel *et al.*, 1988a,b). These changes were detected after 24h whereas the associated biochemical changes disappeared after 3 hours.

In summary, it has been reported that axospinous, perforated synapses increase in number soon after the induction of LTP followed by an increase in multiple spine boutons. 24h later there is an increase in concave perforated synapses and a correlation between the number of synapses per neuron and the degree of LTP. Two weeks later this is manifested as an increase in the number of axodendritic synapses.

However, there are many inconsistencies in the data on synaptic morphological changes after LTP (Table 1.1) that can be explained from several approaches:-

1. The use of inappropriate stereological methods may introduce biases into the investigations and this will be discussed in Chapter Two.

2. The potentiating stimulation may vary between studies of the potentiation of the Schaffer collateral or the perforant path. Most studies of LTP have focused on potentiation that is induced by high frequency stimulation (HFS) of at least 100Hz, although frequencies of 400Hz have been used. Theta–burst stimulation (TBS) of 3-12Hz, that can be recorded by EEG in the rat hippocampus when an animal moves through space (Oddie and Bland, 1998), has also been used to generate LTP. It has generally been assumed that since both are dependent on NMDA receptor activation the molecular mechanisms of LTP produced by HFS are the same as those produced by TBS and that may not be the case.

3. There may be variability between the results of in *vitro* and *in vivo* investigations. Hippocampal slice preparations have been used for extensive *in vitro* studies of LTP mechanisms and although the hippocampal slice is useful, it cannot be viewed as an adequate model of information processing in the *in vivo* hippocampal formation. *In vivo* confirmation of the results of *in vitro*

morphological investigations is required to fully understand the mechanisms involved in the modification of synaptic connectivity after LTP induction.

1.5 Aims of this thesis

Many studies have investigated morphological changes in the first 60min post LTP induction but many of these studies have been non-stereological, *in vitro* and used HFS to induce LTP. (Table 1.1) The widespread use of *in vitro* studies and the difficulty of long-term investigations mean that there are few morphological investigations of the maintenance stages of LTP. This thesis endeavoured to augment the previous studies by using modern unbiased stereological methods and electron microscopy techniques to examine certain aspects of morphological modification, in the dorsal hippocampus.

The first part of the thesis will examine the morphology of synapses in the middle molecular layer of the dentate gyrus, 45min after LTP induction with theta–burst stimulation of the perforant path. If morphological changes observed in previous studies with high frequency stimulation are due to LTP, then similar results should be determined with other stimulating paradigms.

The second part of this thesis will investigate morphological modification that may develop 24h after tetanisation, during the maintenance phase of LTP. To consider the effects of different stimulation protocols, high frequency stimulation and theta–burst stimulation were used to potentiate the perforant path to the dentate gyrus of the hippocampus.

Morphological correlates of LTP might relate to potentiation of synaptic strength in several ways but the normal functioning of the neurons of the brain requires that synapses be continuously remodelled. The final part of this thesis will try to assess whether any morphological changes are the cause of the potentiation, or its consequence and consider how these changes may influence the cellular mechanisms involved in LTP.

Personally, I suspect that there will be some morphological changes after the induction of LTP as it is difficult to believe that a phenomenon that can last for

weeks would not involve synaptic modification of some kind. I am unconvinced the LTP is the mechanism for the induction and storage of memories but it does enhance synaptic efficacy and may be involved in the facilitation of memory formation. I believe that *in vivo* experiments where LTP is induced by more physiological stimulation paradigms are necessary to help to explain the LTP – memory conundrum.

Table 1.1 Morphological studies of the hippocampal formation.

Morphological studies of the hippocampal formation, in the induction and maintenance phases of L-LTP. Biased (B) and unbiased (U) stereological methods of analysis. Serial reconstruction (R).

Pages 50-52

			Hippocampal region	Electrophysiology	Time interval	Results
Van Harreveld and Fifkova 1975	*in vivo*	B	Dentate gyrus	HFS	2-60min	Increase in the mean area of distal spines
Desmond and Levy (1986a)	*in vivo*	B	Dentate gyrus	HFS 400Hz	10 and 60min	Increased incidence of concave synapses.
Desmond and Levy (1986b)	*in vivo*	B	Dentate gyrus	HFS 400Hz	10 and 60min	Increase total PSD surface area (*Sv*). Increase *Sv* of concave spine profiles but decreased *Sv* non-concave spine profiles.
Toni et al (1999)	*in vitro*	R	CA1 organotypic hippocampal slice	TBS	5-120 min	30min - increased incidence of perforated synapses. 60min – increased incidence of multiple synaptic contacts
Lee at al (1980)	*in vivo*	B	CA1	HFS 100Hz	15 min	Increased incidence of axodendritic synapses
Chang and Greenough (1984)	*in vitro*	B	CA1 hippocampal slice	HFS 200Hz	15min-8h	Increase in the numbers of axodendritic and axospinous synapses. Decrease in incidence of concave synapses.
Fifkova and Anderson (1981)	*in vivo*	B	Dentate gyrus	HFS	30min	Increase in the width of spine stalks

Buchs and Muller (1996)	*in vitro*	B	CA1 organotypic hippocampal slice	TBS	30min	Increased incidence of 'activated' perforated synapses. Increased area of spine head profiles, length of PSD profiles and length of AZ profiles.
Trommald *et al* (1997)	*in vivo*	R	Dentate gyrus	HFS 100Hz	30min	Large variability in spine head dimensions, neck length and PSD area. Twin spine heads never shared the same presynaptic bouton.
Trommald *et al* (1990)	*in vivo*	R	Dentate gyrus	HFS 100Hz	30min	Increased spine density.
Desmond and Levy (1990)	*in vivo*	B	Dentate gyrus	HFS 400Hz	60min	Decreased incidence of polyribosomes. Fewer multiple synaptic contacts.
Geinisman *et al* (1991)	*in vivo*	U	Dentate gyrus	HFS 400Hz	60min	Increased frequency of perforated axospinous synapses.
Weeks *et al* (2000)	*in vivo*	U	Dentate gyrus	HFS 400Hz	60min	Significant increase in the proportion of perforated and irregular-shaped synapses, especially those with concave perforated profiles.
Sorra and Harris (1998)	*in vitro*	R	CA1	HFS 100Hz	2h	No changes in synapse number, size or distribution of different synaptic types.
Schuster *et al* (1990)	*in vivo*	B	Dentate gyrus	HFS 200Hz	8h 48h	Increased density of axospinous synapses containing spinules.

Rusakov *et al* (1997)	*in vivo*	U	Dentate gyrus	HFS 200Hz	24h	Decrease in spine density but increased incidence of shorter, thicker spines.
Weeks *et al* (1998)	*in vivo*	U	Dentate gyrus	HFS 400Hz	24hr	Positive correlation between the degree of LTP and the number of synapses per neuron.
Weeks *et al* (1999)	*in vivo*	U	Dentate gyrus	HFS 400Hz	24hr	No overall increase in synaptic number, significant increase in the number of perforated concave synapses.
Geinisman *et al* (1996)	*in vivo*	U	Dentate gyrus	HFS 400Hz	13 days	Increased frequency (28%) of asymmetric axodendritic synapses.

Chapter Two General Methods

2.1 Electrophysiology

2.1.1 Induction of LTP *in vivo*

Male Sprague-Dawley rats (300-400g, 2-3 months old) served as experimental animals and were anaesthetised with chloral hydrate (3.5% in saline, 1ml/100g). The electrophysiology was performed by Dr Gal Richter-Levin in the Department of Psychology, University of Haifa, Israel according to the published protocols for LTP induction with Theta Burst Stimulation (TBS) (Akirav and Richter-Levin, 1999) and High Frequency Stimulation (HFS) (Richter-Levin, Canevari and Bliss, 1998). (Figure 2.1) The electron microscopy, morphological and morphometric studies were performed by Elaine Harrison at the Open University, Milton Keynes.

2.1.2 High Frequency Stimulation

High frequency stimulation (100-400Hz) of the presynaptic neuron, or tetanic stimulation, is commonly used to induce LTP in the laboratory. In stimulated cells, a high-frequency train of action potentials is followed by a period during which action potentials produce successively larger postsynaptic potentials or potentiation. (Figure 2.2) To establish a baseline or control the presynaptic

neuron is stimulated at a steady rate and the presynaptic neuron is then stimulated for several seconds at a higher rate leading to potentiation.

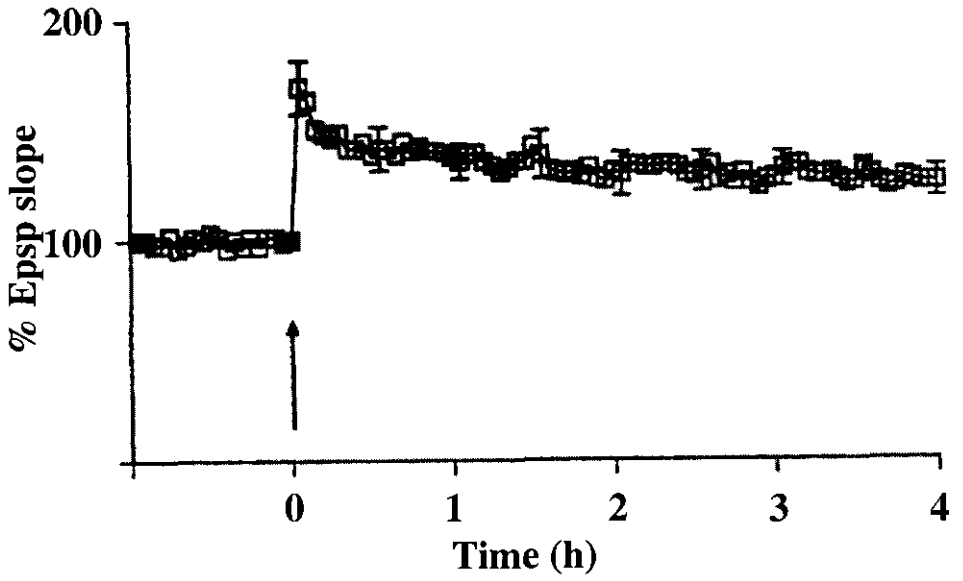

Figure 2.1 A representative graph of the potentiation induced by High frequency or Theta burst stimulation (arrow). % EPSP slope in rat (n=5). The degree of potentiation was assessed before perfusion.

2.1.3 Theta burst stimulation

The hippocampal theta rhythm with a frequency range of 4-12 Hz is one of the largest, most regular EEG rhythms in the rat brain (Skaggs et al 1996) and was a starting point in the search for patterns of naturally occurring activity that produce LTP. Indeed robust LTP can be induced by using stimulus patterns that mimic neuronal activity during theta rhythm. Unlike the long trains of tetanic stimulation, short bursts are sufficient to induce LTP when the bursts are separated by the period of the theta rhythm (approx 200ms). (Figure 2.3) Shorter or longer interburst intervals produce smaller degrees of synaptic change or long-term depression (LTD) (Larson 1986b).

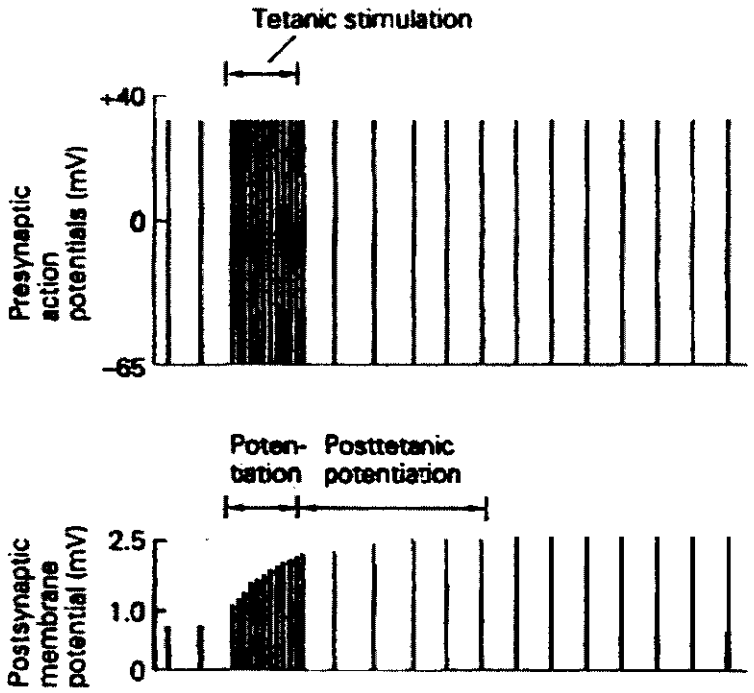

Figure 2.2 The induction of LTP with high frequency stimulation. Long trains of tetanic stimulation to an afferent or presynaptic neuron produce a gradual increase in the amplitude of postsynaptic potentials. Each presynaptic and postsynaptic potential appears as a line indicating its amplitude. Eventually, after weeks in some cases, the postsynaptic potentials decline. After Kandel *et al.*, 2000

The following experiments were performed and the degree of potentiation in each animal, as demonstrated by the % EPSP slope, was monitored for 45-60min post induction depending on the experimental protocol.

1. LTP was induced via theta burst stimulation (TBS) to the perforant path and the animals were sacrificed 45min after LTP induction – within the period of LTP that does not require protein synthesis. Animals demonstrating levels of potentiation in the 130-160% range were taken for perfusion. Five animals fulfilled the criteria.

2. LTP was induced by TBS to the perforant path. The degree of LTP was monitored for one hour and then the animals allowed to recover. The degree of LTP was measured 24h later and again animals demonstrating levels of

potentiation in the 130-160% range were taken for perfusion. Five animals fulfilled the criteria.

3. In order to ensure that putative changes in morphological parameters could be generalised to LTP per se and not to a particular form of LTP induction. LTP was induced by HFS to the perforant path the degree of LTP was assessed as in 2 above and the animals were sacrificed 24h later. Five animals fulfilled the criteria.

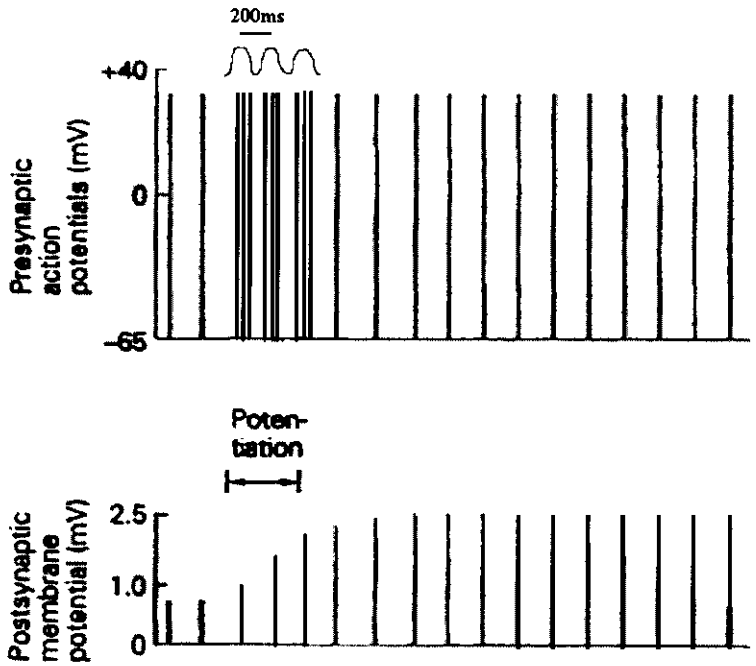

Figure 2.3 The induction of LTP with Theta burst stimulation. Short bursts of stimulation with an interburst interval of 200ms (mimicking theta rhythm), to an afferent or presynaptic neuron produce a gradual increase in the amplitude of postsynaptic potentials. Each presynaptic and postsynaptic potential appears as a line indicating its amplitude. After Kandel *et al.*, 2000

The experimental design included two groups of within-animal control: the contralateral, non-potentiated hemisphere (main control), and the inner molecular layer of the ipsilateral dentate gyrus where the density of perforant path synapses

is known to be negligibly low (Claiborne, *et al.* 1990; Desmond and Levy 1982). The hippocampi from both potentiated, and non-potentiated hemispheres, were dissected (Section 2.2.3) and coded so that all subsequent analyses were carried out blind.

2.2 Tissue preparation

2.2.1 Introduction

In any study that uses microscopy, the quality of fixation of the tissue to preserve the structures of interest is paramount. This is achieved by chemical treatment that terminates the metabolic processes, stabilises components in the cell, and can be quite selective. The most widely used system for ultrastructural analysis of tissue by electron microscopy, is a double fixation with buffered aldehydes (glutaraldehyde and paraformaldehyde) that react primarily with proteins, stabilising the tissue by cross-linkage. This is followed by post-fixation of the dissected region of interest in osmium tetroxide that reacts with various components, but especially unsaturated lipids. During this treatment the blocks of tissue will turn black, harden considerably and become brittle. Such a protocol is preferred because it causes a very fine precipitation of protein and permits a high resolution without appreciable distortion of structure.

After the tissue is fixed it must be sectioned and the slices cut thin enough to transmit electrons and allow clarity of detail. To facilitate sectioning the tissue must be infiltrated with an epoxy resin that can be polymerised (by heat) to become solid. This process has some associated problems because the alcohols used to dehydrate the blocks of tissue before infiltration can extract fat, coagulate protein and cause other chemical changes in the tissue.

2.2.2 Perfusion

After the appropriate time courses each animal was anaesthetised with chloral hydrate (3.5% in saline, 1 ml/100g) by intraperitoneal injection and perfused with a solution of 2% paraformaldehyde and 2% glutaraldehyde in cacodylate buffer at pH 7.4. The animals in the 45-minute experiment were already anaesthetised.

The animal was placed on a dissecting board in a deep dish and the skin and fur was taken back. The peritoneum was opened and, after the rib cage was cut away at each side to expose the heart, the pericardial membrane was removed. The left ventricle was then punctured with a fine needle attached to the tubing of a peristaltic pump and pushed well into the aorta leaving the heart. After clamping the descending aorta, to restrict perfusion to the head and upper limbs, the right atrium was opened to allow blood and fixative to eventually be released from the body. Approximately 50mls of 0.9% saline solution were initially perfused, at a rate of 7mls per minute, to prevent blood clots forming when the 200mls of fixative was pumped into the animal.

After perfusion, the animal was decapitated and the brain excised by penetrating the skull with small bone cutting instruments. The perfused brain should be cream coloured and firm however, all the brains were placed in 20mls of fixative for 24h before dissection to ensure complete fixation.

2.2.3 Dissection

The hippocampus from each hemisphere was dissected by firstly cutting the brain laterally along the mid-line. The hippocampal formation was detached and 1mm saggital slabs, across the entire dorsal hippocampus (~4 mm from the midline), were dissected. The tissue was then trimmed to leave a block containing

CA1, CA3, and dentate gyrus that underwent further fixation and embedding for electron microscopy.

2.2.4 Fixation and embedding for electron microscopy

The tissue slabs were washed in 0.1M sodium cacodylate buffer for 30 min with several changes of buffer and then fixed with 1% osmium tetroxide in buffer, for one hour, at room temperature. The tissue was again washed in buffer for 10 min to remove the fixative and then dehydrated with a series of acetone solutions of increasing concentrations.

Dehydration:

30% Acetone 10 min

50% Acetone 20 min

70% Acetone 20 min

90% Acetone 20 min

100% Acetone, 3 x 10-20 min

100% Acetone (+ molecular sieve) 10-20 min

The hippocampal slabs were then slowly infiltrated with Epon resin, over two days, by initially adding Epon with equal volumes of acetone, allowing the acetone to evaporate, and then fresh 100% Epon. The tissue was then placed in the bottom of flat-bottomed beem capsules, in the required orientation, the capsules filled with fresh Epon and allowed to polymerise overnight at 60°C.

2.3 Electron microscopy

2.3.1 Sectioning

After polymerisation, the blocks were trimmed to remove excess resin and expose the hippocampal formation (Figure 2.4). For stereological assessment of granule cell density, the embedded tissue blocks were cut to collect five to eight serial, 2 μm thick, transverse hippocampal sections containing dentate gyrus. These were stained with toluidine blue and analysed using a modified disector as described below. For electron microscopy, the block was trimmed further to the region of interest, serial ultrathin (~80 nm) sections were cut (to include the entire molecular layer) and collected on carbon-pioloform coated slot grids. The sections were stained with uranyl acetate (Leica Ltd, England) for 50 min at 35°C and lead citrate (Leica Ltd, England) for 10 min at 20°C in an automatic LKB Ultrastainer.

2.3.2 Image acquisition

Digital images of the sections were acquired from a JEOL 1010 transmission electron microscope (Figure 2.5) using a Kodak Megaplus digital camera and stored on magneto-optical discs using a Macintosh Quadra 950 desktop computer equipped with a Perceptics PTDCI frame grabber board (Pixels Tools Digital Camera Interface).

The area for analysis was chosen for each animal by using the large viewing screen of the microscope (~12K) to measure equal distances from the granule cell layer of the dentate gyrus. Cell nuclei were selected at random, along the length of the suprapyramidal blade of the dentate gyrus, until 12 pairs of images were collected from two serial sections. (Figure 2.5) The stage controller on the Joel 1010, that allows co-ordinates to be stored and retrieved easily, greatly enhanced

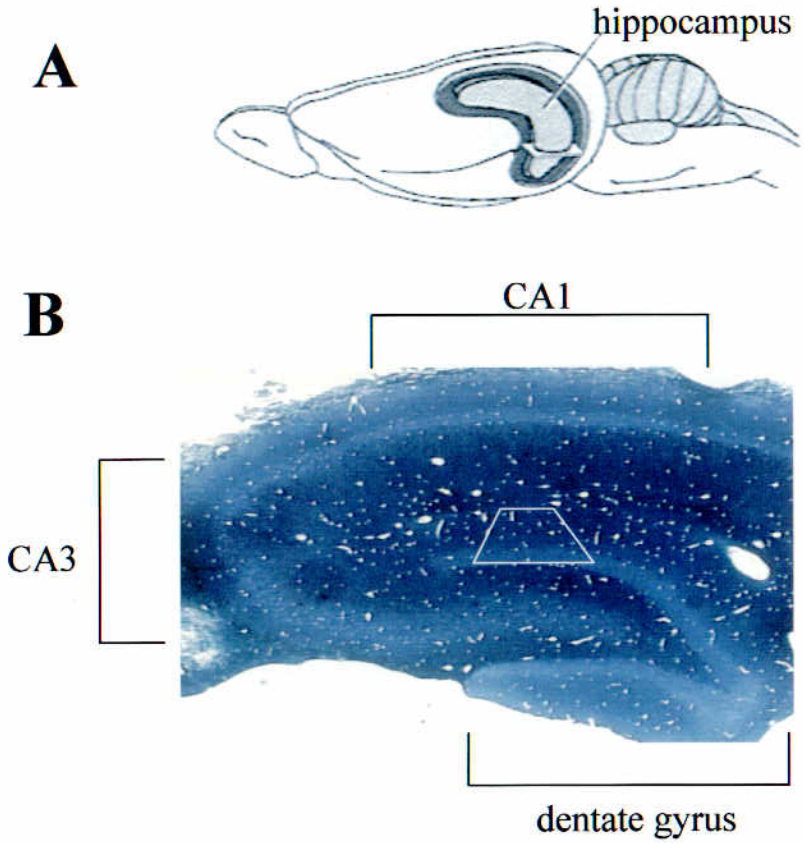

Figure 2.4 Dissection of the hippocampus.

(A) Saggital slices from the dissected dorsal hippocampus were prepared for electron microscopy and semithin, ultramicrotome sections were stained with toluidine blue (B), to identify the hippocampal regions of interest, before further trimming (white trapezium)

this process. The path of the electron beam could clearly be identified due to volatilisation of the resin (Figure 2.6) and low-range magnification images

(~x500) were also taken to ensure the correct location. i.e. Images were captured at a distance of 60-80 μm for the medial molecular layer and 30-40 μm for the inner molecular layer from the proximal edge of the granule cell layer. (Rusakov *et al.* 1997a).

2.3.3 Estimation of ultrathin section thickness.

Section thickness (t) was determined by measuring electron scattering in the section and comparing the result with a standard test curve (De Groot 1988). In such a curve the relative electron transmission (RET) in sections of various thickness is plotted against 'standard' thickness values of the same sections. Each

curve is valid only for a particular embedding resin and a particular setting of the electron microscope. In this instance measurements were carried out at an accelerating voltage of 80Kv and an electron beam size of spot size 2.

The electron scattering was determined directly in the electron microscope by measuring the electron current on the viewing screen with the exposure metre. Measurements of the difference in electron scattering between the section on the support film Es (s) - an area of empty resin, e.g. a blood vessel - and the support film ES (f) were used to calculate RET.

$$R.E.T = (ES\ (s) / ES\ (f)) \times 100$$

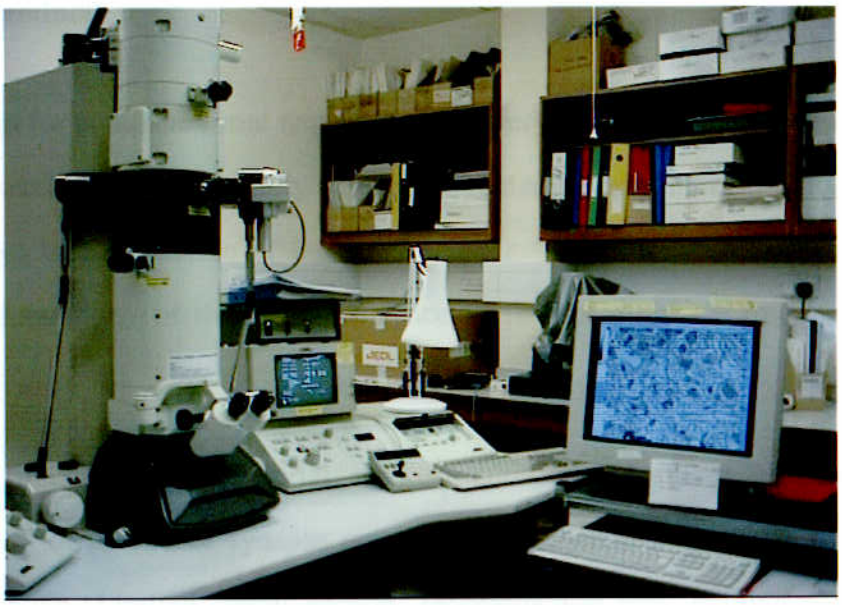

Figure 2.5 The Joel 1010 transmission electron microscope.

Digital images of the sections were acquired from a JEOL 1010 transmission electron microscope using a Kodak Megaplus digital camera and stored on magneto-optical discs using a Macintosh Quadra 950 desktop computer equipped with a Perceptics PTDCI frame grabber board (Pixels Tools Digital Camera Interface).

Figure 2.6 Volatilisation of resin by the electron beam of the Joel 1010 microscope.

The path of the electron beam can clearly be identified due to volatilisation of the resin by the electron beam. Low-range magnification images (x500) were taken to ensure the correct location for image capture.

2.4 Image analysis

2.4.1 Introduction

Except for complete serial reconstruction, every study that reports neuron or synaptic counts in histologically sectioned material determines numbers of counted objects in a fraction of a reference space. The process of counting the objects and sampling of the reference space varies but there are four possible approaches.

The first is complete serial reconstruction, which gives an accurate determination of neuron or synapse numbers but is inefficient because it is too labour intensive. Limited, serial section, reconstruction may involve counting spines along measured lengths of dendrites in thick sections or, using serial, or interrupted electron micrographs for synaptic counts. These methods were considered too inefficient for this study.

The second method involves profile counting, but the number of profiles is being estimated, rather than the number of cells and synapses. If numbers of profiles are to accurately estimate numbers of cells or synapses, each profile must represent a cell or synapse uniquely. Usually, there are more profiles than cells or synapses because the latter are split in the process of histological sectioning and changing section thickness or size of the objects can also change profile number. Total profile numbers in a reference space is estimated by counting profiles at constant intervals through the reference space and multiplying by the interval (e.g. count profiles in every 10^{th} section and then multiply by 10).

Rather than estimating profile numbers, it is more common to estimate densities (number of profiles per unit of size, usually area) or density ratios. These areal densities are determined by counting profiles per unit area (number of profiles per mm^2, per slide etc). Density ratios are calculated from these areal

densities in the control and experimental situation (e.g. numbers of labelled profiles compared to all profiles mm^{-2}). Proportional changes are of interest and not the numbers themselves and the assumption is that changes in profile densities or ratios indicate changes in cell and synapse number.

Nevertheless, cells and synapses can change in size or shape after an event that may modify profile densities and ratios but may be unrelated to changes in cell and synapse number. Furthermore, if a specific population of cells or synapses is lost the resultant change in profile densities and ratios may be disproportionate to alterations in cell or synapse numbers. For example, large cell loss leads to a considerable decrease in profile numbers because large cells are sectioned into more profiles than small cells.

The reference space may also change, perhaps due to oedema, and this changes densities and ratios, even if cell or synapse numbers are constant. Such effects may cause biases and these may balance themselves out but other investigators can be unaware unless the counts are calibrated i.e. make estimations of known populations with the chosen method (Coggeshall *et al.* 1990). Since the effects on synapse size etc of LTP is one of major interest in this investigation this method of counting was disregarded.

Similarly, assumption-based methods make assumptions that allow profiles counts to be converted to cell or synapse numbers. Usually the assumption requires that something else be measured, for example, nuclear diameter. The most frequently used assumption-based method is that of Abercrombie (Abercrombie 1946). In this method, nuclear profile counts (n) are multiplied by mean nuclear diameter (D) divided by mean nuclear diameter plus section thickness (T) to yield neuron number (N).

$$N = (n \times D) / (D + T)$$

Some of these assumptions are that nuclei are spherical, that one can recognise any fragment of a nucleus or synapse sectioned by the microtome knife and that sections are perfectly smooth. The reasoning is sound if the assumptions are met but this is extremely unlikely and these methods tend to be inaccurate.

Finally, stereological methods provide unbiased estimates of cell and synapse numbers relatively efficiently, and they are used to extrapolate 3-D structural quantities (real volumes, surface areas, lengths and numbers) from simple counts made on 2D slice images. The images may take various forms, e.g. physical or optical sections, but they must be sampled randomly, in orientation and /or position, if valid estimates are to be made. Unique associated points are defined by the investigator and can include cell bodies, nuclei or postsynaptic densities.

In this study, an unbiased stereological approach was preferred because, as described above, model or assumption-based methods introduce unknown bias and therefore the validity of biological conclusions is unknown. Specifically, the physical disector method was employed (Sterio 1984) which relies on pairs of parallel sections and the identification and counting of 'particles' by appropriate criteria. This method depends on particle shape and it must be possible to identify all particle profiles on sections that belong to the same parent particle. The disector method yields numerical density rather than number (N) itself. In consequence, estimates are sensitive to preparation artefacts such as fixation distortion (shrinkage or swelling).

2.4.2 Disector Method

The acquired images from the electron microscope were analysed using NIH Image 1.55 software that also allowed the images to be enhanced, by altering contrast, to provide clearer identification of synapses etc. In each animal, disector

windows (7 x 5 μm) were arranged in each of the12 pairs of adjacent ultrathin sections within the medial, or inner molecular layer, from each hemisphere, using an unbiased sampling frame (Braendgaar and Gundersen 1986). Paired images from the serial sections could then be viewed side by side on the large, 20-inch monitor of a Macintosh Quadra 950 computer for analysis.

Only those synapses that appeared in the unbiased counting frame on one section (the *reference* plane) but not on its partner (the *look-up* plane) were counted. Synapses were identified by the presence of a postsynaptic density, indicating an apposition zone (AZ), and at least three presynaptic vesicles. Several unbiased counting rules are available for deciding whether or not synaptic profiles can be regarded as being included in the counting frame on the reference plane (Gunderson and Jensen 1987). In these studies, two sides of the counting frame were considered to be forbidden and any synapse touching these forbidden lines was not counted. (Figure 2.7)

The number of synapses meeting the required criteria (Q^{-}_{syn}) is contained within the volume of the disector. This volume is equal to the area of the counting frame (A) multiplied by the distance between the planes or sections i.e. the thickness of the sections (t). Since these specimens have been sampled by multiple disectors the mean synaptic numerical density N_{Vsyn} can be calculated by the equation:

$$N_{Vsyn} = \Sigma Q^{-}_{syn} / tA$$

Where 't' is the thickness of the section and 'A' is the area of the counting frame and ΣQ^{-}_{syn} is the total number of counted synapse profiles that appear only in the nominated section.

The 40-60 synaptic profiles visible in each window were categorised as axodendritic or axospinous synapses and asymmetric or symmetric depending on

the nature of their postsynaptic density (Gray 1959), although, numbers of symmetric synapses were negligible.

2.5 Morphometry

To determine possible changes in synaptic morphology, other than changes in synaptic density, measurements were taken of various parameters in a fixed area of 10 reference planes.

2.5.1 Lateral surface area

An important synaptic parameter analysed in the present study was the lateral surface area (i.e., membrane area) of AZs per unit tissue volume, or the volume density of AZ areas, S_V (Desmond and Levy 1986b). Estimating this quantity from single section micrographs does not rely on any assumptions about shapes or sizes of AZs and takes the form:

$$S_V = 4/\pi (L_A)$$

Where $\langle L_A \rangle$ is the mean total length of AZ profiles per unit area of sections.

L_A was estimated using the sampling windows described above and because the thickness of ultrathin sections was kept unchanged throughout experimental samples, a potential small over-estimation of $\langle L_A \rangle$ arising from a non-zero thickness of sections was neglected. In each window, all identified AZ profiles (10-20 in each window) were carefully marked as curvilinear binary (white) segments using cursor-editing tools, and the background image was 'cut off '. The total length of the remaining segments was automatically measured and stored to a file using *NIH Image* routines thus giving an estimate of L_A. Combining estimates of S_V and N_V allowed the unbiased estimation of the mean lateral area of individual AZs, S_{AZ}. $S_{AZ} = S_V / N_V$

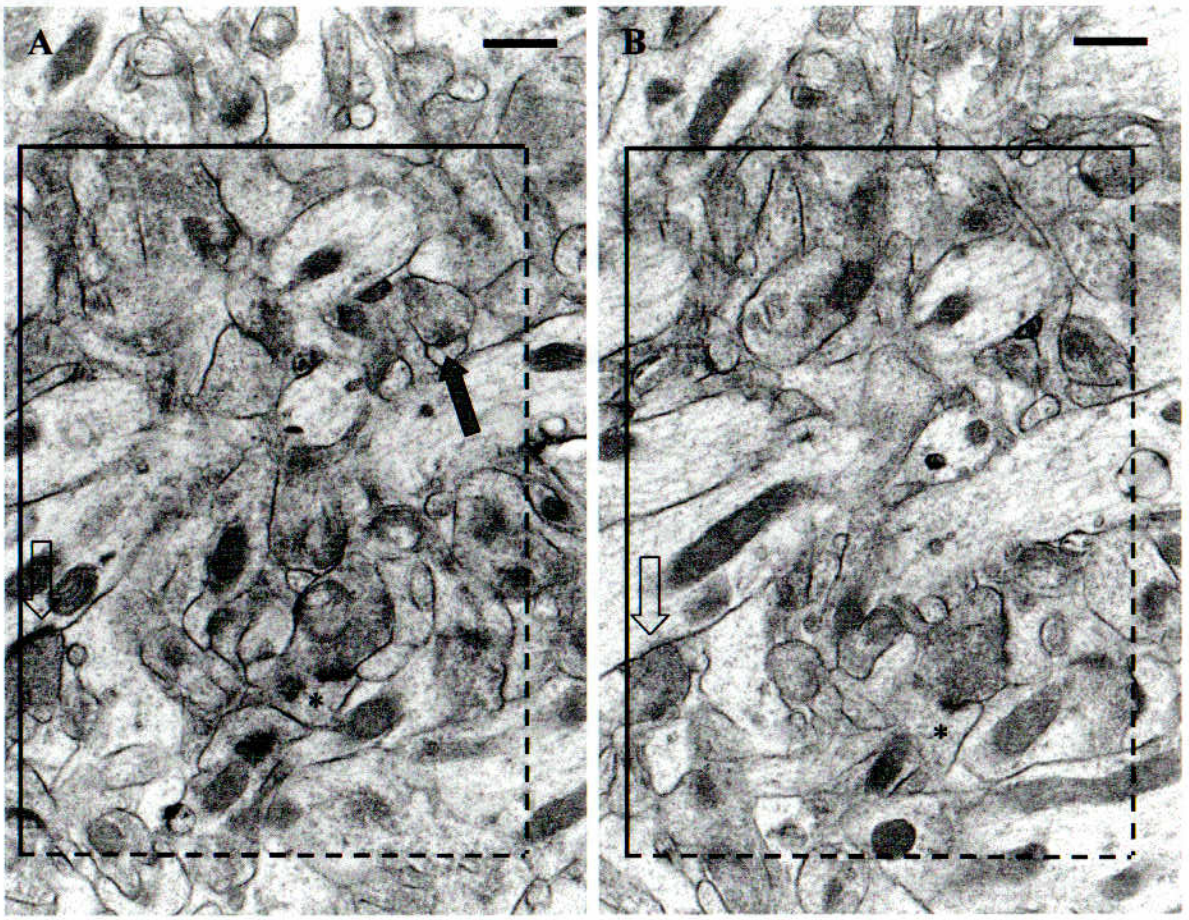

Figure 2.7 The Disector Method

Only those synapses that appeared in the unbiased counting frame on one section, A (the *reference* plane) but not on its partner B, (the *look-up* plane) were counted (grey arrow). When a synapse appeared in both sections it was not counted (*). Two sides of the counting frame were considered to be forbidden and any synapse touching these forbidden lines was not counted. Synapses touching the other sides of the counting frame were counted (open arrows). Magnification x12k, bar = 500nm.

2.5.2 Mean projected synaptic height

The mean projected synapse height H_{syn}, a measure of the size of the postsynaptic density, can be measured using the disector method from

$$H_{syn} = (\Sigma Q_{syn} / \Sigma Q^{-}_{syn})\, t$$

Where Q is the number of synapses in the look-up plane and Q^{-} the number in the reference plane. t is the thickness of the section.

2.5.3 Perforated, concave and non-concave synapses

In each of 10 reference planes, synapses with segmented postsynaptic densities were identified and the number recorded. Similarly, synapses were classified as concave, if the postsynaptic membrane curved towards the presynaptic bouton, or not. (Figure 2.8). This was established by comparing the membrane with a straight line drawn through the middle of the synaptic cleft.

2.6 Neuronal volume determination

2.6.1 Stereological correction 'per neuron' using disector

Because numerical synaptic density also depends on the 'reference volume' of the tissue (Braendgaar and Gundersen 1986), it was important to assess possible dentate volume changes associated with LTP. Ideally, one would measure whole hippocampal volume using systematic sampling based on the Calvalieri principle (Geinisman *et al.* 1996). However, since the number of granule cells in the dentate is unlikely to change significantly 24 h after LTP induction, shrinkage or expansion of this hippocampal area would increase, or decrease, respectively, numerical volume densities of the cells.

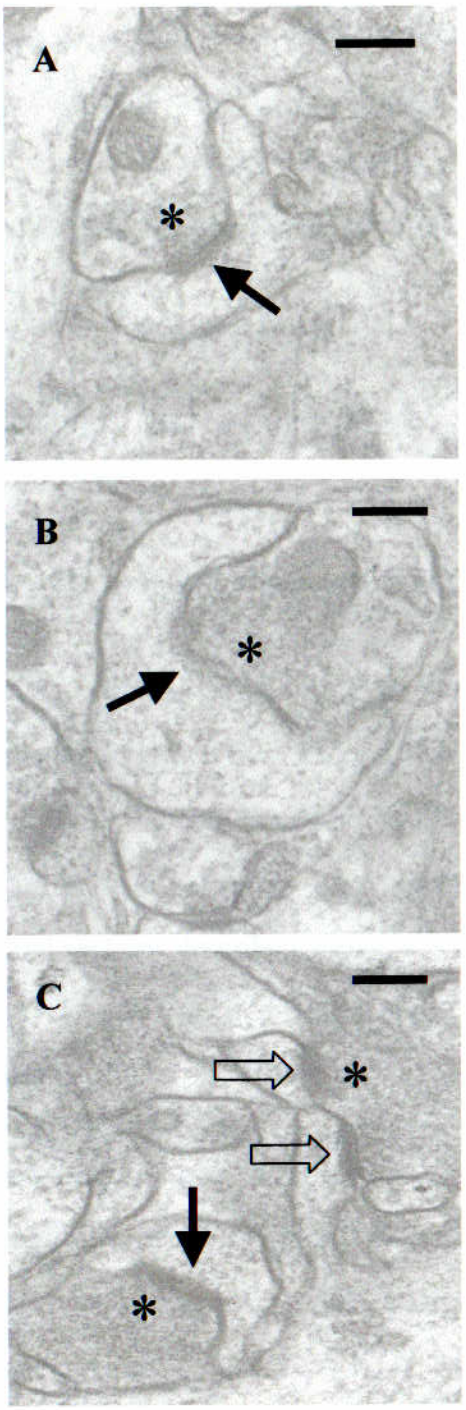

Figure 2.8 Electron micrographs of concave and macular synapses

(A,B) Synapses with concave postsynaptic profiles. (C) Concave synapses and two simple, macular synapses (open arrows) with the the same presynaptic bouton (multiple synapse bouton). The postsynaptic densities are indicated by arrows and the presynaptic boutons by *. Magnification x40k, bar = 200nm

Therefore, comparison of granule cell densities in the control versus potentiated hemisphere (in the area where synaptic images were sampled) would serve as a 'local' volume correction control. Thus, the numerical synaptic density is corrected 'per neuron' where local synaptic density is weighted with respect to local granule cell density (Braendgaar and Gundersen 1986).

$$\text{Number of synapses per neuron} = Nv_{syn} / N$$

Where N is the number of neurons, μm^{-3} and Nv_{syn} is the mean numerical density of synapses, μm^{-3}.

2.6.2 Neuronal cell density counting with image analysis

Images were acquired with the MicroComputer Imaging Device (MCID) system, developed by Imaging Research Inc., Brock University, Ontario, Canada. This system uses a digital CCTV camera to capture images from a light box or a light microscope, in this case an Axiophot light microscope. In two of the toluidine blue stained serial sections described above, 4-6 sequential fragments of the granule cell body layer were viewed in the microscope (magnification ~500x) and captured as image files.

Images taken from adjacent (2 μm thick) sections of dentate were analysed using a stereological design illustrated in Figure 2.9. In each image, an unbiased disector frame was arranged by placing two straight, nearly parallel lines (located at ~230 μm apart) perpendicular to the cell body layer, with the 'exclusion line' (Braendgaar and Gundersen 1986) being one of the borders. The routine was repeated in the adjacent section, disector counts of the cell nuclei were made in each look-up and reference window and displayed simultaneously on the monitor screen (Figure 2.9 A-B).

The mean cell density value D was derived as:

$$D = N_+/sT$$

where $\langle N_+ \rangle$ is the mean number of disector scores (over all windows), T is the section thickness (2 μm), and s stands for the window length along the cell body layer (distance between the lines in Figure 2.9 A-B).

Therefore, D represents the number of cells contained with a parallelepiped of unit area passing through the granule cell layer (Figure 2.9 C-D). In each animal, 4-5 disector pairs of sampling windows, each containing 40-50 profiles of cell nuclei, were examined giving 100-120 disector scores per hemisphere.

2.7 Statistical methods

As each animal had an experimental and control hemisphere the Student t-test paired two sample for means was applied.

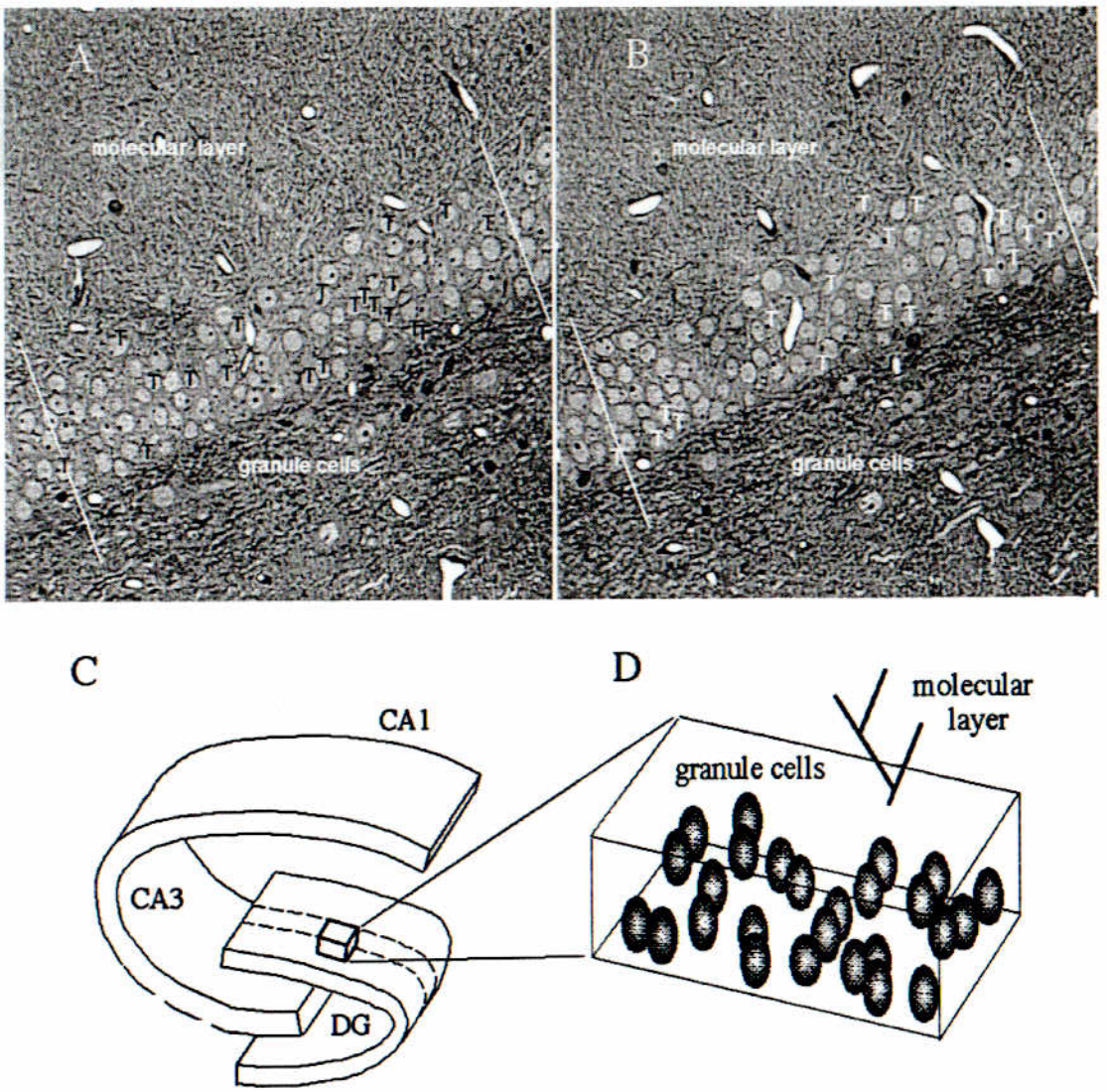

Figure 2.9 Neuronal density estimation using a modified disector method.

Disector counts of cell nuclei were made, between the designated exclusion lines, in each look-up and reference window displayed simultaneously on the monitor screen (A-B). The number of cells contained with a parallelepiped of unit area passing through the granule cell layer (C-D) was then calculated.

Chapter Three Estimation of morphological and morphometric correlates 45 min after the induction of LTP by Theta Burst Stimulation (TBS)

3.1 Introduction

The physiological paradigm of long-term potentiation (LTP) of synaptic transmission in the hippocampus (Bliss and Lomo, 1973) has been extensively studied but the cellular basis of LTP expression (in particular the relative importance of pre- versus postsynaptic components) still remains the subject of considerable debate (Bliss and Lomo, 1973; Larkman and Jack, 1995; Lynch *et al.*, 1990; McNaughton, 1993; Nicoll and Malenka, 1995). Whilst it is reasonable to assume that long-lasting changes of synaptic efficacy must be supported by structural alterations no universal agreement exists concerning the significance of these alterations. However, the plausibility of real-time, function-dependent changes in the appearance of living synaptic elements (dendritic spines) has been demonstrated *in vitro* (Hosokawa *et al.*, 1995; Segal, 1995).

Although there have been many investigations of morphological correlates of synaptic plasticity in the first hour post–tetanisation, the results are disparate. *In vivo* investigations of the dentate gyrus after stimulation of the perforant path (Geinisman *et al.*, 1991,1993) have reported some changes in synapse number and/or structure as early as 2 min after the induction of LTP (Van Harreveld and Fifkova, 1975; Fifkova and Anderson, 1982; Desmond and Levy, 1986a,b; Desmond and Levy, 1990;

Trommald, *et al.* 1990). Various changes have also been reported in the hippocampal CA1 region of brain slices after electrical or chemically induced LTP (Lee *et al.*, 1980; Chang and Greenough, 1984; Buchs and Muller, 1996; Toni *et al.*, 1999). Many of these studies were single section analyses, therefore liable to the inaccuracies outlined previously (Coggeshall *et al,*. 1990), and the data from unbiased serial reconstruction may be more reliable (Sorra and Harris, 1998; Trommald and Hulleberg, 1997).

At the electron microscope level, a large proportion of ultrastructural studies concerning hippocampal LTP has explored a relatively homogeneous population of perforant path synapses on granule cell dendrites (confined mostly to the medial molecular layer of the dentate gyrus). Van Harreveld and Fifkova (1975) demonstrated an increased width of dendritic spine profiles in the potentiated tissue 6min to 23h after the induction of LTP. Wenzel *et al.* (1980) presented a set of synaptic changes induced by high-frequency stimulation of the perforant path. In parallel, it was reported that high frequency stimulation of the perforant path results in an increased number of synaptic vesicles located in the proximity of the AZ membrane (Applegate and Landfield, 1988; Desmond and Levy, 1988), and in formation of spinule-like membrane invaginations into presynaptic terminals (Schuster *et al.*, 1990). In area CA1 of the hippocampus, a profound (up to 48%) increase in the number of axodendritic synapses was found following the induction of LTP with high-frequency stimulation *in vitro* (Chang and Greenough, 1984).

Most *in vivo* studies of morphological changes in the molecular layer of the dentate gyrus have been performed after high frequency stimulation of the perforant path (Geinisman *et al.*, 1991; Geinisman *et al.*, 1996; Weeks *et al.*, 1998; Weeks *et al.*, 1999). However, another effective protocol for inducing robust and persistent LTP is Theta burst stimulation (TBS), which is designed to mimic the firing patterns of hippocampal neurons recorded during exploratory behaviour in intact, awake animals. The objectives of this study were twofold. Firstly, to ensure that putative changes in morphological parameters can be generalised to LTP per se and not to a particular

form of LTP induction, by testing changes in morphology with alternative stimulation paradigms, i.e. TBS. Secondly, to attempt to verify results from some 'single section' analyses by the use of unbiased stereological methods.

The experimental design included two groups of within-animal control: the contralateral, non-potentiated hemisphere (main control), and the inner molecular layer of the ipsilateral dentate gyrus where the density of perforant path synapses is known to be negligibly low (Claiborne, *et al.* 1990; Desmond and Levy 1982). The hippocampi from both potentiated, and non-potentiated hemispheres, were dissected as detailed previously and coded so that all subsequent analyses were carried out blind. Low-range magnification images (x500) were also taken to ensure that images were acquired from the correct location: areas irradiated by the electron beam were clearly identified as paler circles, as demonstrated previously (Rusakov, *et al.* 1997a). (Figure 2.3) There were few symmetric, or inhibitory, synapses, identified in this study and the results reflect the density and morphometry of asymmetric synapses.

3.2 Results

3.2.1 Mean numerical synaptic density

There were no significant differences in the mean numerical synaptic density of axodendritic or axospinous synapses in the middle or inner molecular layers of the dentate gyrus. In the MML the mean axodendritic, synaptic density was 0.14 μm^{-3} in the potentiated hemisphere and 0.17 μm^{-3} in the control hemisphere ($p<0.21$). (Figure 3.1) In the IML the results were similar with a synaptic density of 0.16 μm^{-3} in the potentiated hemisphere and 0.17 μm^{-3} in the control hemisphere ($p<0.42$). (Figure 3.2)

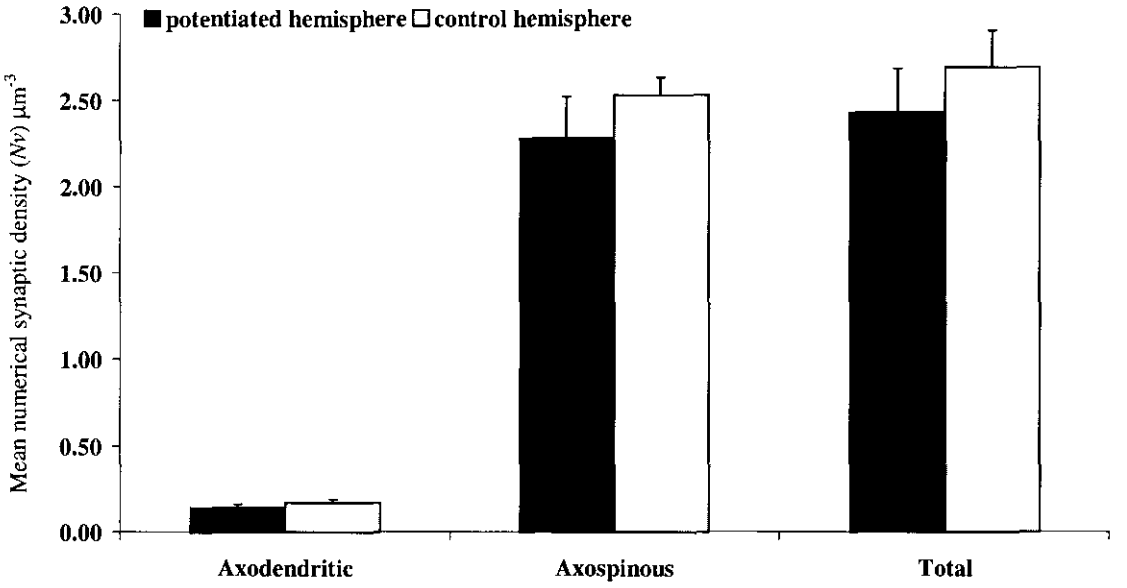

Figure 3.1 Mean numerical synaptic density (*Nv*) of synapses in the middle molecular layer of the dentate gyrus, in potentiated and control hemispheres, 45min after the induction of LTP by TBS. Mean (± S.E.M.) of 5 animals

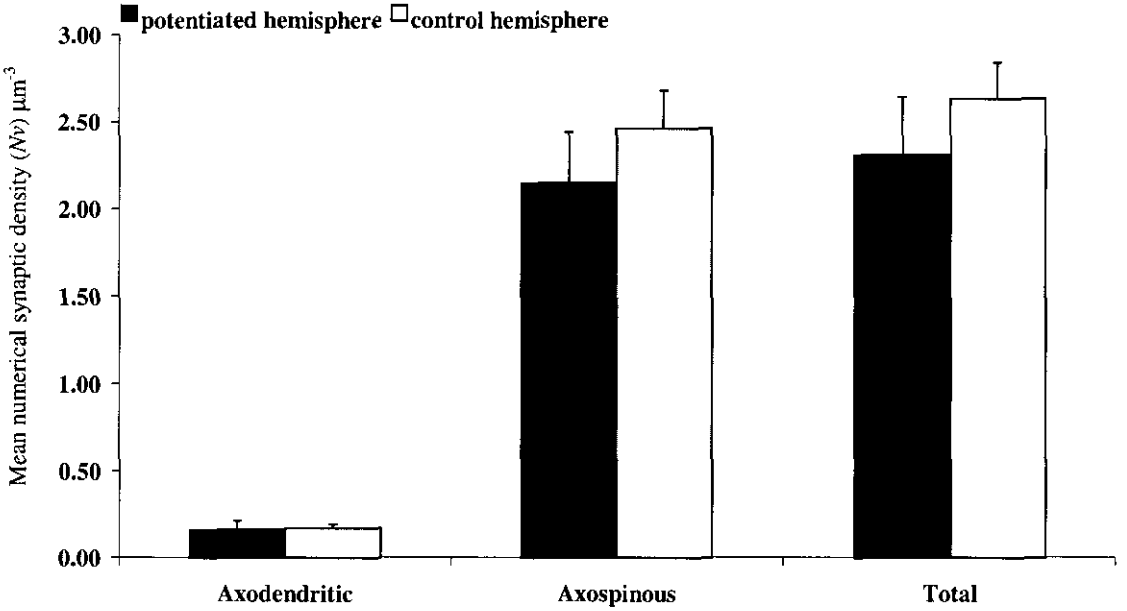

Figure 3.2 Mean numerical synaptic density (*Nv*) of synapses in the inner molecular layer of the dentate gyrus, in potentiated and control hemispheres, 45min after the induction of LTP by TBS. Mean (± S.E.M.) of 5 animals

Mean numerical axospinous synaptic densities of 2.28 μm^{-3} and 2.53 μm^{-3} were determined in the potentiated and control hemispheres in the MML ($p<0.18$). In the IML, the mean numerical density of asymmetric axospinous synapses was 2.15 μm^{-3} in the stimulated hemisphere and 2.46 μm^{-3} in the contralateral hemisphere ($p<0.08$).

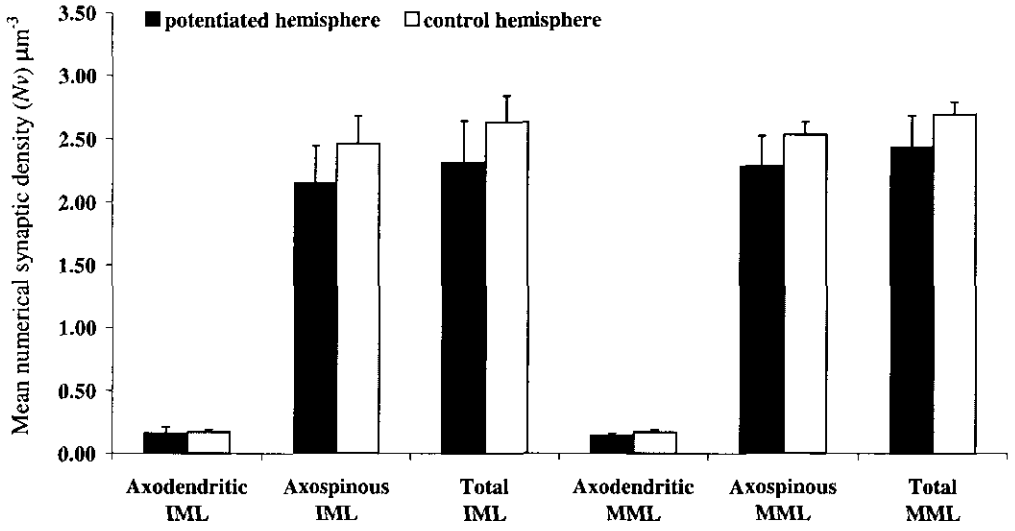

Figure 3.3 Mean numerical synaptic density (*Nv*) of synapses in the inner and middle molecular layers of the dentate gyrus, in potentiated and control hemispheres, 45min after the induction of LTP by TBS. Mean (± S.E.M.) of 5 animals.

There were no significant differences in the mean numerical total synaptic density between the IML and MML in the control hemisphere ($p<0.39$) or the potentiated hemisphere ($p<0.23$). Neither were there significant differences in the axospinous mean numerical synaptic density between the IML and MML in the control hemisphere ($p<0.38$) or the potentiated hemisphere ($p<0.17$). (Figure 3.3)

3.2.2 Neuronal density

The mean neuronal density of the potentiated hemisphere was 0.0087μm^{-3} and 0.0098μm^{-3} in the control hemisphere ($p<0.07$) (Figure 3.4). This difference was not

significant, but is has been suggested that there may there be some swelling in the tissue of the potentiated hemispheres, due to the experimental protocol. Shrinkage or swelling would have a detrimental effect on the accuracy of the mean numerical density results and the corrected synapse per neuron number may be more meaningful. However, shrinkage due to the processing of tissue for electron microscopy has been previously investigated (Rusakov, *et al.* 1998) and shown to be minimal. Since all the tissue in these experiments was from the hippocampus, we must assume that the relative shrinkage was the same for all tissue examined.

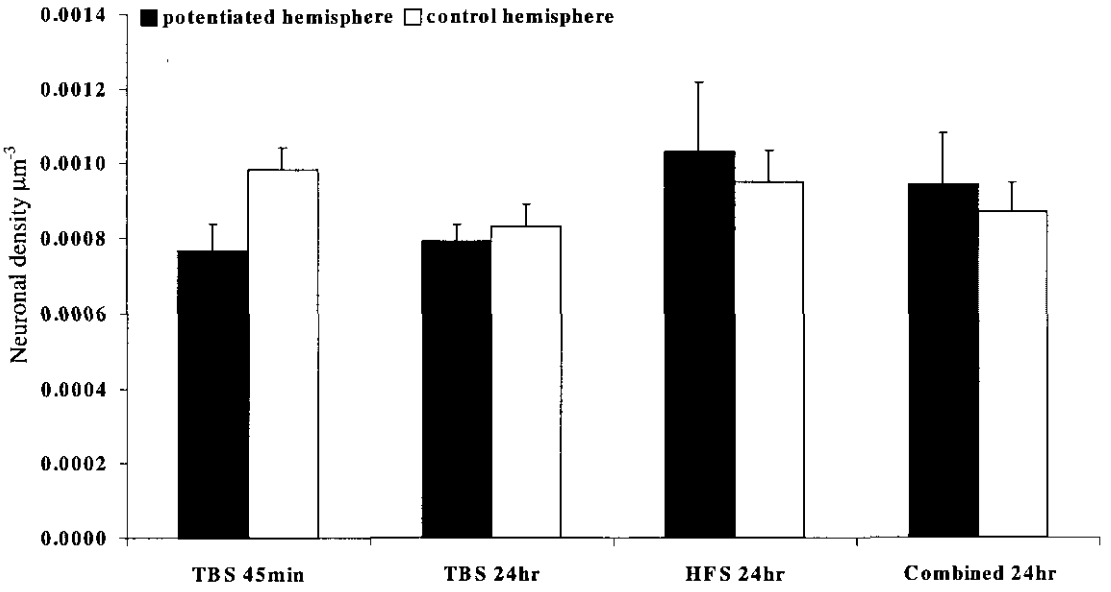

Figure 3.4 Neuronal density per μm^3 in the granule cell layer of the dentate gyrus, at various time points, after the induction of LTP by TBS and HFS. Mean (± S.E.M.) of 5 animals except Combined 24hr where mean (± S.E.M.) of 6 animals.

There were no significant differences in the mean number of synapses per neuron. In the MML (Figure 3.5), there was a mean of 185 axodendritic synapses in the potentiated hemisphere and 170 in the control hemisphere ($p<0.35$). There were 2993 axospinous synapses, versus a control mean of 2576, in the potentiated hemisphere ($p<0.13$).

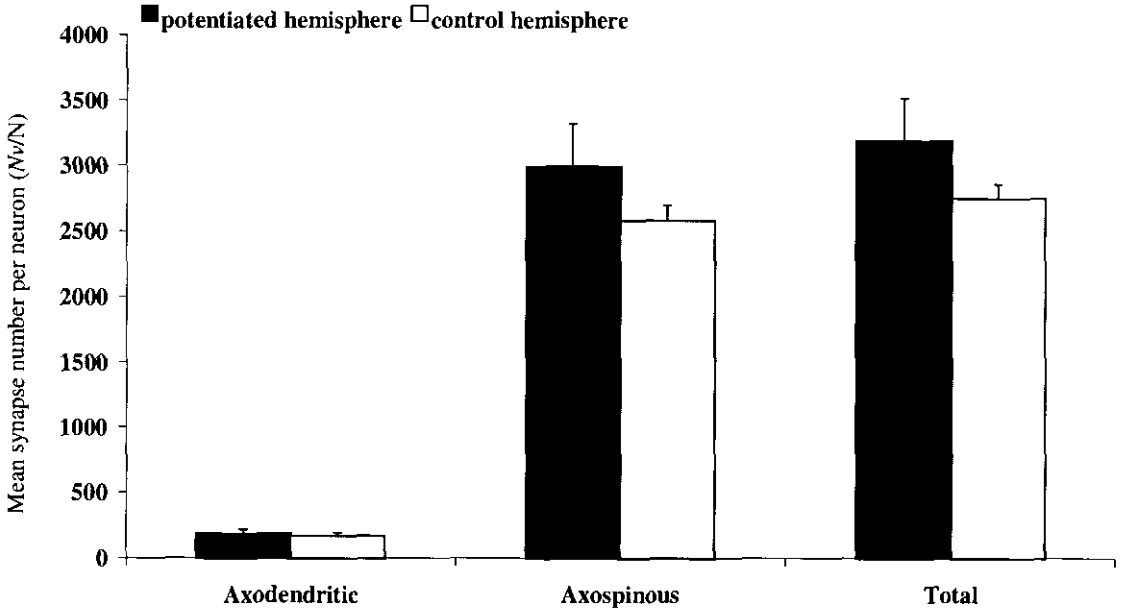

Figure 3.5 Mean synapse number per neuron in the middle molecular layer of the dentate gyrus, in potentiated and control hemispheres, 45min after the induction of LTP by TBS. Mean (± S.E.M.) of 5 animals.

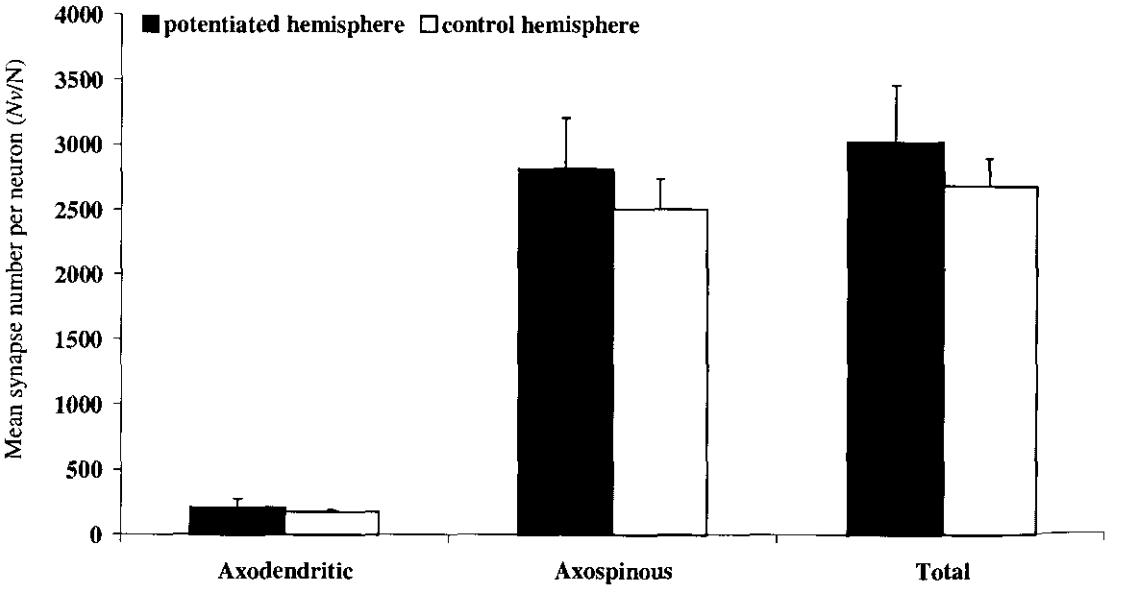

Figure 3.6 Mean synapse number per neuron in the inner molecular layer of the dentate gyrus, in potentiated and control hemispheres, 45min after the induction of LTP by TBS. Mean (± S.E.M.) of 5 animals.

In the IML (Figure 3.6) the mean number of axodendritic synapses per neuron, in the potentiated and control hemispheres, was calculated as 210 and 175 ($p<0.31$) respectively. The mean number of axospinous synapses was 2814 and 2505 ($p<0.15$). Total mean numbers of synapses per neuron were similar in the middle and inner molecular layer, with values of 3185 (MML) and 3024 (IML) in the potentiated hemisphere. In the control hemisphere there was a mean of 2746 synapses per neuron in the MML and 2681 in the IML.

3.2.3 Mean projected synaptic height

There was no significant difference in the mean projected synaptic height of axodendritic synapses in the middle molecular layer, 227nm in the potentiated hemisphere and 211nm in the control ($p<0.43$). Although the axodendritic synapses in the IML appeared to be smaller, again there was no significant difference between hemispheres: 156nm in the potentiated and 148nm in the control ($p<0.38$). (Figure 3.7)

There was a similar trend towards slightly larger axospinous synapses in the potentiated hemisphere in both the MML and IML. In the MML, mean projected synaptic height was calculated as 142nm in the experimental hemisphere and 137nm in the control ($p<0.36$). Mean values of 145nm and 133nm ($p<0.06$) respectively were recorded for the IML of the ipsilateral and contralateral hemispheres. (Figure 3.7)

3.2.4 Volume density of total axospinous AZ area (*Sv*)

In the middle molecular layer, there was no significant difference between the mean volume density of the apposition zone area i.e. $0.14\mu m^2/\mu m^3$ tissue in the potentiated hemisphere, and $0.13\mu m^2/\mu m^3$ in the control hemisphere ($p<0.34$). In the inner third of the molecular layer there was a significant difference between hemispheres with a mean volume density of $0.11\mu m^2/\mu m^3$ in the tetanised hemisphere and $0.12\mu m^2/\mu m^3$ in the control hemisphere ($p<0.03$). (Figure 3.8)

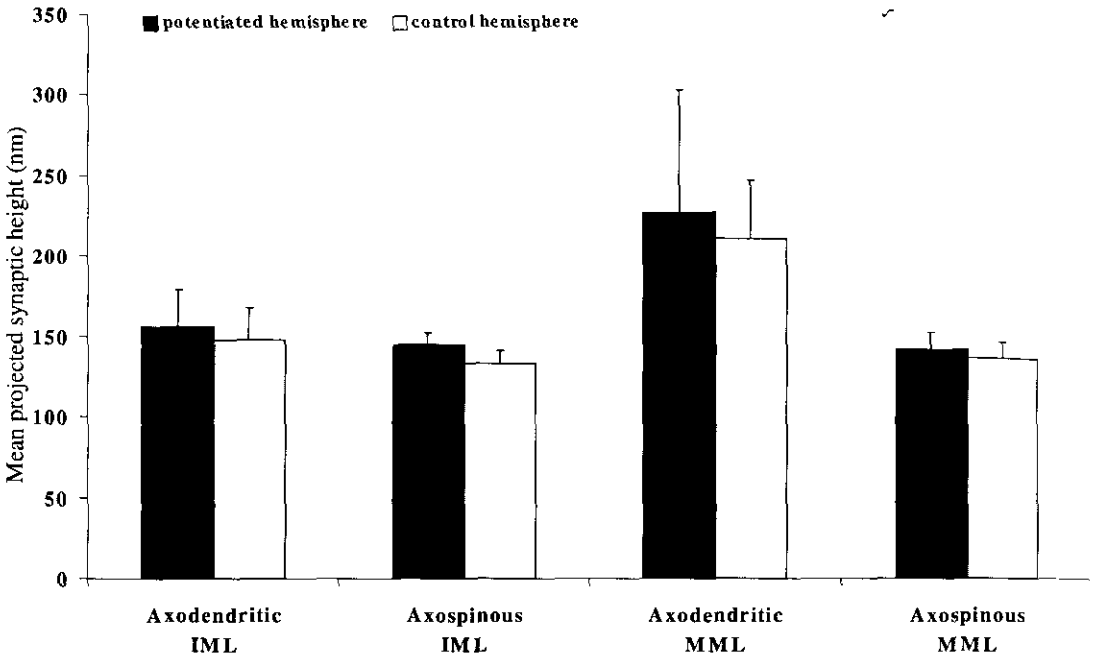

Figure 3.7 Mean projected synaptic height of axospinous and axodendritic synapses, in the inner and middle molecular layers of the dentate gyrus, 45min after the induction of LTP by TBS. Mean (± S.E.M.) of 5 animals.

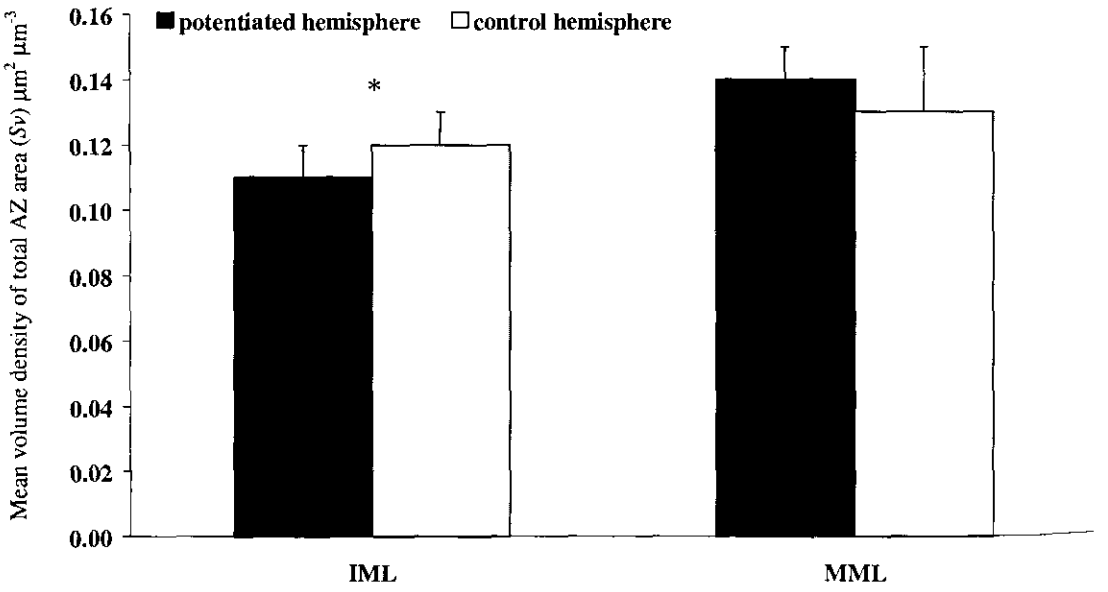

Figure 3.8 Mean volume density of total axospinous apposition zone (AZ) area (*Sv*) in the inner and middle molecular layers of the dentate gyrus, 45min after the induction of LTP by TBS. (* indicates significant difference $p<0.05$). Mean (± S.E.M.) of 5 animals.

3.2.5 Volume density of individual axospinous AZ area

Individual synapses were larger, but not significantly so, in the MML of the tetanised hemisphere with a volume density of 0.06$\mu m^2/\mu m^3$, whilst the mean volume density of synapse in the contralateral hemisphere was 0.05$\mu m^2/\mu m^3$ ($p<0.20$). In the IML the mean volume density of an asymmetric synapse was the same in each hemisphere, 0.05$\mu m^2/\mu m^3$ ($p<0.42$). (Figure 3.9)

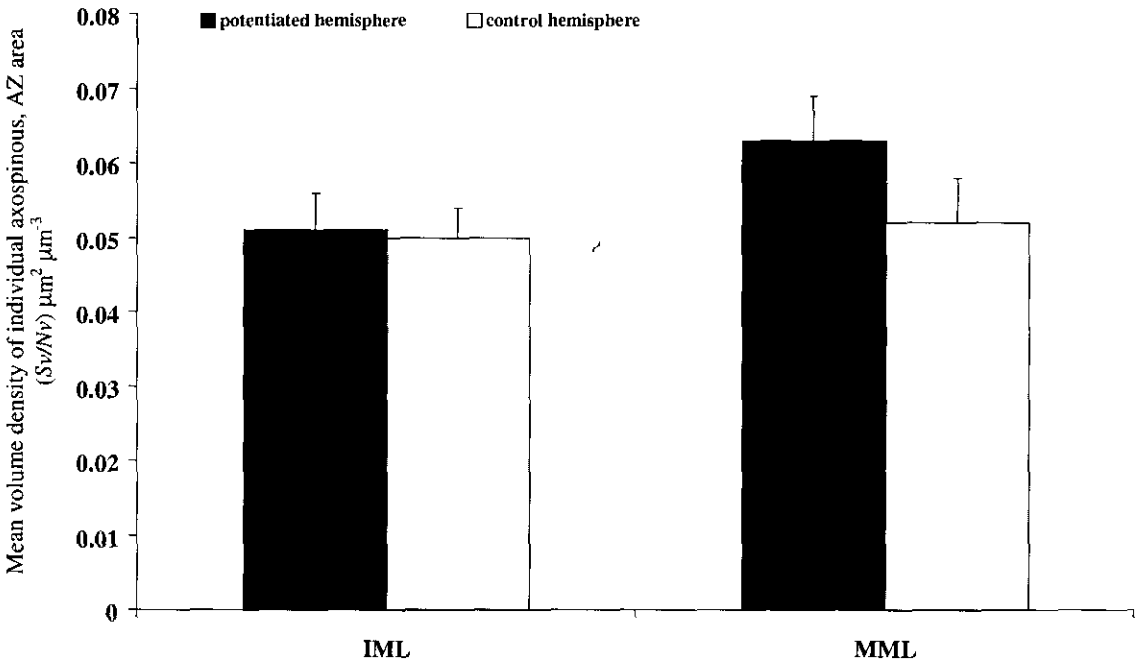

Figure 3.9 Mean volume density of individual axospinous apposition zone (AZ) area (*Sv/Nv*) in the inner and middle molecular layers of the dentate gyrus, 45min after the induction of LTP by TBS. Mean (± S.E.M.) of 5 animals.

3.2.6 Characterisation of synaptic profiles

Each synapse was identified in 10 reference planes, characterised and the means calculated; therefore results represent the mean number of synapses found in a reference area of 350μm^2. A mean of 132.8 (potentiated) and 135.4 (control) synapses were classified in the designated area of the MML. (Figure 3.10) An average of 8.60 (6.42%) perforated synapses were identified in the potentiated hemisphere and 8.40 (6.11%) in the contralateral hemisphere ($p<0.47$). The respective values for synapses

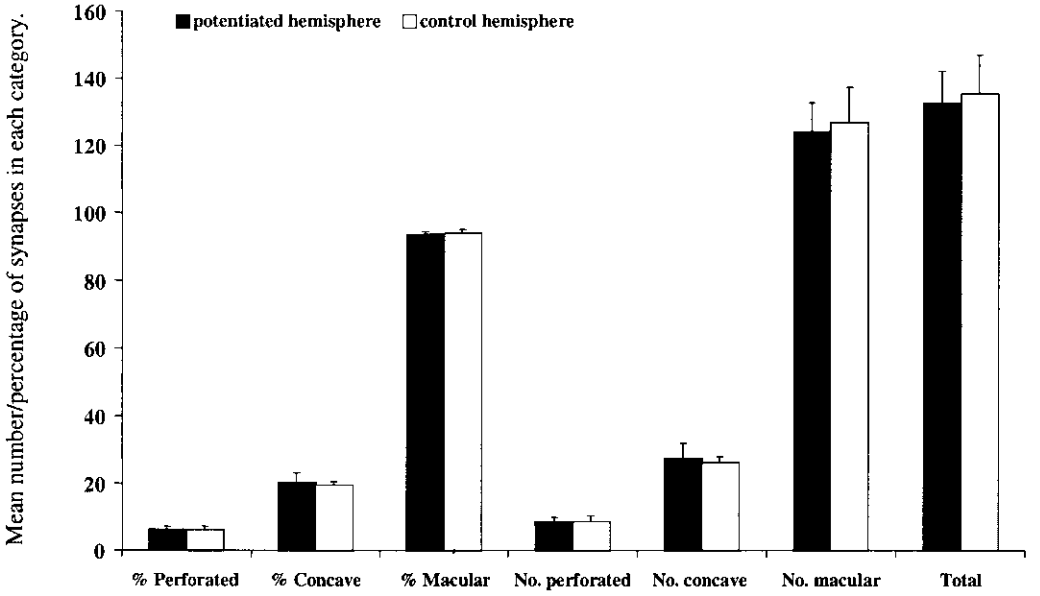

Figure 3.10 Morphology of axospinous synapses in an area of 350μm^2, in the middle molecular layer of the dentate gyrus, 45min after the induction of LTP by TBS. Mean (± S.E.M.) of 5 animals.

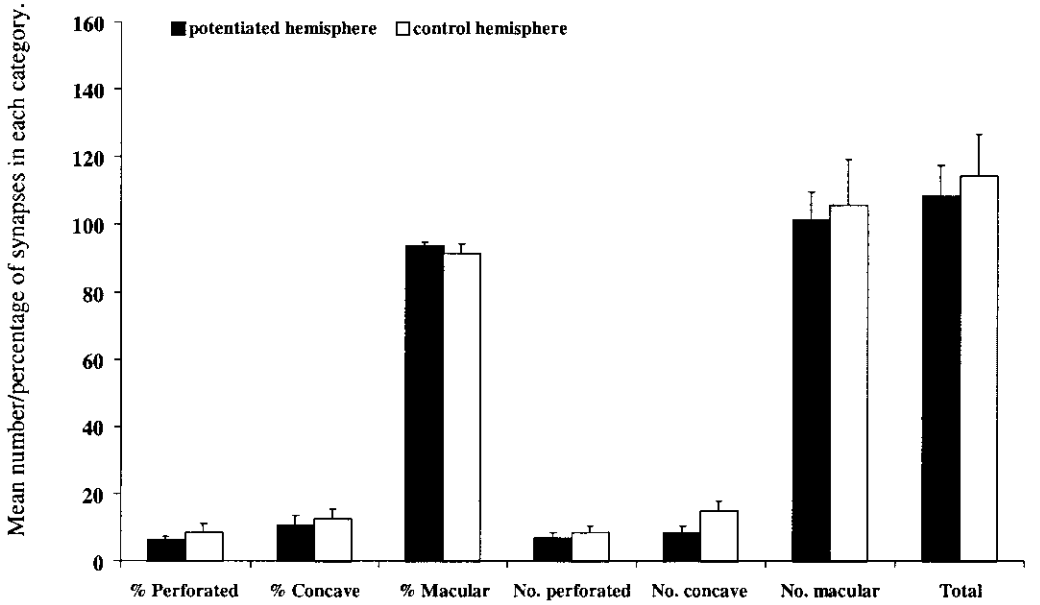

Figure 3.11 Morphology of axospinous synapses in an area of 350μm^2, in the inner molecular layer of the dentate gyrus, 45min after the induction of LTP by TBS. Mean (± S.E.M.) of 5 animals.

with concave profiles were 27.4 (20.24%) and 26.0 (19.42%) ($p<0.39$) and for simple, macular synapses 124.2 (93.58%) and 127.0 (93.89%) ($p<0.37$).

In the IML (Figure 3.11), from a total of 108.4 in the potentiated hemisphere and 114.2 in the contralateral hemisphere there was a mean of 7.0 (6.39%) perforated synapses in the potentiated hemisphere and 8.6 (8.50%) in the contralateral hemisphere ($p<0.32$). A mean of 12.4 (10.70%) concave synapses were identified in the tetanised hemisphere and 13.4 (12.43%) in the control hemisphere ($p<0.44$). Again most of the synapses identified were macular synapses with a mean of 101.4 (93.61%) in the potentiated hemisphere and 105.6 (91.5%) in the control hemisphere ($p< 0.31$).

3.2.6.1 Morphometry of perforated and concave profiles of synaptic active zones

In the MML, the *Nv* of concave synapses was $0.85\mu m^{-3}$ in the potentiated hemisphere and $1.00\mu m^{-3}$ in the control hemisphere ($p<0.27$) and the mean numerical density of perforated synapses was $0.03\mu m^{-3}$ in the potentiated hemisphere and $0.07\mu m^{-3}$ in the control hemisphere ($p<0.18$). (Figure 3.12) Further investigations in the MML, established a mean projected synaptic height of perforated synapses of 493nm in the potentiated hemisphere and 389nm in the contralateral hemisphere ($p<0.10$). Synapses with concave profiles measured 188nm in both the potentiated and control hemispheres ($p<0.50$). (Figure 3.13)

The mean volume density of the total contact area of the spine head of perforated synapses was $0.06\mu m^2,\mu m^{-3}$ in the potentiated hemisphere and $0.05\mu m^2$, μm^3 in the control hemisphere ($p<0.07$). The mean total contact area of spines with concave profiles was $0.18\mu m^2,\mu m^{-3}$ in the potentiated hemisphere and $0.18\mu m^2,\mu m^{-3}$ in the contralateral hemisphere ($p<0.49$). (Figure 3.14)

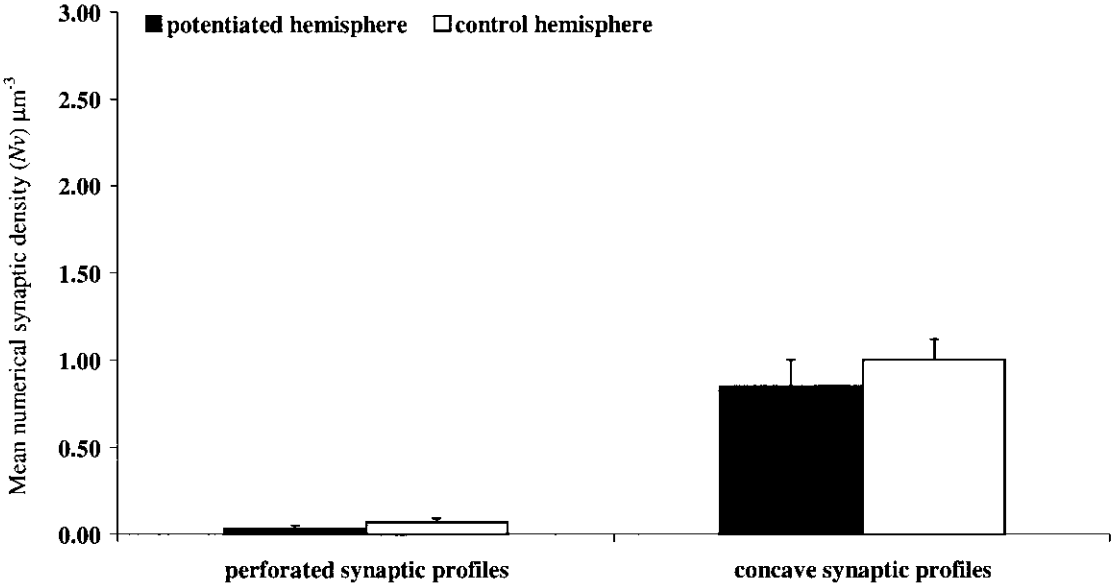

Figure 3.12 Mean numerical synaptic density (*Nv*) of axospinous synapses with perforated or concave profiles, in the middle molecular layer of the dentate gyrus, 45min after the induction of LTP by TBS. Mean (± S.E.M.) of 5 animals.

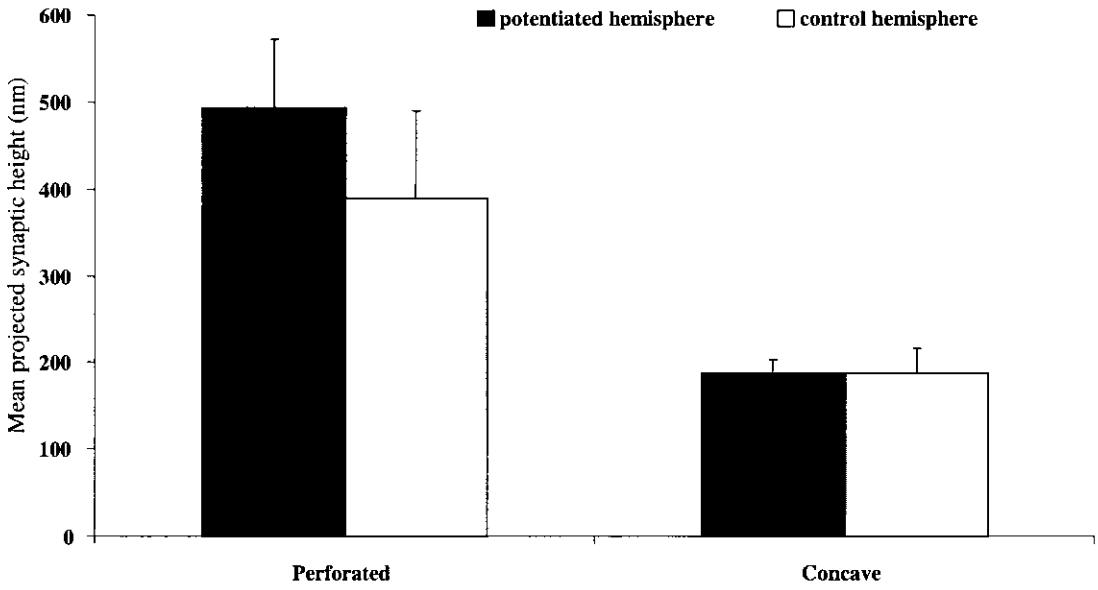

Figure 3.13 Mean projected synaptic height of axospinous synapses with perforated and on concave profiles, in the middle molecular layer of the dentate gyrus, 45min after the induction of LTP by TBS. Mean (± S.E.M.) of 5 animals.

3.3 Discussion

The results indicate that 45min after the induction of LTP with TBS there are no significant differences, between the hemispheres, in any of the morphological parameters examined in the middle molecular layer. (Table 3.1) However, this may not indicate an absence of plasticity as concurrent synaptogenesis and synapse elimination could result in no net change in synapse number or size.

Earlier non-stereological investigations in hippocampal slices have observed increases in the number of axodendritic and axospinous synapses 10-15min after LTP induction (Chang and Greenough, 1984; Lee *et al.*, 1980). These changes persisted for up to 8 hours although (Sorra and Harris, 1998) reported no increase in synapse number 2h post-tetanus, in the CA1 region of hippocampal slices after serial reconstruction. The present study failed to find any significant differences in axodendritic or axospinous asymmetric synaptic densities 45min post-tetanisation and a recent stereological study reported similar results 60min after the induction of LTP with HFS (Weeks *et al.*, 2000).

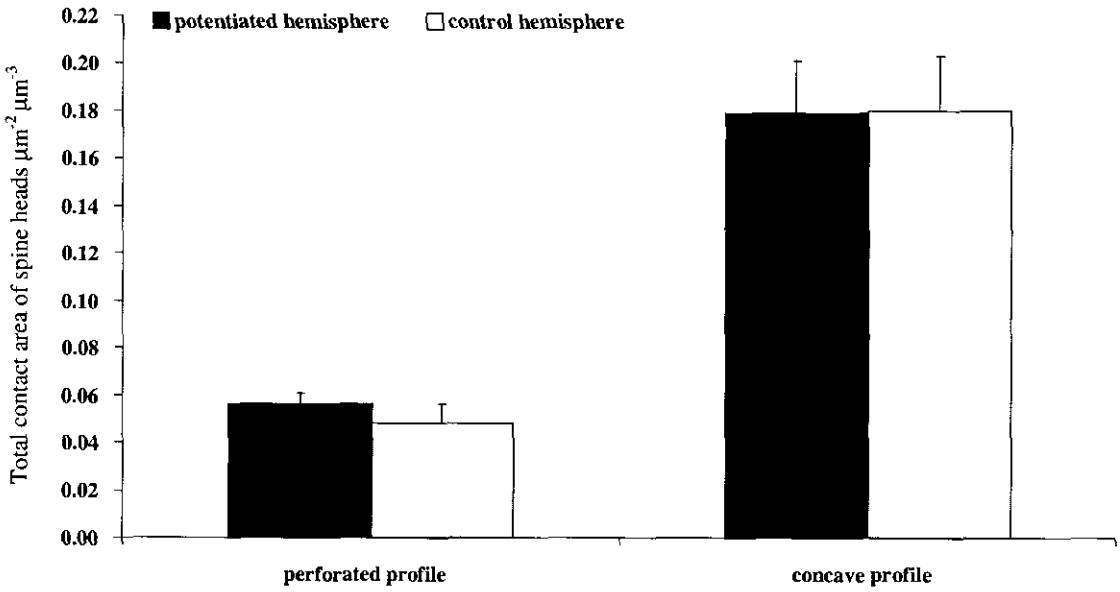

Figure 3.14 Total contact area of spine heads with perforated or concave profiles, in the middle molecular layer of the dentate gyrus, 45min after the induction of LTP by TBS. Mean (± S.E.M.) of 5 animals.

There is however a trend towards larger synapses in the potentiated hemisphere. The volume density (*Sv*) of synapses in the potentiated hemisphere was greater per unit volume although the mean numerical density of synapses in that volume was less. This total increase in area, which can be correlated with total spine volume (Harris, 1989), is supported by a larger mean surface area of individual synapses and is reflected in the slightly longer PSDs in this hemisphere. Other studies with HFS have reported a similar trend (Desmond and Levy, 1986b).

Serial reconstruction has shown that a spine head can appear large and indented on one section and small and convex two sections later (Sorra and Harris, 1998) and it is not always possible to identify segmented PSDs. It is difficult to identify spine or synapse profiles on single sections, and although, in this study, there were serial sections to refer to, there may be an underestimation of concave and perforated profiles. However, as this underestimation would affect stimulated and control groups equally these results should provide an adequate comparison.

There was no significant difference, between the hemispheres, in the *Nv* of synapses with concave profiles, the size of the PSDs of these synapses or the contact area of their spine profiles. Non-stereological studies have reported a decrease in the number of synapses with concave profiles of synaptic active zones, two hours post-tetanisation, in CA1 (Chang and Greenough, 1984), while in the dentate gyrus an increase in the number of these synapses was reported 60 min after LTP induction (Desmond and Levy, 1986a; Desmond and Levy, 1988). A significantly increased PSD surface area (Desmond and Levy, 1986b) and an increased synaptic length per neuron (Weeks *et al.*, 2000) of concave spine profiles has been reported after HFS of the perforant path. In the present study, there was no change in the morphometry of concave profiles between hemispheres and although concave synapses were larger than average in the potentiated hemisphere, this applied equally to the contralateral hemisphere.

Desmond and Levy (Desmond and Levy, 1986b) also found a decrease in the Sv of non-concave synapses, and suggested that spine heads activated by conditioning stimulation enlarge and become concave in shape (Desmond and Levy, 1986a). They suggest that the conversion of spine heads from non-concave to concave occurs rapidly after conditioning stimulation (within 2-3min) and persists for at least 60min and propose that concave spine profiles are a correlate of LTP in the dentate gyrus. They hypothesise that PSD material is added with this conversion as the active zone of the potentiated synapses enlarges. These larger concave synapses may be important, although studies of 'activated' synapses have not reported any associated differences in the induction phase of LTP after TBS (Buchs and Muller, 1996; Toni *et al.*, 1999). Changes in the incidence and morphology of concave synapses may be a phenomenon related to the stimulation protocol employed as suggested by the varied results reported after HFS or TBS. However, larger spines are reported to have more receptors (Nusser *et al.*, 1998; Takumi *et al.*, 1999; Baude *et al.*, 1995) and the present study has concluded that concave synapses are larger than the average axospinous synapse. The influence of synaptic size and shape on receptor availability and synaptic efficacy will be discussed later.

The most interesting results concern the morphology of those synapses with segmented PSDs. The difference in the Nv of perforated synapses was not significant but the lower mean numerical density, per unit volume, suggested a trend towards larger synapses. This was supported by the increased size of the PSDs, as reflected in the mean projected synaptic height estimation, in the potentiated hemisphere and the larger contact area suggesting larger spines. Measurement of the spine contact area was judged to avoid the inaccuracies of attempting to measure segmented PSDs from single sections.

Although changes in the incidence of perforated synapses has been observed previously within 60min of stimulation (Geinisman *et al.*, 1996), this may be a transient change. Recent experiments in hippocampal CA1 of cultured slices have

employed a calcium marking technique to identify activated synapses (Buchs and Muller, 1996), and found a 3-fold increase in the frequency of perforated synapses in this population. However, Ca^{2+} precipitates are more likely to be detected in spines that contain calcium-sequestering tubules of smooth endoplasmic reticulum (SER) and only 20% of spines with macular PSDs contain SER unlike 100% of the spines with perforated PSDs (Spacek and Harris, 1997). It is conceivable that this analysis was restricted to large spines that already had perforated PSDs. Alternatively, more bound calcium may be sequestered in spines with SER after LTP.

Further studies reported that within this group of activated synapses there was a gradual increase in the percentage of perforated synapses until 30min after TBS. This transient increase was not significant at 45min and had returned to control levels 60min after TBS (Toni *et al.*, 1999). This seems to substantiate my findings at 45min post-tetanisation and it would be expected that an approach that examined only activated synapses could detect more subtle changes in morphometry than the inclusive process employed here.

Recent studies of LTP induction of the perforant path, with HFS, have reported significantly more perforated synapses 60min after tetanisation (Weeks *et al.*, 2000). In dissociated hippocampal cell cultures, 15min stimulation with the $GABA_A$–antagonist picrotoxin (PTX) selectively increases the percentage of perforated synapses while other morphological parameters were not affected (Neuhoff *et al.*, 1999). This increase was blocked when PTX was added with DL-2-amino-5 phosphonovaleriac acid (APV), indicating that the formation of perforated synapses depends on the activation of NMDA receptors. Longer periods of stimulation increased the frequency of perforated synapses significantly. This phenomenon may explain the increased numbers of perforated synapses observed (Geinisman *et al.*, 1991; Geinisman *et al.*, 1996; Weeks *et al.*, 2000) where the protocol employed to induce potentiation requires 400Hz HFS for up to four days. However, treatment of slice cultures with PTX for two weeks blocked the ability of the slices to express LTP

(Collin *et al.*, 1997), suggesting that chemically induced saturation of LTP induction and perforated synapse formation are functionally related.

As already mentioned the failure to find any change in synaptic number may be a result of spine pruning that counteracts novel spine development. Three-dimensional reconstruction techniques to examine synapses in slice culture after LTP have reported multiple spine synapses (Figure 2.5) between a single axon terminal and a dendrite within 60 minutes of TBS (Toni *et al.*, 1999). This is a time course consistent with that of new spine formation observed by (Engert and Bonhoeffer, 1999) but fewer multiple synaptic contacts have been reported within 60min after HFS (Desmond and Levy, 1990) in the dentate gyrus. In hippocampal CA1, no change in the incidence of multiple synaptic contacts was reported two hours after HFS (Sorra and Harris, 1998).

The most robust phenomenon, regardless of the stimulating protocol used and controversy regarding the methods employed, is the involvement of synapses with segmented PSDs in the induction of LTP. The formation of perforated synapses seems to be an early morphological consequence of synaptic activation. There may be either an increased incidence, or enlargement of these synapses to evolve into several separate active zones. Presynaptic boutons may undergo parallel changes with postsynaptic changes, as demonstrated by experiments where the administration of estradiol results in an increase in spine density. A corresponding increase in the number of synaptic terminals staining for synaptophysin was reported, indicating that presynaptic boutons were expanding (Murphy and Segal, 1996). The effect of LTP would be to increase the number of release sites per bouton and eventually lead to the formation of separate synapses, as suggested by the presence of multiple synaptic contacts.

Spines expand the connective prospects for a dendrite that effectively enlarges the area occupied by a given dendrite, while permitting tight packing of synapses. They are dynamic structures that can undergo fast morphological variations - shrinkage of spines can take place within a minute (Halpain *et al.*, 1998). This activity

may explain the conflicting reports of activity-dependent changes in axospinous synapse morphology during the first few hours post LTP induction.

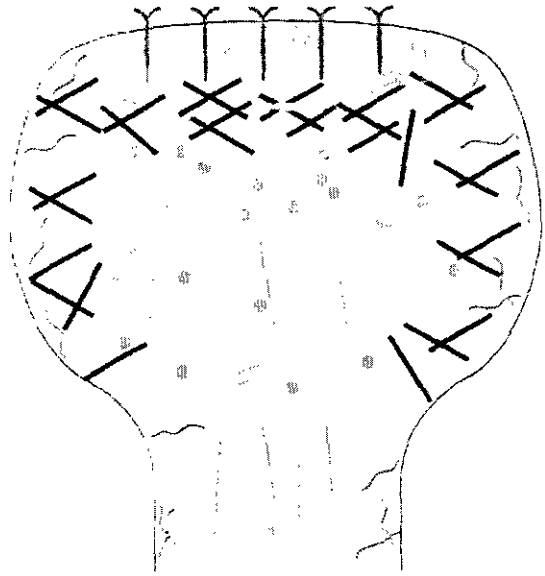

Figure 3.15 The hypothesised configuration of the actin cytoskeleton in dendritic spines.

The spine head is believed to comprise at least two pools of actin. One set of filaments forms a stable core of F-actin in the central region of the spines whereas dynamic filaments exist towards the periphery. Actin filaments in the core are rendered stable and resistant to polymerisation by end capping proteins. Activation of glutamate receptors is likely to modulate multiple actin-dependent processes in spines. Stable actin (━), dynamic actin (╾), glutamate receptor (Y) and capping protein (●). After Halpain 2000.

Local and central factors have a role in the regulation of spine morphology. Local changes in [Ca^{2+}] will change spine length, while a central somatic change in [Ca^{2+}] will lead to the formation of novel spines or their elimination throughout the dendritic tree, via nuclear signalling cascades. e.g. after estradiol administration the phosphorylation of cAMP-response-element-binding protein (CREB) leads to an increase in dendritic spine density that is not restricted to a single dendrite (Murphy and Segal, 1996).

A moderate and transient postsynaptic increase in [Ca^{2+}], equivalent to the release of Ca^{2+} from internal stores, will cause elongation of spines and the formation of new ones *in vitro* (Korkotian and Segal, 1998). A large increase in [Ca^{2+}] resulting

from seizure will cause shrinkage of spines and lead to their eventual disappearance (Segal *et al.,* 2000). Generally, shrinkage of spines is associated with a stronger link between the spine and parent dendrite and spine elongation with independence of the spine from the parent dendrite (Korkotian and Segal, 1998; Volfovsky *et al.,* 1999). Spine length modification has been demonstrated in the same spine population where a short pulse application of glutamate causes elongation of spines, whereas a larger pulse of glutamate results in shrinkage of the same spines (Korkotian, 1999). The length of the spine neck does not determine synaptic efficiency (Harris and Kater, 1994), but it could affect the efficiency of the molecular machinery involved in the modification of glutamate receptors, or the availability of cytoskeletal elements associated with changes in glutamate mediated function (van Rossum and Hanisch, 1999). In this way, alteration of spine neck length acts as a 'fine tuning' mechanism for continuous adjustment of synaptic modification (Segal *et al.,* 2000).

Spines have heterogeneous populations of actin filaments that provide the main structural basis for cytoskeletal organisation as most spines lack microtubules and intermediate filaments. (Figure 3.15) EM studies have reported a greater density of actin filaments in spines than in dendritic shafts (Fifkova and Delay, 1982) while microtubule components, including tubulin and MAP2, are restricted to the dendritic shaft domain (Kaech *et al.,* 1997). Two forms of actin are present in spines, polymerised filaments (F-actin) or unpolymerised globular subunits (G-actin). Their states are regulated locally by various actin-associated proteins (Littlefield and Fowler, 1998; Hall, 1998) and hence the amount of stability and motility of the spine is controlled. The rapid motility of spines depends on dynamic, F- actin fibres (Fischer *et al.*, 1998) and, the application of actin depolymerisation drugs prevents the formation of stable LTP in hippocampal slices (Kim and Lisman, 1999).

It has also been shown that intense glutamate-receptor stimulation induces the disassembly of F-actin in spines within minutes, an event that is correlated with the collapse of spine structure (Halpain *et al.,* 1998). Inhibitors of calcineurin, a Ca^{2+}-

dependent phosphatase, block this effect and calcineurin has been proposed as a potential regulator of actin filament integrity in spines. Interestingly, behavioural studies, to investigate the role phosphatases play in hippocampal-dependent memory, suggest that calcineurin has a function in the transition from short-to long-term memory, which correlates with a novel intermediate phase of LTP (Mansuy *et al.*, 1998). The close association of cytoplasm actins with spines, together with the presence of biochemical pathways that support rapid motility under basal conditions and can induce rapid actin collapse under excitotoxic conditions, supports the idea that actin motility-based changes in spine shape may contribute to synaptic plasticity.

How can the capacity of spines to modify their morphology improve their ability to transduce synaptic signals? Many signalling complexes and receptor clusters are anchored to the actin cytoskeleton until a synaptic signal causes actin depolymerisation. e.g. clusters of glutamate receptors and the β subunit of CaMKII, two components of the postsynaptic density, have been shown to be tethered to actin filaments (Allison *et al.*, 1998; Shen *et al.*, 1998). Changes in actin depolymerisation may be used to dynamically regulate mechanosensitive ion channels (Paoletti and Ascher, 1994) and to position macromolecular complexes in a signal-dependent manner. Therefore, glutamate receptors, or CaMKII, could be released for fusion with the PSD by an activity-dependent alteration in actin filament assembly. Dynamic actin could also participate in the coupling of other signalling enzymes with their appropriate substrates; hence, activity -dependent changes in actin stability could alter the number or functional state of proteins clustered at the synaptic junction.

It is uncertain whether spines, that are seen to move freely *in vitro*, can be as mobile *in vivo*, but these actin based morphological control mechanisms are still relevant to the understanding of the mechanisms of LTP. The distribution of receptors in segmented PSDs and the insertion of AMPA receptors into 'silent synapses' after potentiating stimulation will be discussed in Chapter 5.

Dynamic actin may also control the position of organelles inside the spine such as polyribosomes or SER (Halpain, 2000) and play a role in the production of new membrane proteins or the synthesis of novel spines. During development, dendrites of immature neurons can bear numerous transient spine-like projections, or filopodia, that do not correspond to authentic spines and only occasionally bear synaptic contacts (Fiala *et al.,* 1998). Electrical stimulation, similar to afferent activity, has been reported to augment dendritic filopodia and they are proposed to be the precursors of spines at developing synapses (Maletic-Savatic *et al.,* 1999; Dailey and Smith, 1996; Ziv and Smith, 1996). *In vivo* electron microscopy studies have shown that incoming fibres make synapses with dendritic filopodia that then become mature spines, suggesting that spines follow synapse formation (Fiala *et al.,* 1998).

While there is some indirect evidence for the formation of novel spines after LTP *in vitro* (Toni *et al.,* 1999), unbiased *in vivo* studies have failed to find an increase in synaptic density or multiple synaptic contacts (Weeks *et al.,* 2000) in the first hour post tetanisation. Indeed, one *in vivo* study that recorded the incidence of polyribosomes at the base of dendritic spines, in the first hour post HFS, concluded that new synapses do not form with the induction of LTP (Desmond and Levy, 1990). If new synapses are formed, then spine pruning may occur to keep the synaptic number constant. It is not clear whether spine pruning is an active process associated with an increase in synaptic activity or a passive process caused by lack of afferent activation of the pruned spine.

Since serial studies have suggested only a redistribution of synaptic weight (Sorra and Harris, 1998), other morphological modification may be occurring. It has been shown that the distribution of spines along dendrites is not evenly random, but includes dense clusters of spines surrounding the dendritic shaft (spine 'collars') (Rusakov and Stewart, 1995). Partial fusion of active spines, and more subtle changes which result in formation of spine branches, or changes in spine branch positions, could significantly increase synaptic signal transfer (Rusakov *et al.,* 1996). Spine

density in the cultured neuron can be 10-30% lower than spine density in its *in vivo* counterpart (Collin *et al.*, 1997). However, investigations using this system, plus confocal microscopy techniques, will allow minute by minute changes in receptor insertion and spine orientation to be investigated and will play an important role in directing future *in vivo* studies.

	Mean of potentiated hemispheres	Mean of control hemispheres	Potentiated v control
Axodendritic (*Nv*) μm^{-3}	0.14 ± 0.02	0.17 ± 0.02	$p < 0.21$
Axospinous (*Nv*) μm^{-3}	2.28 ± 0.24	2.53 ± 0.10	$p < 0.18$
Number of axodendritic synapses per neuron	185 ± 31	170 ± 23	$p < 0.35$
Number of axospinous synapses per neuron	2993 ± 321	2576 ± 115	$p < 0.13$
Axodendritic PSD height (nm)	227 ± 0.08	211 ± 0.04	$p < 0.43$
Axospinous PSD height (nm)	142 ± 0.01	137 ± 0.01	$p < 0.36$
Axospinous (*Sv*) $\mu m^2 \mu m^{-3}$	0.14 ± 0.01	0.13 ± 0.02	$p < 0.34$
Sv/Nv $\mu m^2 \mu m^{-3}$	0.059 ± 0.006	0.049 ± 0.006	$p < 0.20$
% synapses with perforated profiles	6.42 ± 0.82	6.11 ± 1.08	$p < 0.43$
% synapses with concave profiles	20.24 ± 2.84	19.42 ± 1.14	$p < 0.42$
% macular synapses	93.58 ± 0.82	93.89 ± 1.08	$p < 0.43$
Number of synapses with perforated profiles	8.60 ± 1.33	8.40 ± 2.01	$p < 0.47$
Number of synapses with concave profiles	27.4 ± 4.49	26.0 ± 1.92	$p < 0.39$
Number of macular synapses	124.2 ± 8.52	127.0 ± 10.34	$p < 0.37$
Perforated profile (*Nv*) μm^{-3}	0.03 ± 0.02	0.07 ± 0.02	$p < 0.18$
Concave profile (*Nv*) μm^{-3}	0.85 ± 0.15	1.00 ± 0.12	$p < 0.27$
Perforated PSD height (nm)	493.4 ± 78.9	388.8 ± 101.0	$p < 0.10$
Concave PSD height (nm)	188.4 ± 15.0	188.2 ± 28.4	$p < 0.50$

Table 3.1 Morphological and morphometric parameters, in the middle molecular layer of the dentate gyrus, 45 min after the induction of LTP with TBS.

Results (± S.E.M.) of morphological and morphometric investigations, in the middle molecular layer of the dentate gyrus, 45 min after the induction of LTP with TBS.

	Mean of potentiated hemispheres	Mean of control hemispheres	Potentiated v control
Axodendritic (*Nv*) μm^{-3}	0.16 ± 0.05	0.17 ± 0.02	p < 0.42
Axospinous (*Nv*) μm^{-3}	2.15 ± 0.29	2.46 ± 0.22	p < 0.08
Number of axodendritic synapses per neuron	210 ± 67	175 ± 17	p < 0.31
Number of axospinous synapses per neuron	2814 ± 389	2505 ± 231	p < 0.14
Axodendritic PSD height nm	156 ± 23	148 ± 20	p < 0.38
Axospinous PSD height nm	145 ± 7	133 ± 8	p < 0.06
Axospinous (*Sv*) $\mu m^2 \mu m^{-3}$	**0.11 ± 0.01**	**0.12 ± 0.01**	**p < 0.03**
Axospinous *Sv/Nv* $\mu m^2 \mu m^{-3}$	0.05 ± 0.005	0.05 ± 0.004	p < 0.42
% of synapses with perforated profiles	6.39 ± 1.08	8.50 ± 2.72	p < 0.29
% of synapses with concave profiles	10.70 ± 2.84	12.43 ± 3.06	p < 0.38
% of macular synapses	93.61 ± 1.08	91.50 ± 2.72	p < 0.29
Number of synapses with perforated profiles	7.0 ± 1.41	8.60 ± 1.78	p < 0.32
Number of synapses with concave profiles	12.40 ± 1.95	13.40 ± 2.97	p < 0.44
Number of macular synapses	101.4 ± 8.38	105.6 ± 13.72	p < 0.31

Table 3.2 Morphological and morphometric parameters, in the inner molecular layer of the dentate gyrus, 45 min after the induction of LTP with TBS.

Results (± S.E.M.) of morphological and morphometric investigations, in the inner molecular layer of the dentate gyrus, 45 min after the induction of LTP with TBS.

	Mean of potentiated hemispheres	Mean of control hemispheres	Potentiated v control
Axodendritic (*Nv*) μm^{-3}	0.16 ± 0.05	0.17 ± 0.02	p < 0.42
Axospinous (*Nv*) μm^{-3}	2.15 ± 0.29	2.46 ± 0.22	p < 0.08
Number of axodendritic synapses per neuron	210 ± 67	175 ± 17	p < 0.31
Number of axospinous synapses per neuron	2814 ± 389	2505 ± 231	p < 0.14
Axodendritic PSD height nm	156 ± 23	148 ± 20	p < 0.38
Axospinous PSD height nm	145 ± 7	133 ± 8	p < 0.06
Axospinous (*Sv*) $\mu m^2 \mu m^{-3}$	**0.11 ± 0.01**	**0.12 ± 0.01**	**p < 0.03**
Axospinous *Sv/Nv* $\mu m^2 \mu m^{-3}$	0.05 ± 0.005	0.05 ± 0.004	p < 0.42
% of synapses with perforated profiles	6.39 ± 1.08	8.50 ± 2.72	p < 0.29
% of synapses with concave profiles	10.70 ± 2.84	12.43 ± 3.06	p < 0.38
% of macular synapses	93.61 ± 1.08	91.50 ± 2.72	p < 0.29
Number of synapses with perforated profiles	7.0 ± 1.41	8.60 ± 1.78	p < 0.32
Number of synapses with concave profiles	12.40 ± 1.95	13.40 ± 2.97	p < 0.44
Number of macular synapses	101.4 ± 8.38	105.6 ± 13.72	p < 0.31

Table 3.2 Morphological and morphometric parameters, in the inner molecular layer of the dentate gyrus, 45 min after the induction of LTP with TBS.

Results (± S.E.M.) of morphological and morphometric investigations, in the inner molecular layer of the dentate gyrus, 45 min after the induction of LTP with TBS.

Chapter Four Estimation of morphological and morphometrical correlates, 24h after induction of LTP with either Theta Burst Stimulation (TBS) or High Frequency Stimulation (HFS).

4.1 Introduction

While early restructuring of synapses may occur in minutes, the phase of LTP, which requires enhanced protein synthesis (both *in vivo* and *in vitro*), is believed to begin hours after induction of potentiation (Buchs and Muller, 1996). This argues that more prominent structural change, if any is likely to occur after that period. Recent investigations have reported no overall increase in synaptic number 24h post tetanization but an increase in the number of perforated concave synapses and in the proportion of pre-synaptically concave-shaped synapses (Weeks, *et al.,* 1999). However, an earlier study at this time point by the same authors (Weeks, *et al.,* 1998) found that synaptic number was positively correlated with the degree of potentiation. An increased number of axodendritic synapses in the dentate gyrus has been reported thirteen days after the induction and maintenance of LTP (Geinisman, *et al.,* 1996). Therefore, 24h post-induction would appear to represent an intermediate stage between shorter- and longer-term correlates of synaptic potentiation.

In this study, to ensure that any changes could be generalised to LTP, two different stimulating protocols were applied. Changes in morphology were then examined 24h after LTP was induced with either HFS or TBS.

4.2 Results 24h after the induction of LTP with Theta Burst Stimulation

4.2.1 Mean numerical synaptic density

In the MML of the potentiated hemisphere, the mean density of asymmetric axospinous synapses was 2.55 μm^{-3} and 1.90μm^{-3} in the control hemisphere ($p<0.08$). There was a significant difference ($p<0.05$) in the density of axodendritic asymmetric synapses with 0.17μm^{-3} in the experimental hemisphere and 0.07μm^{-3} in the contralateral hemisphere. Total synaptic density of 2.72μm^{-3} and 1.97μm^{-3} reflected these results but did not reach the 95% level of significance ($p< 0.07$). (Figure 4.1)

In the IML, no significant differences were demonstrated. Mean axodendritic synaptic densities of 0.08μm^{-3} and 0.09μm^{-3} ($p<0.33$) and axospinous synaptic densities of 2.24μm^{-3} and 2.43μm^{-3} ($p<0.28$) were recorded from the potentiated and control hemispheres. (Figure 4.2)

4.2.2 Neuronal density

There was no significant difference in the mean neuronal density of the hemispheres and the results were used to correct the synapse per neuron estimation for any swelling or shrinkage. (A mean of 0.0079 neurons, μm^{-3} in the potentiated hemisphere and 0.0083 neurons, μm^{-3} in the contralateral hemisphere, $p<0.28$). (Figure 3.4)

4.2.3 Mean Synapse Number per Neuron

The MML of the potentiated hemisphere presented significantly different results to those of the contralateral hemisphere. The mean number of axodendritic synapses per neuron was 213 versus 81 ($p< 0.04$) and the mean total number of synapses per neuron was 3421in the potentiated hemisphere and 2373 in the control ($p< 0.05$). The

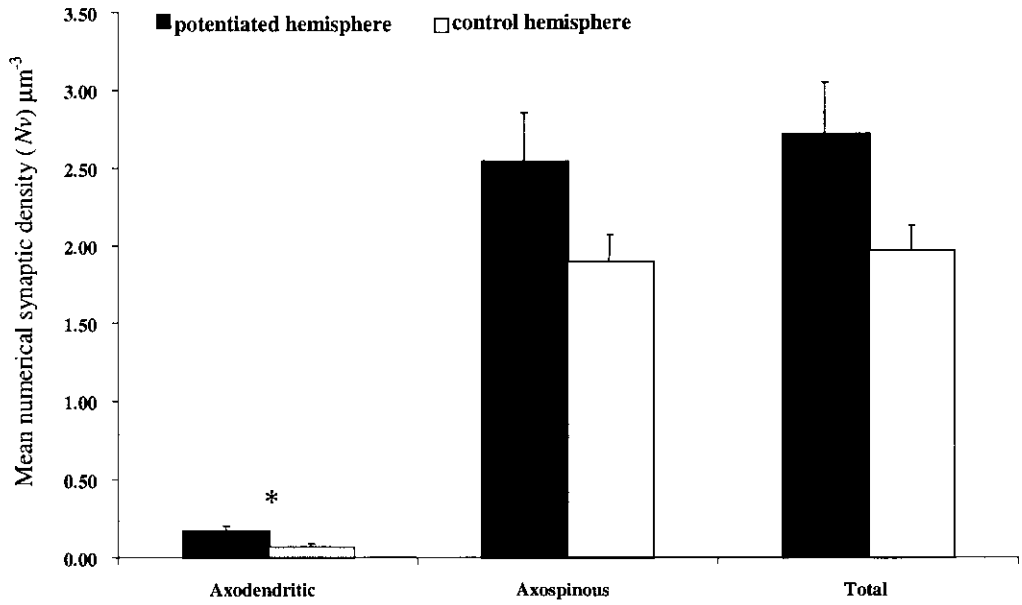

Figure 4.1 Mean numerical synaptic density *(Nv)* of synapses in the middle molecular layer of the dentate gyrus, in potentiated and control hemispheres, 24 h after the induction of LTP by TBS. (* indicates significant difference $p<0.05$) Mean (± S.E.M.) of 5 animals.

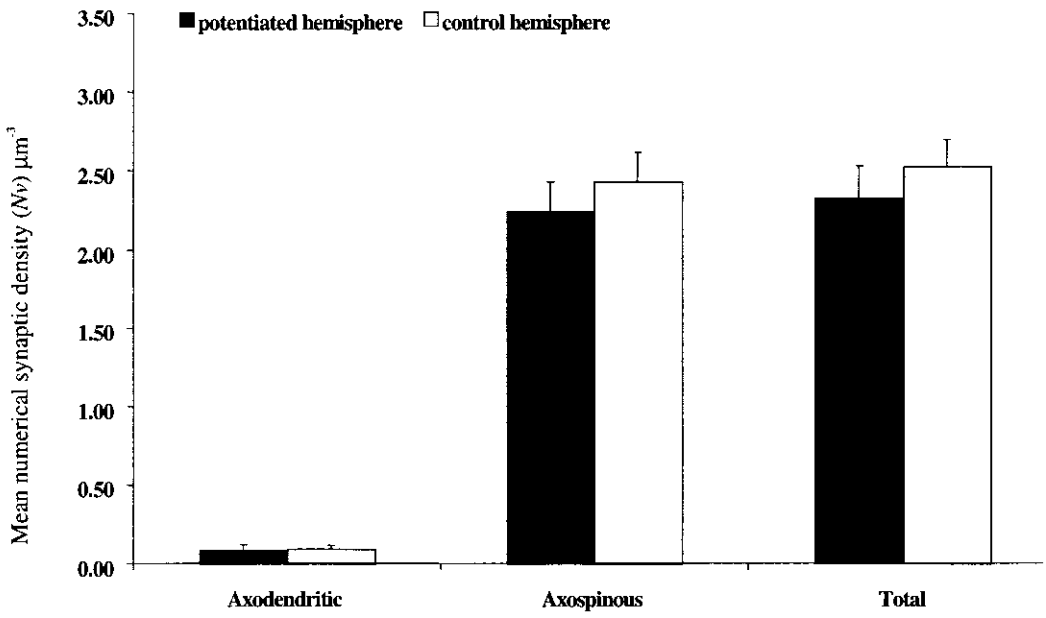

Figure 4.2 Mean numerical synaptic density *(Nv)* of synapses in the inner molecular layer of the dentate gyrus, in potentiated and control hemispheres, 24h after the induction of LTP by TBS. Mean (± S.E.M.) of 5 animals.

mean number of axospinous synapses per neuron, in the stimulated and control hemispheres respectively, was 3230 and 2292. Although the difference between the hemispheres was 41%, this did not reach the level of significance ($p< 0.06$). (Figure 4.3)

The mean synapse per neuron numbers in the inner molecular layer did not show any significant differences between the hemispheres. In the potentiated hemisphere, there was a mean of 97 axodendritic synapses per neuron and 2840 axospinous synapses per neuron (2937 synapses in total). In the contralateral hemisphere, the mean synapse per neuron values were 113 axodendritic ($p<0.37$) and 2919 axospinous ($p<0.42$) yielding a mean total synapse per neuron value of 3028 ($p<0.41$). (Figure 4.4)

4.2.4 Mean projected synaptic height

The mean projected synaptic height of axodendritic synapses in the MML of the potentiated hemisphere was 178nm and 171nm in the control hemisphere ($p<0.46$). For axospinous synapses, values of 135 and 139nm were recorded in the experimental and control hemispheres ($p<0.33$). (Figure 4.5)

In the inner molecular layer, the mean projected synaptic height of the axodendritic synapse was 122nm, in the potentiated hemisphere, and 145nm in the control hemisphere ($p<0.21$). There was a significant difference in the mean synaptic height of axospinous synapses in the IML with values of 139nm in the experimental hemisphere and 121nm in the control hemispheres ($p<0.02$). (Figure 4.5)

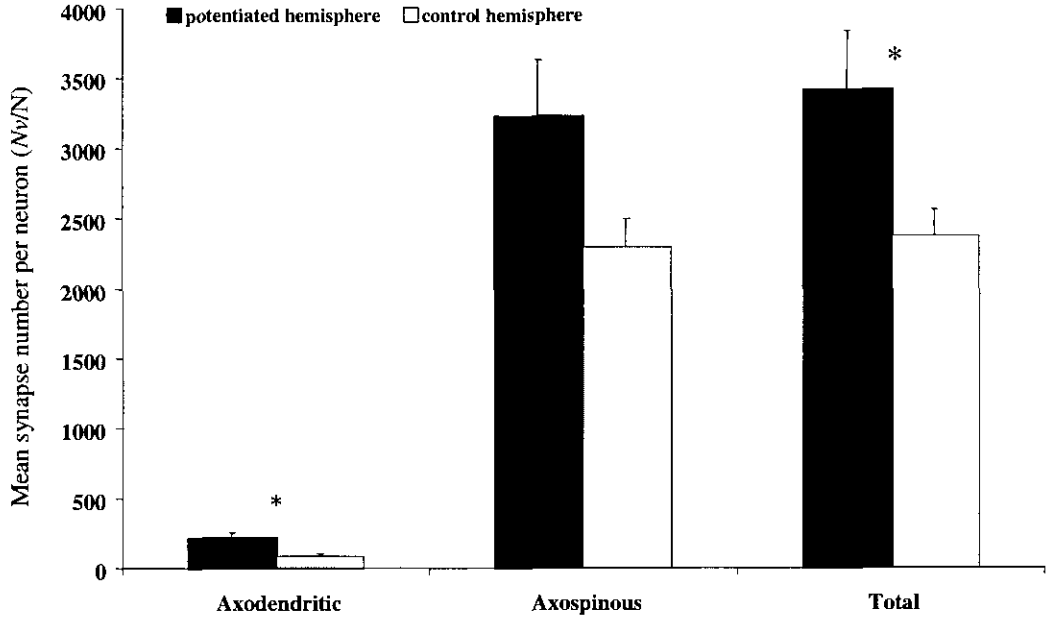

Figure 4.3 Mean synapse number per neuron in the middle molecular layer of the dentate gyrus, in potentiated and control hemispheres, 24h after the induction of LTP by TBS. . (* indicates significant difference $p<0.05$). Mean (± S.E.M.) of 5 animals.

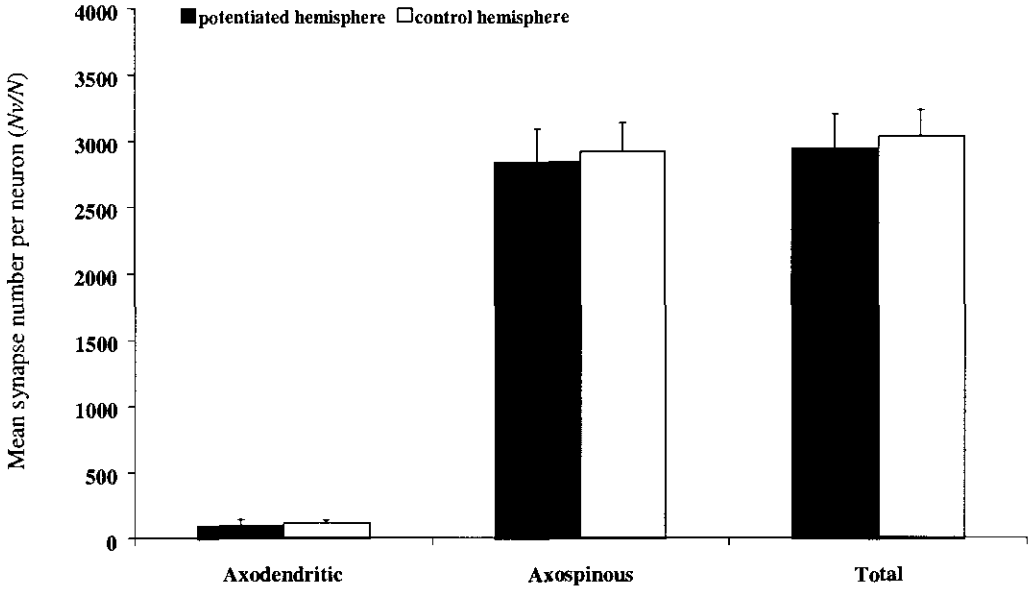

Figure 4.4 Mean synapse number per neuron in the inner molecular layer of the dentate gyrus, in potentiated and control hemispheres, 24h after the induction of LTP by TBS. Mean (± S.E.M.) of 5 animals.

4.2.5 Total volume density of axospinous AZ area (*Sv*)

The total volume density of axospinous synapses in the MML of the tetanised hemisphere was significantly different to the control hemisphere with a *Sv* of $0.13\mu m^2/\mu m^3$ and $0.09\mu m^2/\mu m^3$ respectively ($p<0.03$). In the IML the *Sv* was $0.11\mu m^2/\mu m^3$ in both hemispheres ($p<0.041$). (Figure 4.6)

4.2.6 Volume density of individual axospinous synapses (*Sv/Nv*)

In the MML, there was no difference in the volume density of individual axospinous synapses with an average volume density of 0.05 $\mu m^2/\mu m^3$ in both hemispheres ($p<0.39$). (Figure 4.8) In the IML the mean volume density was 0.05 $\mu m^2/\mu m^3$ in the potentiated hemisphere and 0.04 $\mu m^2/\mu m^3$ in the control hemisphere ($p<0.07$). (Figure 4.7)

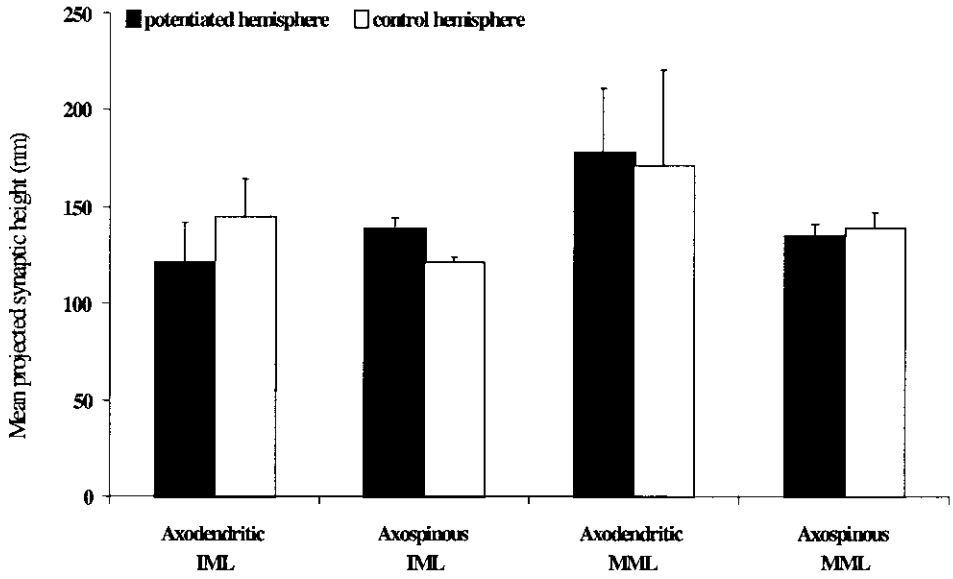

Figure 4.5 Mean projected synaptic height of synapses, in the inner and middle molecular layers of the dentate gyrus, 24h after the induction of LTP by TBS. Mean (± S.E.M.) of 5 animals.

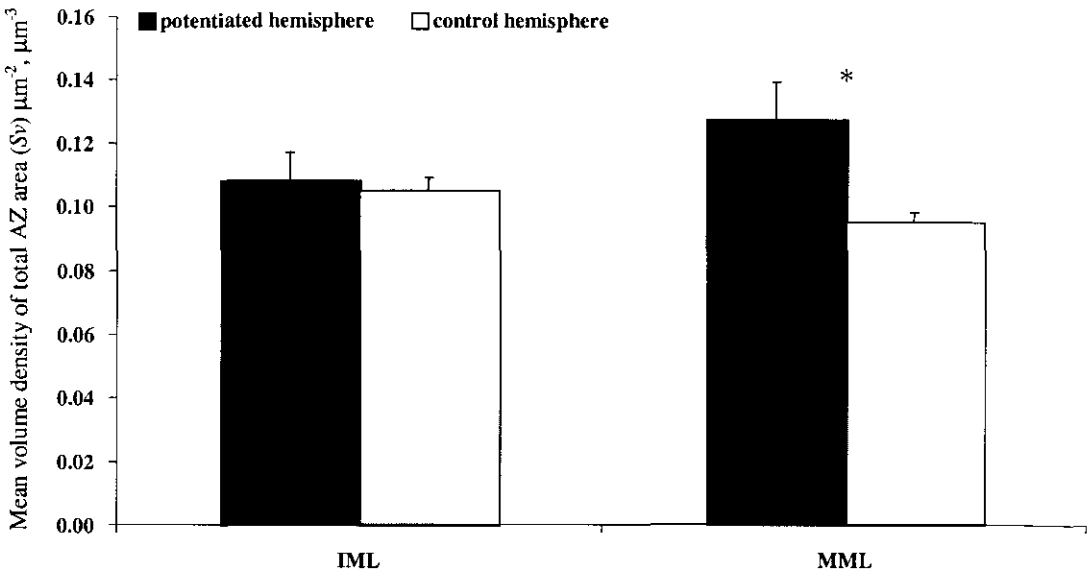

Figure 4.6 Mean volume density of total axospinous apposition zone (AZ) area (*Sv*) in the inner and middle molecular layer of the dentate gyrus, 24h after the induction of LTP by HFS. (* indicates significant difference $p<0.05$). Mean (± S.E.M.) of 5 animals.

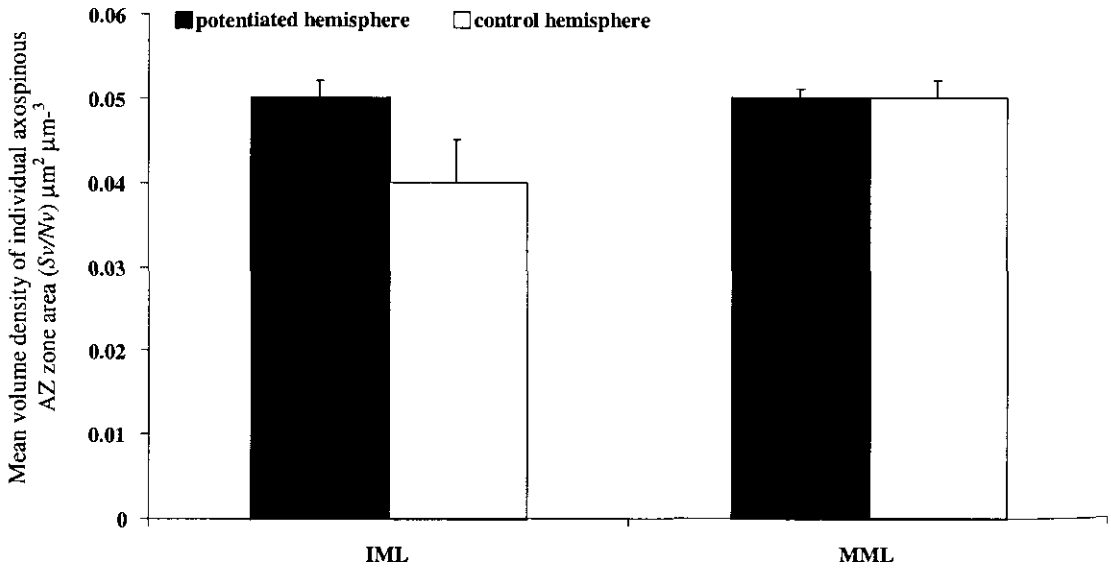

Figure 4.7 Mean volume density of individual axospinous apposition zone (AZ) area (*Sv/Nv*) in the inner and middle molecular layers of the dentate gyrus, 24h after the induction of LTP by TBS. Mean (± S.E.M.) of 5 animals.

4.2.7 Characterisation of synaptic profiles

As before synapses were identified in an area of 350 μm^2 and classified according to their synaptic profiles. In the MML, there was a mean of 10.2 (8.57 %) synapses with perforated profiles in the potentiated hemisphere and 9.8 (11.10 %) in the control hemisphere ($p<0.42$). There was a mean of 14.8 (13.09%) synapses with concave profiles in the potentiated and 12.0 (13.45%) in the control ($p<0.38$) hemispheres. There was a significant difference in the mean numbers of macular synapses between the hemispheres with 115.8 (92.0%) in the potentiated and 81.8 (88.9%) in the contralateral hemisphere ($p<0.05$). (Figure 4.8)

In the IML, there were no significant differences in the numbers of synapses between the hemispheres. There was a mean of 6.80 (6.90%) synapses with perforated profiles and 13.8 (14.06%) synapses with concave profiles in the potentiated hemisphere and 5.60 (5.31%) ($p<0.31$) and 10.0 (9.58%) ($p<0.16$) respectively in the control hemisphere. In the potentiated hemisphere, there was a mean of 89.4 (93.10%) macular synapses with 98.20 (94.69%) in the control hemisphere (0.16). (Figure 4.9)

4.3 Results 24h after the induction of LTP with High Frequency Stimulation

4.3.1 Mean numerical synaptic density (*Nv*)

The mean numerical density of axodendritic synapses in the middle molecular layer was $0.23\mu m^{-3}$ in the potentiated hemisphere and $0.26\mu m^{-3}$ in the control hemisphere ($p<0.33$). In the inner molecular layer the results were $0.16\mu m^{-3}$ and $0.08\mu m^{-3}$ respectively ($p<0.09$). In the MML, the mean *Nv* of axospinous synapses in the potentiated hemisphere was $2.50\mu m^{-3}$ and $2.00\mu m^{-3}$ in the control hemisphere ($p<0.03$). (Figure 4.10)

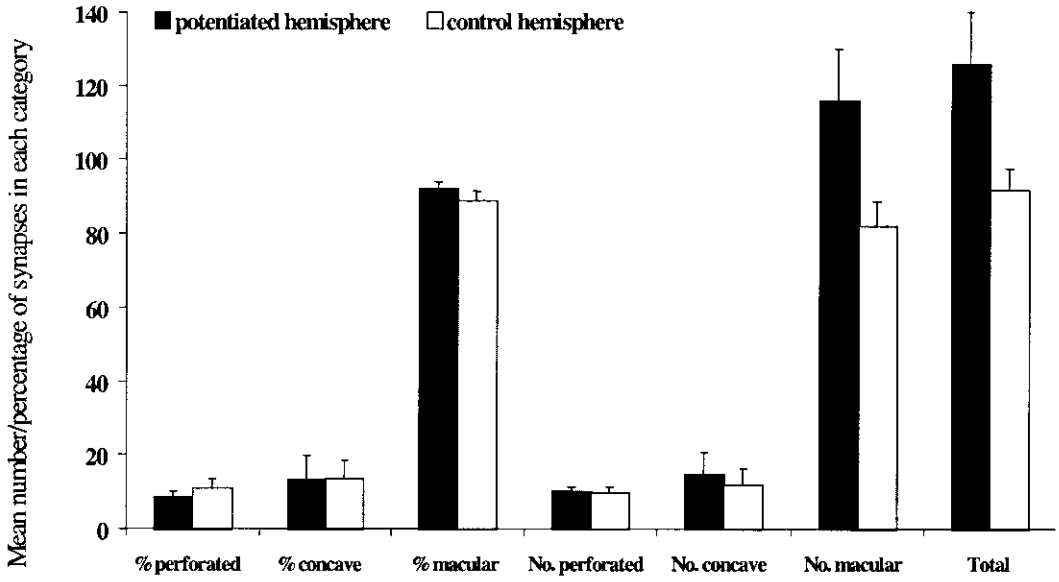

Figure 4.8 Morphology of axospinous synapses in an area of 350 μm^2, in the middle molecular layer of the dentate gyrus, 24h after the induction of LTP by TBS. (* indicates significant difference $p<0.05$). Mean (± S.E.M.) of 5 animals.

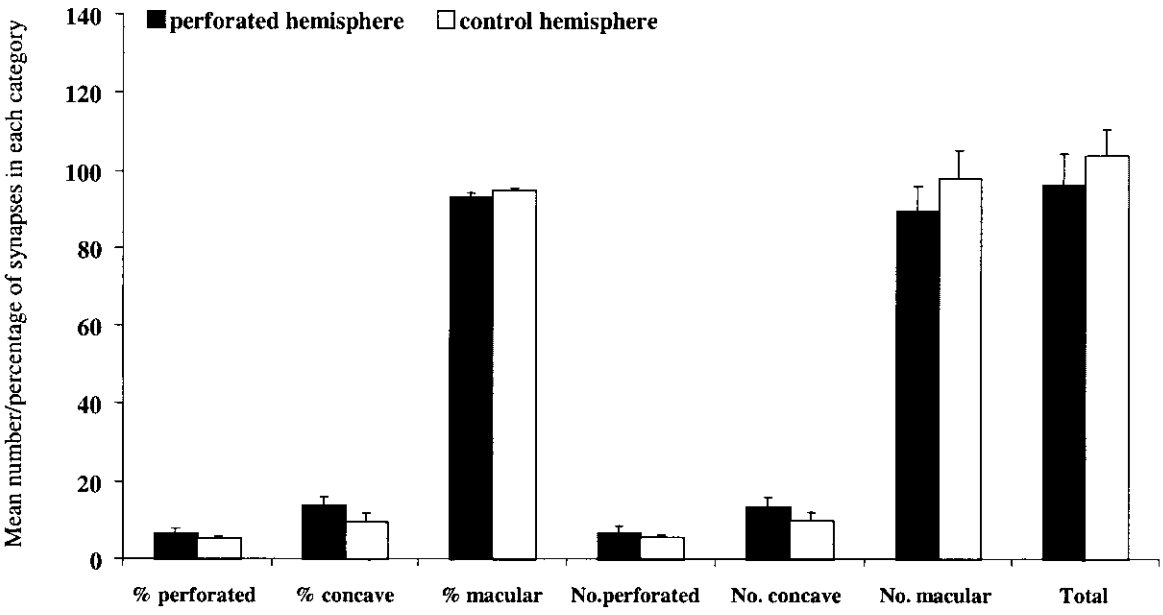

Figure 4.9 Morphology of axospinous synapses in an area of 350 μm^2, in the inner molecular layer of the dentate gyrus, 24h after the induction of LTP by TBS. Mean (± S.E.M.) of 5 animals.

In the IML, there was a mean *Nv* of 2.57μm^{-3} axospinous synapses in the stimulated hemisphere and 2.14 μm^{-3} in the control hemisphere ($p<0.17$). The total asymmetric synaptic density results reflect these findings, with an *Nv* of 2.73μm^{-3} in the MML of the potentiated hemisphere and 2.27μm^{-3} in the control hemisphere ($p<0.04$). In the IML the respective *Nv*s were 2.73μm^{3} and 2.22μm^{-3} ($p>0.14$). (Figure 4.11)

4.3.2 Neuronal density

The mean neuronal density of the potentiated hemisphere was 0.0010 μm^{-3} and 0.0095 μm^{-3} in the control hemisphere ($p<0.35$) (Figure 3.4). This difference was not significant suggesting minimal shrinkage or swelling due to the experimental protocol. The neuronal density value was used to calculate the number of synapses per neuron as previously described.

4.3.3 Synapse per neuron number

The number of axodendritic synapses per neuron in the MML of the potentiated hemisphere was 219 compared to 271 in the control hemisphere ($p<0.25$). (Figure 4.12) In the IML, the mean value in the potentiated hemisphere was 171 and 192 in the control hemisphere ($p<0.40$). (Figure 4.13)

There was no significant difference in the number of axospinous synapses per neuron between hemispheres, in the molecular layer of either hemisphere. In the MML of the potentiated hemisphere, the mean value was 2415 synapses per neuron and 2110 in the control hemisphere ($p<0.10$). In the IML, the mean value was 2423 asymmetric axospinous synapses per neuron in the potentiated hemisphere and 2276 in the control hemisphere ($p<0.38$).

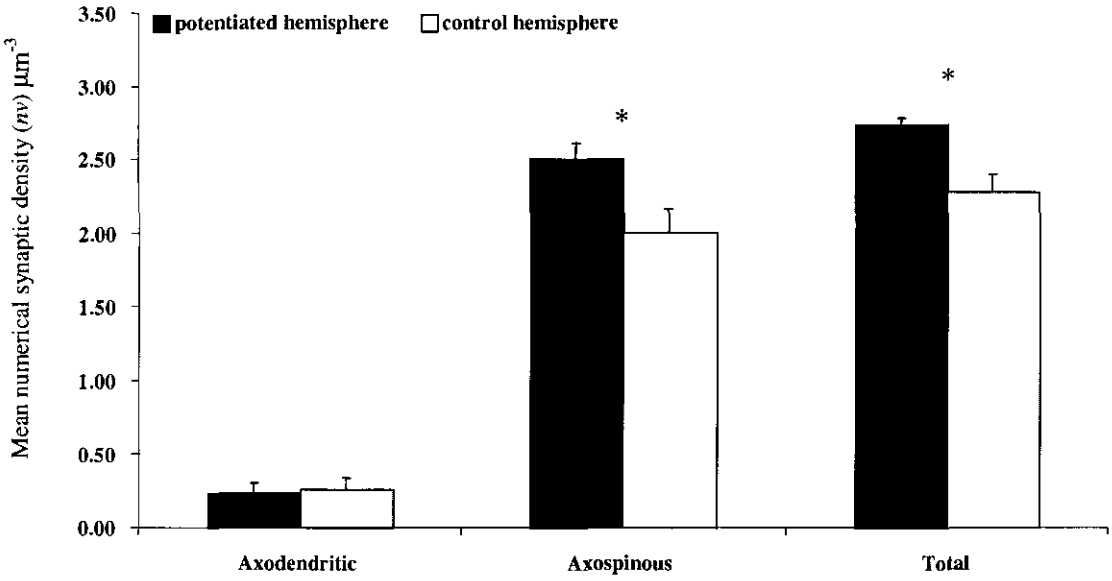

Figure 4.10 Mean numerical synaptic density (*Nv*) of synapses in the middle molecular layer, in potentiated and control hemispheres, 24h after the induction of LTP by HFS. (* indicates significant difference $p<0.05$). Mean (± S.E.M.) of 5 animals.

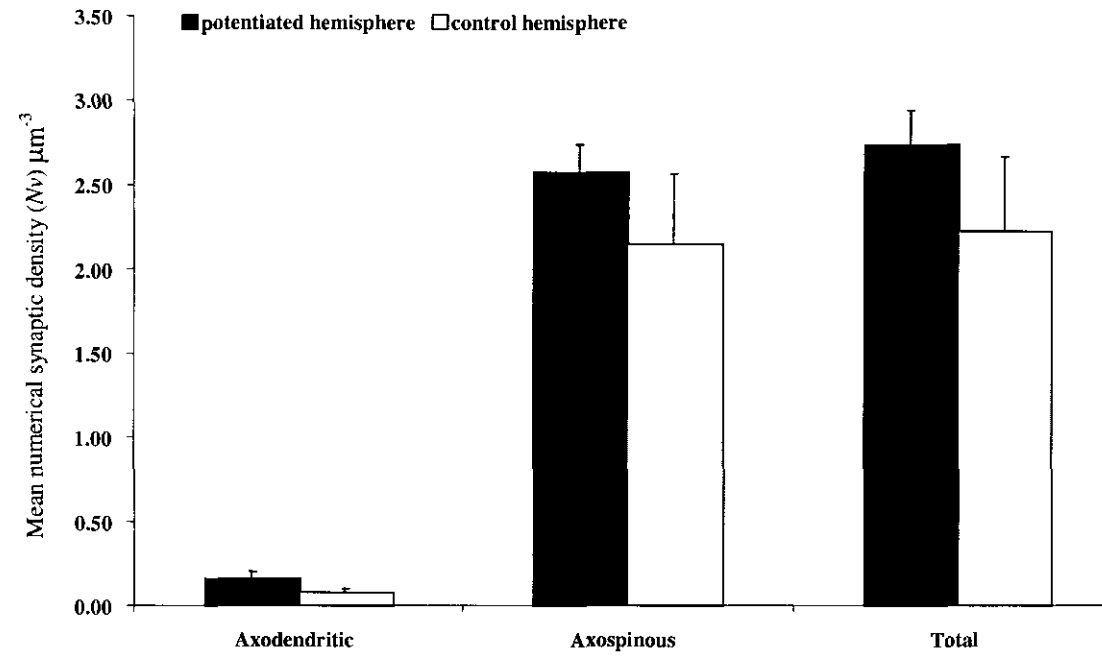

Figure 4.11 Mean numerical synaptic density (*Nv*) of synapses in the inner molecular layer, in potentiated and control hemispheres, 24h after the induction of LTP by HFS. Mean (± S.E.M.) of 5 animals.

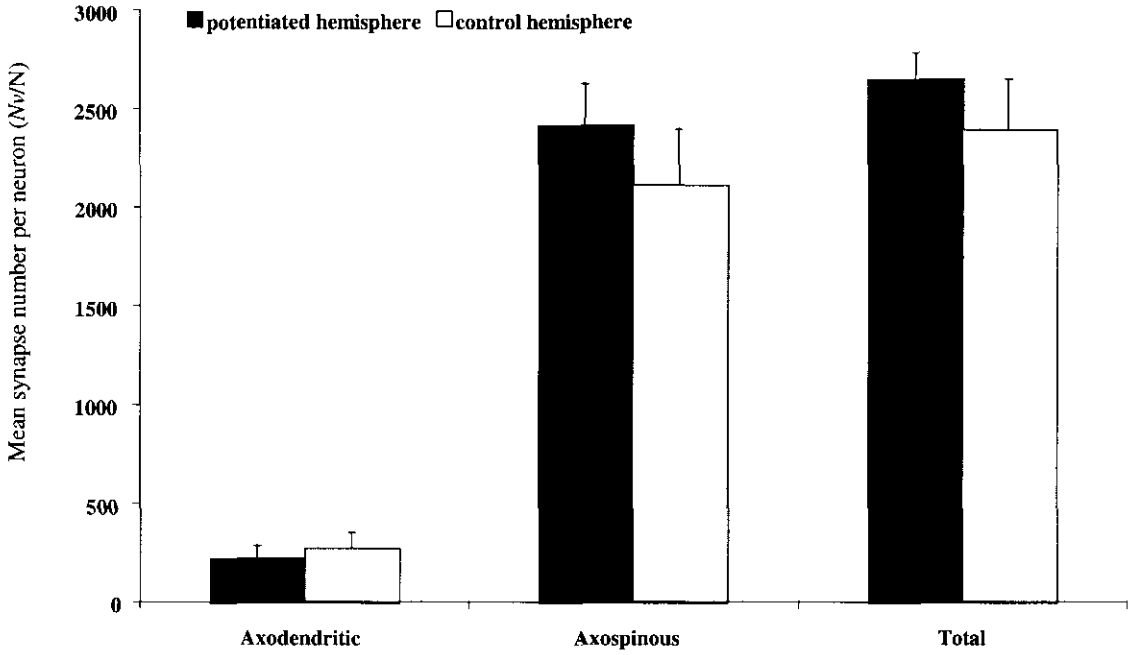

Figure 4.12 Mean synapse number per neuron in the middle molecular layer of the dentate gyrus, in potentiated and control hemispheres, 24h after the induction of LTP by HFS. Mean (± S.E.M.) of 5 animals.

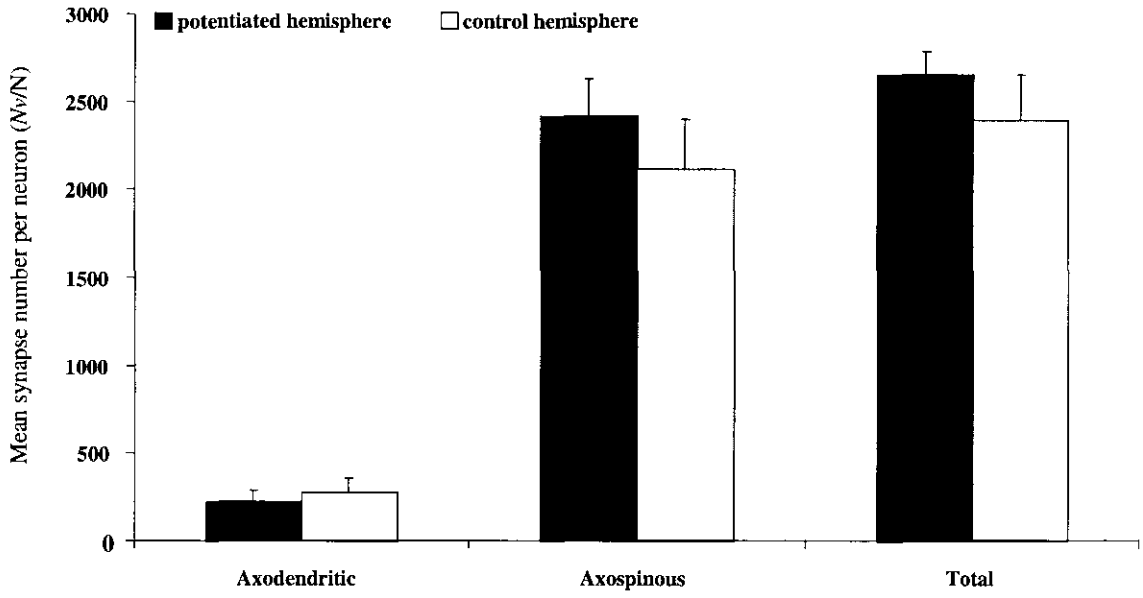

Figure 4.13 Mean synapse number per neuron in the inner molecular layer of the dentate gyrus, in the potentiated and control hemispheres, 24h after the induction of LTP by HFS. Mean (± S.E.M.) of 5 animals.

4.3.4 Mean projected synaptic height.

In the MML the mean projected synaptic height of axodendritic synapses was 190nm in the potentiated hemisphere and 156nm in the control group ($p<0.19$). In the same region, the mean synaptic height of axospinous synapses was 119nm and 131nm ($p<0.26$). In the IML, axodendritic synapses had a mean synaptic height of 99nm in the experimental and 106nm in the control hemisphere ($p<0.43$) and axospinous synapses were 128nm and 159nm respectively ($p<0.16$). (Figure 4.14)

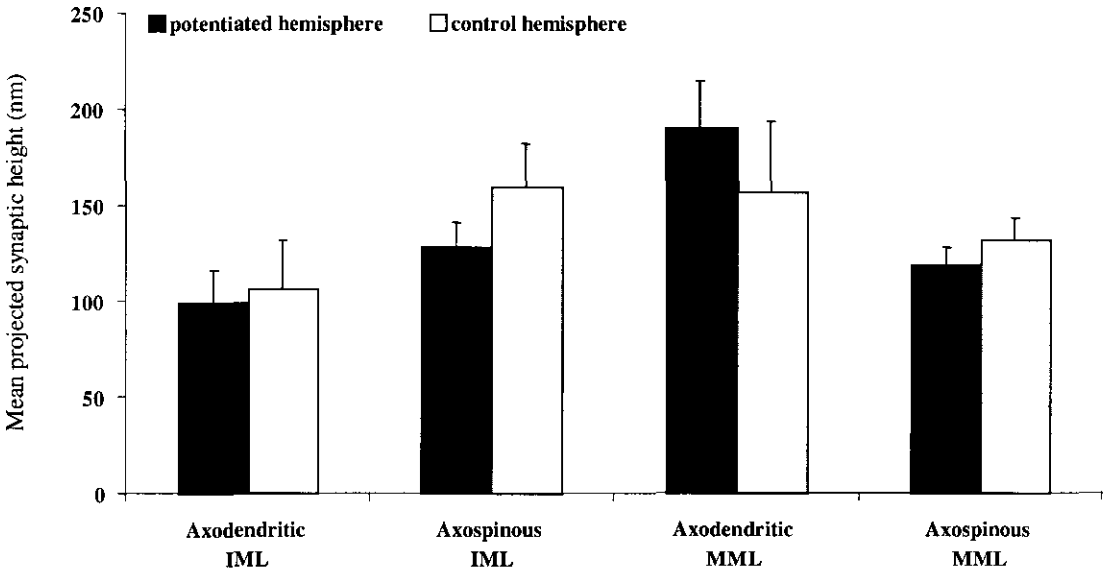

Figure 4.14 Mean projected synaptic height of synapses, in the inner and middle molecular layers of the dentate gyrus, 24h after the induction of LTP by HFS. Mean (± S.E.M.) of 5 animals

4.3.5 Total volume density of AZ area (*Sv*)

There were no significant differences in the mean total volume density of synapses between the potentiated and contralateral hemispheres. In the MML the *Sv* was $0.09\mu m^2/\mu m^3$ and $0.08\mu m^2/\mu m^3$ respectively ($p<0.12$) and in the IML $0.11\mu m^2/\mu m^3$ and $0.10\mu m^2/\mu m^3$ ($p<0.41$). (Figure 4.15)

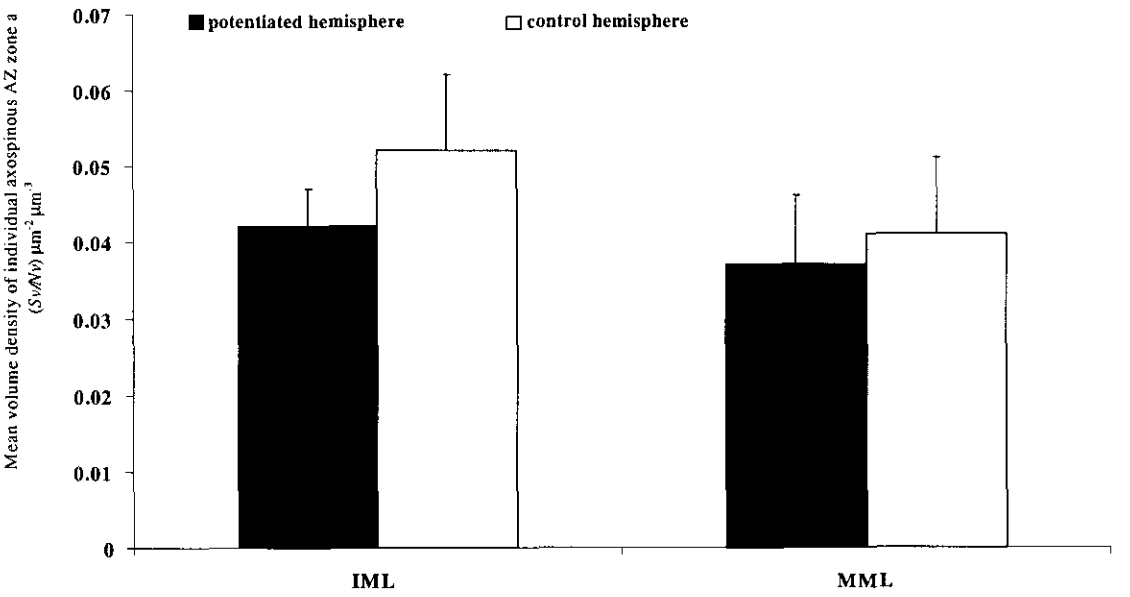

Figure 4.16 Mean volume density of individual axospinous apposition zone (AZ) area (*Sv/Nv*) in the inner and middle molecular layers of the dentate gyrus, 24h after the induction of LTP by HFS. Mean (± S.E.M.) of 5 animals.

In the IML, there were no significant differences in the numbers of synapses between the hemispheres. There were means of 5.60 (4.97%) perforated and 33.6(29.76%) concave profiles in the potentiated hemisphere and 3.20 (3.55%) ($p< 0.15$) and 31.6 (30.23%) ($p<0.43$) respectively in the control hemisphere. There was a mean of 72.8 (65.28%) macular synapses in the potentiated hemisphere and 66.8 (66.21%) in the control hemisphere ($p<0.20$). (Figure 4.18)

4.4 Pooled results

The morphological results from the molecular layer after each of the stimulation protocols produced some similar trends but also some differing results. Animals were perfused for morphological examination if the degree of potentiation measured after 24h was between 130 and 160%. To attempt to elucidate these findings the results from three animals that demonstrated the greatest degree of LTP, from each group, were pooled i.e. after TBS those animals with potentiation levels of 143%, 152% and 146% and after HFS 136%, 160% and 143%. For many parameters studied, there was

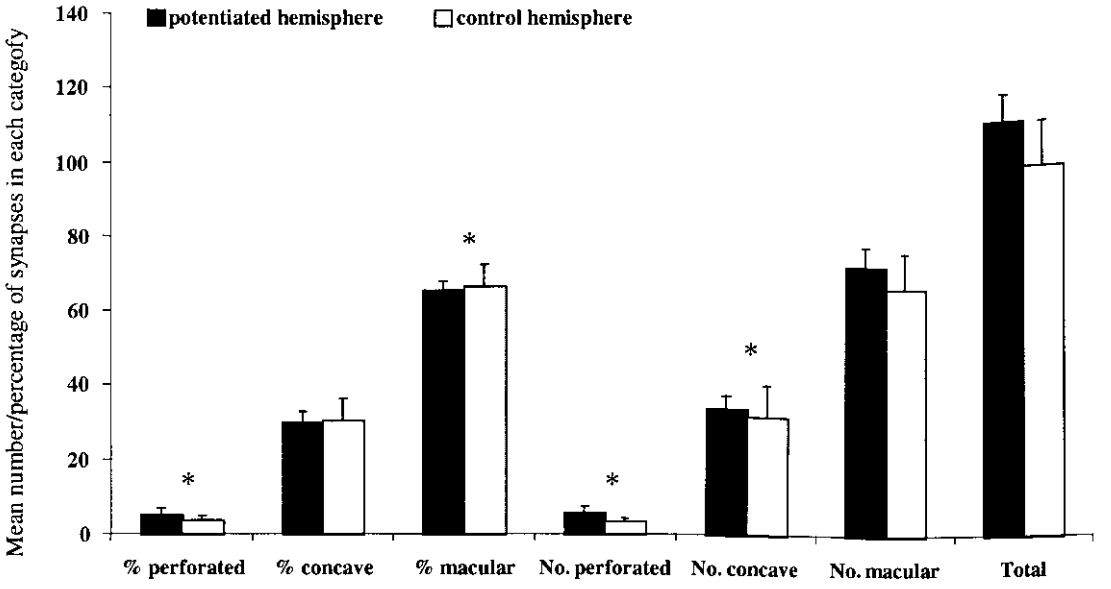

Figure 4.17 Morphology of axospinous synapses in an area of 350μm^2, in the middle molecular layer of the dentate gyrus, 24h after the induction of LTP by HFS. (* indicates significant difference $p<0.05$). Mean (± S.E.M.) of 5 animals.

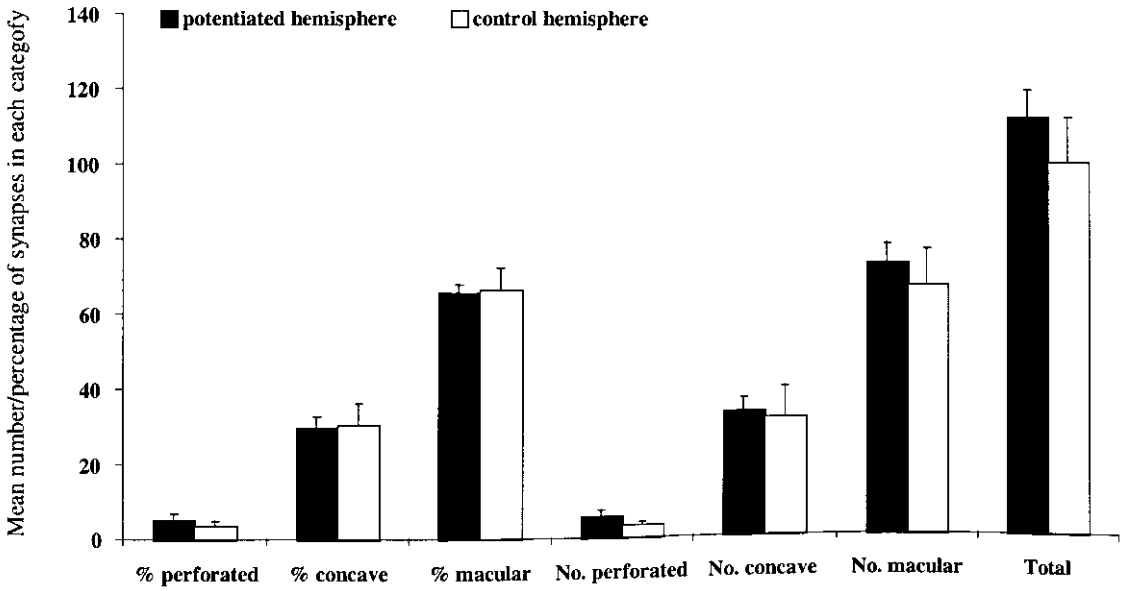

Figure 4.18 Morphology of axospinous synapses in an area of 350μm^2, in the inner molecular layer of the dentate gyrus, 24h after the induction of LTP by HFS. Mean (± S.E.M.) of 6 animals.

no significant difference between the hemispheres in the MML or IML. However there were some interesting differences in morphology and morphometry.

4.4.1 Neuronal density

There was no significant difference in the neuronal density of the granule cell layer between the potentiated and control hemispheres ($p<0.29$). (Figure 3.14) In the potentiated hemisphere there were an estimated 0.0094 neurons per μm^3 and in the control hemisphere 0.0087 neurons per μm^3.

4.4.2 Mean numerical synaptic density (*Nv*)

The pooled results confirmed the increased mean numerical density of axospinous synapses with an *Nv* of 2.60 μm^{-3} in the potentiated hemisphere and 1.76 μm^{-3} in the control hemisphere ($p<0.01$). (Figure 4.19) The differences in axospinous mean numerical synaptic density between the IML and MML in the potentiated ($p<0.31$) and control hemispheres ($p<0.16$) were not significant. There was also a significant difference in the number of axospinous synapses per neuron i.e. 2955 in the potentiated hemisphere and 2019 in the control hemisphere ($p<0.03$). (Figure 4.20) None of these parameters was shown to demonstrate any significant differences, between hemispheres, in the IML.

4.4.3 Morphometry

There were no significant differences in any of the morphometric parameters in the middle (Table 4.2), or inner molecular layers. (Table 4.5) The mean total *Sv* of all axospinous synapses was larger in the potentiated hemisphere but just outside the level of significance ($p<0.06$).

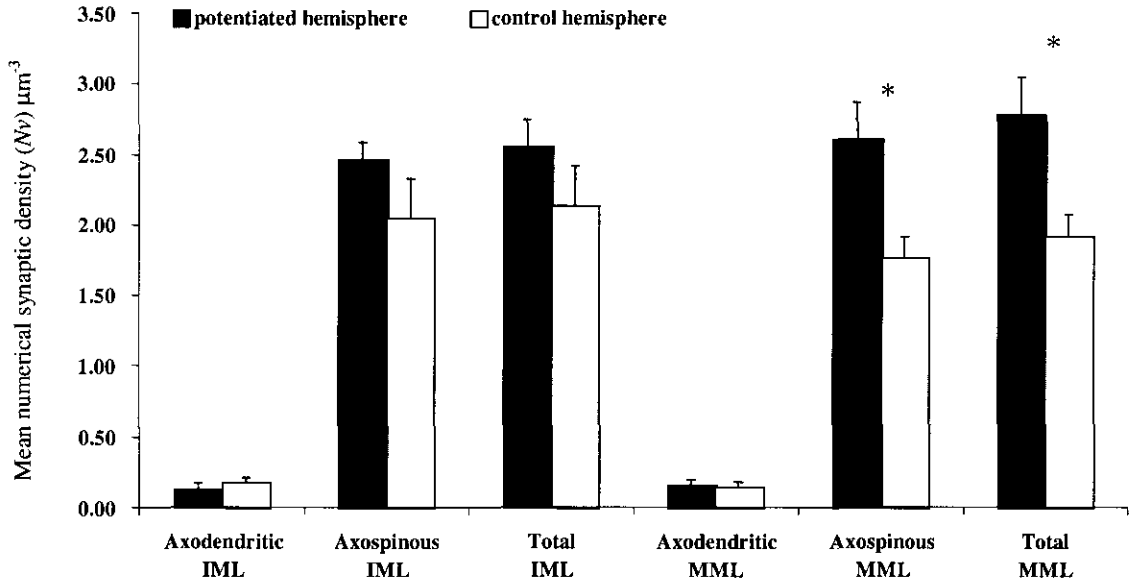

Figure 4.19 Mean numerical synaptic density (*Nv*) of synapses in the inner and middle molecular layer of the dentate gyrus, in potentiated and control hemispheres, 24h after the induction of LTP. Pooled results with 3 animals potentiated with TBS and 3 animals with HFS. (* indicates significant difference $p<0.05$). Mean (± S.E.M.) of 6 animals.

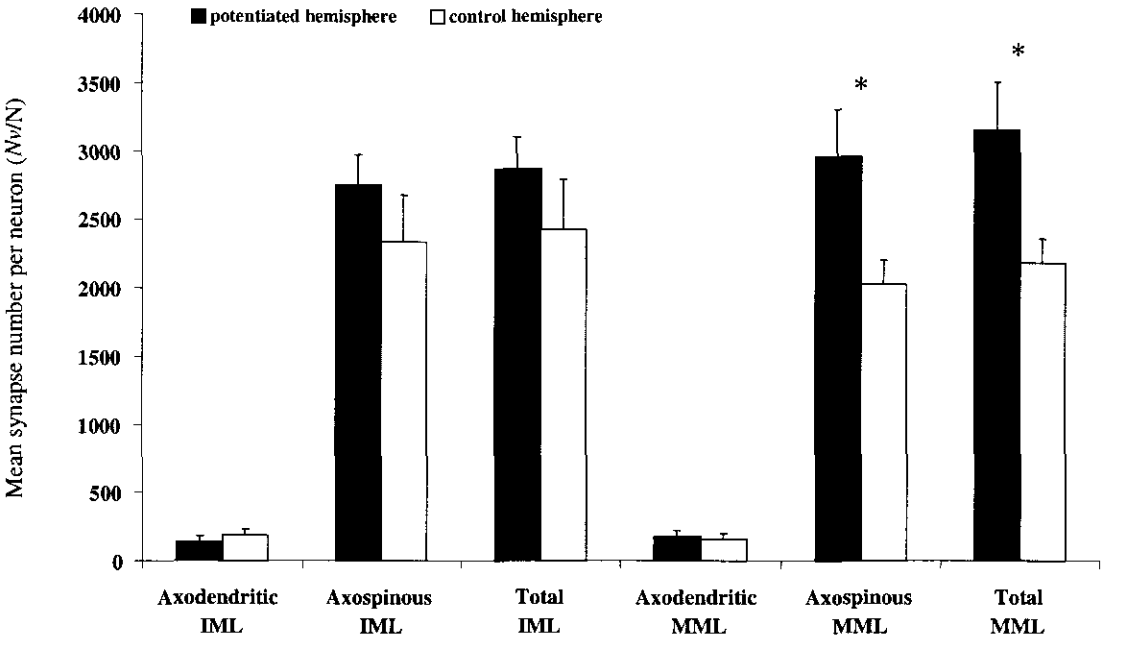

Figure 4.20 Mean number of synapses per neuron in the inner and middle molecular layers of the dentate gyrus, in potentiated and control hemispheres, 24h after the induction of LTP. Pooled results with 3 animals potentiated with TBS and 3 animals with HFS. Mean (± S.E.M.) of 6 animals.

4.4.4 Synaptic Morphology

There was a significant increase in the number of synapses with concave profiles in the MML ($p<0.04$) but this was replicated in the IML ($p<0.02$). There was also a significant increase in the number of perforated synapses in the IML ($p<0.05$). (Figure 4.21)

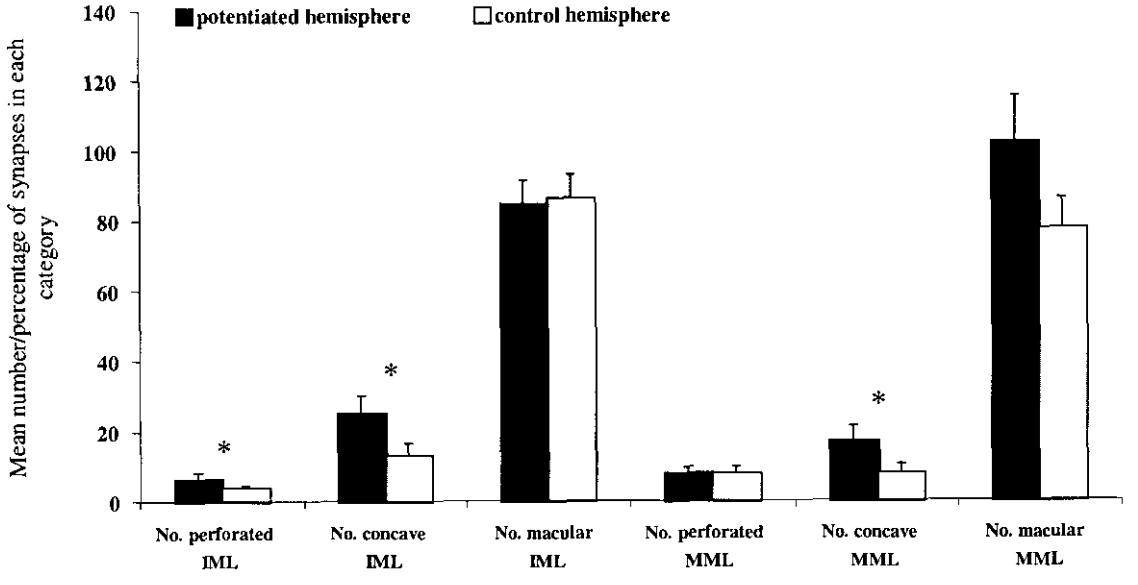

Figure 4.21 Morphology of axospinous synapses in the inner and middle molecular layers of the dentate gyrus, in potentiated and control hemispheres, 24h after the induction of LTP. Pooled results with 3 animals potentiated with TBS and 3 animals with HFS. (* indicates significant difference $p<0.05$). Mean (± S.E.M.) of 6 animals.

4.5 Discussion

These data demonstrate that in young adult rats there are significant differences in the numerical density of synapses in the middle molecular layer of the dentate gyrus 24h after tetanisation in the potentiated compared with the control hemisphere. The level of significance varies according to the stimulation protocol but, coupled with the pooled results, they suggest that there is a bonafide increase in the number of asymmetric axospinous synapses 24h after LTP induction.

A similar study, also using unbiased stereological techniques, reported an 11% increase in the total number of synapses per neuron, in the MML, 24h after the induction of LTP with HFS (Weeks *et al.,* 1999). There were some methodological differences between the studies: they used higher frequency stimulation (400Hz as opposed to the 200 Hz and TBS used here) and the control group consisted of implanted non-stimulated animals. This increase was not significant but, interestingly, synaptic number was positively correlated with the degree of potentiation (Weeks *et al.,* 1998). Animals with a higher *a priori* number of synapses could show a greater degree of potentiation, however, as found in the present study, dissimilar distributions of synapses per neuron were reported and the mean for LTP tissue was higher and the variance greater.

Whilst there was a trend towards a reduction in synaptic size in the potentiated hemisphere following LTP, this was not significant. The changes in the MML might be achieved in two ways: splitting of existing synapses with complete partitioning of AZs, or shrinkage of some AZs while new synapses are formed. Studies, including those reported in the previous chapter, have shown that from 45min post-tetanisation there is no significant difference in the incidence of perforated synapses. However, increases in spine density (Trommald and Hulleberg, 1997) and in multiple synaptic contacts (Toni *et al.,* 1999) have been reported from around this time. This suggests that synapses with segmented PSDs may develop separate presynaptic boutons and form new synapses with spines with a divided stem and two heads (bifurcating spines), or new dendritic spines.

There is some disagreement whether segmented synapses are indeed the precursors of new macular synapses as previously suggested (Nieto-Sampedro, 1982). Spines with perforated PSDs could arise directly from the dendritic shaft during development and not need a cycle of synapse splitting and spine retraction to form. (Geinisman *et al.,* 1996) Studies of the maturation of synapses in immature hippocampal CA1 have determined that perforated synapses increase their number in

parallel with macular synapses (Sorra and Harris, 1998). Since almost no splitting of dendritic spines occurs at postnatal day 15, splitting is unlikely to be important during development. As different parts of a perforated PSD make contact with the same presynaptic bouton, different branches of a splitting dendritic spine should also synapse with the same presynaptic bouton. During development, different branches of the same spine never synapse with the same presynaptic bouton, therefore bifurcating spines are unlikely to be transient intermediates in the process of dividing from perforated synapses (Sorra and Harris, 1998).

Similar observations have been made after LTP induction where an increase in spine density, particularly bifurcating spines, has been observed (Trommald and Hulleberg, 1997; Andersen and Soleng, 1998). However, when reconstructed, the twin spine heads never share the same presynaptic bouton (Trommald and Hulleberg, 1997) - arguing against PSD division as an intermediate step in synapse formation. However, when activated synapses, identified by the accumulation of calcium in dendritic spines, were examined 60min after the induction of LTP with HFS there was a marked increase in the proportion of axon terminals contacting two or more dendritic spines. Three-dimensional reconstruction revealed that these spines arose from the same dendrite thereby duplicating activated synapses (Toni *et al.,* 1999) and were not usually bifurcated. Confocal microscopy studies have indicated that LTP induction invokes the growth of small filipodia-like protrusions in CA1 neurons. 27% of these new filipodia developed a bulbous head within 60min post stimulation, which suggests that the filopodia might mature to become spines (Maletic-Savatic *et al.,* 1999).

There is no reason to believe that both mechanisms cannot be mutually employed in synaptogenesis. However, this new synapse formation, 40-60min after the induction of LTP, can only contribute to a later stage of LTP and may represent a way of consolidating changes in synaptic efficacy that are initiated by receptor insertion (Muller, 2000). Two hours after tetanisation, serial reconstruction failed to find any changes in synaptic morphology (Sorra and Harris, 1998). This suggests that

synapse populations could replace one and other and not be detected as a shift in the overall number, or a more plausible explanation may be the difficulty in detecting any change, as only a fraction of synapses undergo this duplication (Toni *et al.*, 1999).

Twenty-four hours after the induction of LTP, the increased number of axospinous synapses may be due to the maturation of synapses at filipodia or further synaptogenesis in the interim period. Neural cell adhesion molecules (NCAMs) are believed to play a role in the synaptic remodelling accompanying LTP e.g. the selective removal of polysialic acid (PSA) from NCAM can prevent the induction of LTP (Muller *et al.*, 1996). The major isoform (NCAM 180) is predominantly localised in postsynaptic membranes and the PSDs of hippocampal neurons (Schuster *et al.*, 1998) and strengthening of synaptic efficacy leads to an increase in expression of NCAM isoforms (Wheal *et al.*, 1998). The percentage of spine synapses expressing the NCAM 180 isoform increased in the dentate molecular layer 24h after tetanisation of the perforant path with HFS (Schuster *et al.*, 1998). As cells expressing polysialylated isoforms of NCAM have an increased capacity for structural plasticity (Doherty *et al.*, 1990; Doherty *et al.*, 1995) this would suggest that synaptic remodelling is a result of LTP.

Further evidence suggests that modification of synapses is a result of LTP. Synapsins, proteins associated with the cytoplasmic surface of the vesicle membrane are thought to play an important role in presynaptic function and synaptogenesis. Mice lacking synapsins suffer from impaired presynaptic function and a depletion of synaptic vesicles in nerve terminals (Ferreira *et al.*, 1998; Rosahl *et al.*, 1995). Synapsin I mRNA expression increases in dentate granule cells between 8h and 24h post LTP-inducing stimulation (Morimoto *et al.*, 1998) and increased synthesis of synapsin I protein, has been confirmed in the MML at a similar time point (Sato *et al.*, 2000). Synaptic spinules, protrusions of the postsynaptic membrane into presynaptic invaginations (Tarrant and Routtenberg, 1977), are thought to be involved in the process of synaptic turnover that enhances synaptic efficacy. Therefore, it is

interesting that an increased incidence of spinules has been reported 8h and 48h after LTP induction (Schuster *et al.*, 1990) and this morphological correlate may reflect the combined activity of the pre- and postsynaptic neuron.

A significant increase in the proportion of presynaptically concave synapses and perforated concave synapses, between potentiated and control animals has been reported 24h after the LTP induction with HFS (Weeks *et al.*, 1999). I have found a significant increase in the number of concave and perforated synapses after HFS but not TBS and, although the pooled results indicate a significant increase in the number of concave synapse in the MML, similar results were determined in the IML. Concavity may allow for more efficient uptake of released neurotransmitter but the incidence of synapses with concave profiles may be dependent on the stimulation protocol (See Chapter 5) as no correlation has been reported between the degree of potentiation and the number of concave synapses (Weeks *et al.*, 1998). Differences in the mechanisms of LTP induction and expression may also explain the increased incidence of axodendritic synapses after the induction of LTP with TBS. While LTP induction may or may not be associated with the production of concave or perforated synapses, synaptic number appears to be important for the degree of LTP expressed.

Paradoxically, a decrease in spine density and an increase in the relative frequency of shorter, thicker spines has been indicated 24h after the induction of LTP (Rusakov *et al.*, 1997b). There is no discrepancy between these two results because the number of synapses accommodated by each individual spine could increase while the spine densities fall. Computer simulations demonstrated that potentiation of postsynaptic responses was compatible with branching of a proportion of spines with their neighbours but was not compatible with retraction of spines (Rusakov *et al.*, 1997b). Partial fusion of active spines, which result in formation of spine branches, could significantly increase synaptic signal transfer (Rusakov *et al.*, 1996).

13 days after the induction and maintenance of LTP it has been demonstrated that the numbers of axodendritic synapses in the dentate gyrus increase (~28%) *in vivo*

(Geinisman *et al.,* 1996). Earlier studies from the same laboratory showed that the major structural correlate of the earlier phase of LTP (up to one-two hours) is an increased number of multiple, completely partitioned AZs at axospinous synapses (Geinisman *et al.,* 1993). By combining these results Geinisman and colleagues have suggested a scenario where the transition from the induction phase, to the maintenance phase of LTP is characterised by partitioning of axospinous synapses, a proportion of which gradually becomes axodendritic synapses (Geinisman *et al.,* 1996). (Figure 4.23)

My results from the intermediate stage of LTP consolidation, coupled with the study of Rusakov *et al.,* 1997b could complement this scenario. Partitioning of AZs, combined with spine fusion and/or retraction, may lead to an increased number of axospinous synapses 24h after the induction of LTP. Alternatively synaptogenesis may increase the number of axospinous synapses but in turn, there may be a transformation of some axospinous synapses into axodendritic synapses at a later stage. (Figure 5.2)

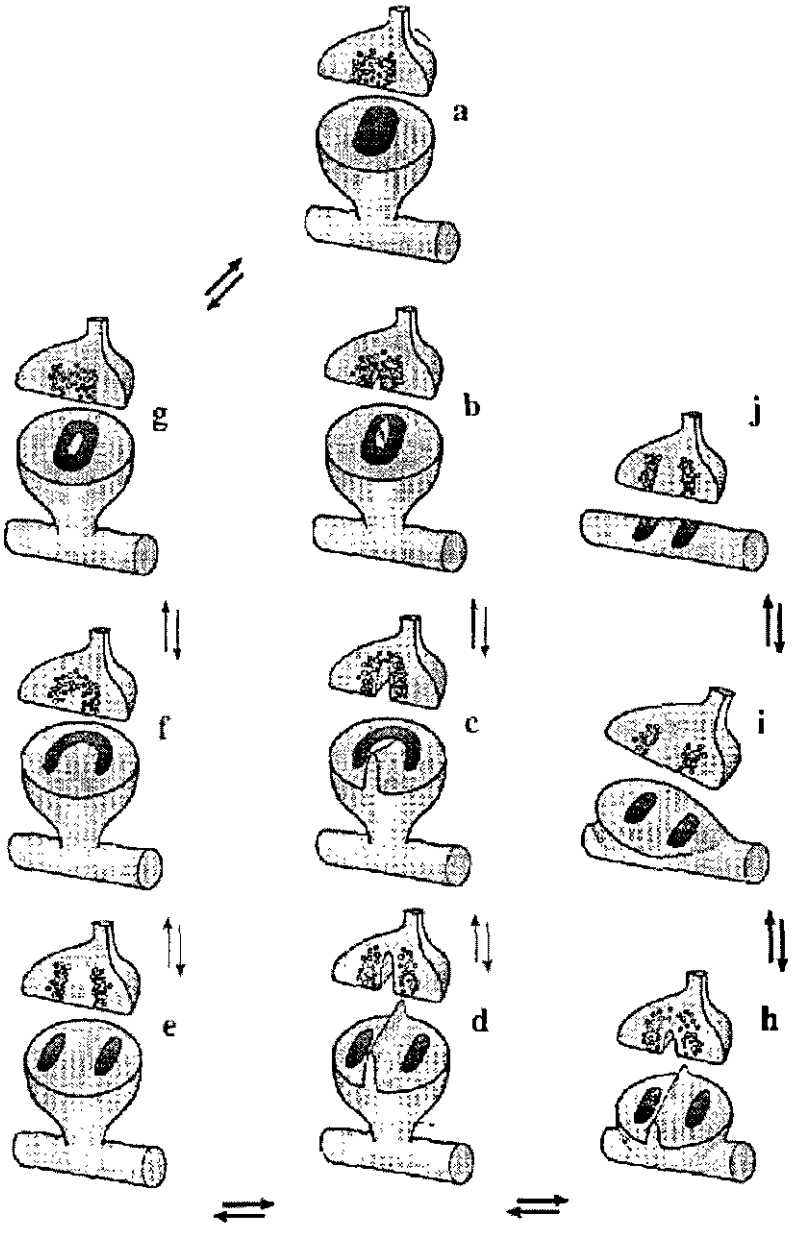

Figure 4.22 Schematic diagram of structural synaptic plasticity associated with LTP.

Geinisman suggests that a remodelling of pre-existing synaptic contacts underlies the selective increases in the number of either axospinous synapses with multiple completely partitioned transmission zones (d) following the induction of LTP or asymmetrical axodendritic synapses (j) during the maintenance phase of LTP. There may be many intermediates in synaptic plasticity from (a) a non-perforated axospinous synapse to various subtypes of perforated axospinous synapses. Those with partitions (spinules) include (b) a focal partition and fenestrated PSD, (c) a sectional spine partition and horseshoe shaped PSD, (d) complete spine partition and segmented PSD. Non-partitioned synapses may exhibit the same segmentation (e), horseshoe shape (f) or fenestration (g). The conversion of a perforated axospinous synapse to an axodendritic synapse may include subtypes of synapses involving a dendritic spine that does not have a neck (h); or a dendritic spine that is partially retracted into the parent dendrite (i); leading to an asymmetric axodendritic synapses with a perforated PSD (j). After Geinisman 1996.

		TBS	HFS	Combined
Mean numerical axodendritic synapse density (Nv) μm^{-3}	Potentiated hemispheres	**0.17 ± 0.03**	0.23 ± 0.07	0.16 ± 0.04
	Control Hemispheres	**0.07 ± 0.02**	0.26 ± 0.08	0.14 ± 0.04
	Potentiated v control	**p< 0.05**	p< 0.33	p< 0.39
Mean numerical axospinous synapse density (Nv) μm^{-3}	Potentiated hemispheres	2.55 ± 0.31	**2.50 ± 0.11**	**2.60 ± 0.26**
	Control Hemispheres	1.90 ± 0.17	**2.00 ± 0.16**	**1.76 ± 0.15**
	Potentiated v control	p< 0.08	**p< 0.03**	**p< 0.01**
Mean number of axodendritic synapses per neuron	Potentiated hemispheres	**213 ± 41**	219 ± 67	176 ± 44
	Control Hemispheres	**81 ± 24**	272 ± 80	157 ± 43
	Potentiated v control	**p< 0.04**	p< 0.25	p< 0.40
Mean number of axospinous synapses per neuron	Potentiated hemispheres	3230 ± 396	2415 ± 210	**2955 ± 345**
	Control Hemispheres	2292 ± 202	2110 ± 282	**2019 ±178**
	Potentiated v control	p< 0.06	p< 0.10	**p< 0.03**
Mean number of asymmetric synapses per neuron	Potentiated hemispheres	**3421 ± 425**	2644 ± 138	**3150 ± 347**
	Control Hemispheres	**2373 ± 194**	2390 ± 255	**2177 ± 176**
	Potentiated v control	**p< 0.05**	p< 0.15	**p< 0.03**

Table 4.1 Mean numerical synaptic density and synapse number per neuron, in the middle molecular layer of the dentate gyrus, 24h after the induction of LTP.

Results (± S.E.M.) of the numerical synaptic density (Nv) and synapse number per neuron, in the middle molecular layer of the dentate gyrus, 24h after the induction of LTP by theta-burst (TBS) or high frequency stimulation (HFS). The combined category represents the results from 3 animals with the highest levels of potentiation from each stimulation protocol (n=6).

		TBS	HFS	Combined
Axodendritic PSD height (nm)	Potentiated hemispheres	178 ± 33	190 ± 24	213 ± 26
	Control Hemispheres	171 ± 49	156 ± 37	199 ± 31
	Potentiated v control	p< 0.46	p< 0.19	p< 0.40
Axospinous PSD height (nm)	Potentiated hemispheres	135 ± 6	119 ± 9	122 ± 7
	Control Hemispheres	139 ± 8	131 ± 12	139 ± 11
	Potentiated v control	p< 0.33	p< 0.26	p< 0.12
Axospinous (*Sv*) $\mu m^2, \mu m^{-3}$	Potentiated hemispheres	**0.13 ± 0.012**	0.09 ± 0.02	0.11 ± 0.01
	Control Hemispheres	**0.10 ± 0.003**	0.08 ± 0.02	0.08 ± 0.01
	Potentiated v control	**p< 0.03**	p< 0.12	p< 0.06
Axospinous *Sv/Nv* $\mu m^2, \mu m^{-3}$	Potentiated hemispheres	0.05 ± 0.001	0.04 ± 0.004	0.04 ± 0.005
	Control Hemispheres	0.05 ± 0.002	0.04 ± 0.10	0.05 ± 0.009
	Potentiated v control	p< 0.39	p< 0.34	p< 0.15

Table 4.2 Synaptic morphometry, in the middle molecular layer of the dentate gyrus, 24h after the induction of LTP.

Results (± S.E.M.) of morphometric estimations of synaptic profiles in the middle molecular layer of the dentate gyrus, 24 h after the induction of LTP by theta-burst stimulation (TBS) or high frequency stimulation (HFS). The combined category represents the results from 3 animals with the highest levels of potentiation from each stimulation protocol (n=6).

		TBS	HFS	Combined
% Perforated profiles	Potentiated hemispheres	8.57 ± 1.35	**4.34 ± 1.50**	7.05 ± 1.67
	Control Hemispheres	11.10 ± 2.37	**1.93 ± 1.22**	8.27 ± 2.94
	Potentiated v control	p< 0.17	**p< 0.01**	p< 0.31
% Concave profiles	Potentiated hemispheres	13.09 ± 6.59	13.24 ± 0.77	15.31 ± 4.91
	Control Hemispheres	13.45 ± 4.93	9.23 ± 3.17	7.83 ± 1.99
	Potentiated v control	P< 0.49	P< 0.12	P< 0.10
% Macular profiles	Potentiated hemispheres	92.0 ± 1.72	**82.42 ± 1.88**	86.48 ± 2.69
	Control Hemispheres	88.9 ± 2.37	**88.85 ± 3.74**	86.96 ± 2.56
	Potentiated v control	p< 0.12	**p< 0.02**	p< 0.44
Mean number of perforated profiles	Potentiated hemispheres	10.2 ± 1.07	**4.34 ± 1.86**	8.0 ± 1.53
	Control Hemispheres	9.8 ± 1.66	**2.20 ± 1.95**	7.5 ± 2.40
	Potentiated v control	p< 0.42	**p< 0.03**	p< 0.38
Mean number of concave profiles	Potentiated hemispheres	14.8 ± 5.86	**15.0 ± 0.95**	**16.83 ± 4.22**
	Control Hemispheres	12.0 ± 4.38	**8.60 ± 3.66**	**7.83 ± 2.73**
	Potentiated v control	p< 0.38	**p< 0.05**	**p< 0.04**
Mean number macular synapses	Potentiated hemispheres	**115.8 ± 14.10**	94.4 ± 7.71	102.17 ± 13.16
	Control Hemispheres	**81.8 ± 6.72**	75.8 ± 9.36	77.33 ± 8.68
	Potentiated v control	**p< 0.05**	p< 0.15	p< 0.11

Table 4.3 Classification of synaptic profiles in the middle molecular layer of the dentate gyrus, 24h after induction of LTP.

Results (± S.E.M.) of the classification of synaptic profiles in 350μm^2 of the middle molecular layer of the dentate gyrus, 24 h after the induction of LTP by theta-burst stimulation (TBS) or high frequency stimulation (HFS). The combined category represents the results from 3 animals, with the highest levels of potentiation, from each stimulation protocol (n=6).

		TBS	HFS	Combined
Mean numerical axodendritic synapse density (Nv) μm^{-3}	Potentiated hemispheres	0.08 ± 0.04	0.16 ± 0.04	0.13 ± 0.04
	Control Hemispheres	0.09 ± 0.02	0.08 ± 0.02	0.17 ± 0.04
	Potentiated v control	p< 0.33	p< 0.09	p< 0.26
Mean numerical axospinous synapse density (Nv) μm^{-3}	Potentiated hemispheres	2.24 ± 0.19	2.57 ± 0.17	2.46 ± 0.12
	Control Hemispheres	2.43 ± 0.18	2.14 ± 0.42	2.05 ± 0.27
	Potentiated v control	p< 0.28	p< 0.17	p< 0.14
Mean number of axodendritic synapses per neuron	Potentiated hemispheres	97 ± 44	171 ± 42	136 ± 43
	Control Hemispheres	113 ± 21	192 ± 50	186 ± 42
	Potentiated v control	p< 0.37	p< 0.40	p< 0.23
Mean number of axospinous synapses per neuron	Potentiated hemispheres	2841 ± 245	2423 ± 113	2746 ± 225
	Control Hemispheres	2919 ± 214	2276 ± 465	2334 ± 339
	Potentiated v control	p< 0.42	p< 0.38	p< 0.13
Mean number of asymmetric synapses per neuron	Potentiated hemispheres	2937 ± 267	2475 ± 102	2861 ± 237
	Control Hemispheres	3028 ± 203	2311 ± 446	2426 ± 357
	Potentiated v control	p< 0.41	p< 0.38	p< 0.14

Table 4.4 Mean numerical synaptic density and synapse number per neuron, in the inner molecular layer of the dentate gyrus, 24h after the induction of LTP.

Results (± S.E.M.) of the numerical synaptic density (Nv) and synapse number per neuron, in the inner molecular layer of the dentate gyrus, 24h after the induction of LTP by theta-burst (TBS) or high frequency stimulation (HFS). The combined category represents the results from 3 animals with the highest levels of potentiation from each stimulation protocol (n=6).

		TBS	HFS	Combined
Axodendritic PSD height nm	Potentiated hemispheres	122 ± 20	99 ± 17	128 ± 16
	Control Hemispheres	145 ± 19	106 ± 26	106 ± 14
	Potentiated v control	p< 0.21	p< 0.43	p< 0.12
Axospinous PSD height nm	Potentiated hemispheres	139 ± 5	128 ± 13	136 ± 9
	Control Hemispheres	121 ± 3	159 ± 23	150 ± 20
	Potentiated v control	p< 0.02	p< 0.16	p< 0.31
Axospinous (*Sv*) $\mu m^2, \mu m^{-3}$	Potentiated hemispheres	0.11 ± 0.009	0.11 ± 0.007	0.11 ± 0.008
	Control Hemispheres	0.11 ± 0.004	0.10 ± 0.016	0.10 ± 0.012
	Potentiated v control	p< 0.41	p< 0.41	p< 0.20
Sv/Nv $\mu m^2, \mu m^{-3}$	Potentiated hemispheres	0.05 ± 0.001	0.04 ±0.005	0.05 ± 0.003
	Control Hemispheres	0.04 ± 0.002	0.05 ± 0.010	0.05 ± 0.008
	Potentiated v control	p< 0.07	p< 0.23	p< 0.28

Table 4.5 Synaptic morphometry in the inner molecular layer of the dentate gyrus, 24hr after the induction of LTP.

Results (± S.E.M.) of morphometric estimations of synaptic profiles, in the inner molecular layer of the dentate gyrus, 24 h after the induction of LTP by theta-burst stimulation (TBS) or high frequency stimulation (HFS). The combined category represents the results from 3 animals with the highest levels of potentiation from each stimulation protocol (n=6).

		TBS	HFS	Combined
% Perforated profiles	Potentiated hemispheres	6.90 ± 1.18	4.97 ± 1.83	5.76 ± 1.49
	Control Hemispheres	5.31 ± 0.67	3.55 ± 1.28	3.92 ± 0.93
	Potentiated v control	p< 0.21	p< 0.27	p<0.09
% Concave profiles	Potentiated hemispheres	14.06 ± 1.88	29.76± 3.05	**21.90 ± 3.74**
	Control Hemispheres	9.58 ± 2.25	30.23 ± 5.99	**14.03 ± 4.28**
	Potentiated v control	p< 0.09	p< 0.47	**p< 0.02**
% Macular profiles	Potentiated hemispheres	93.10 ± 1.18	65.28 ± 2.63	79.45 ± 5.66
	Control Hemispheres	94.69 ± 0.67	66.21 ± 5.99	86.17 ± 11.81
	Potentiated v control	p< 0.21	P< 0.43	p< 0.23
Mean number of perforated profiles	Potentiated hemispheres	6.80 ± 1.77	5.60 ± 1.94	**6.33 ± 1.74**
	Control Hemispheres	5.60 ± 0.68	3.20 ± 1.02	**3.67 ± 0.76**
	Potentiated v control	p< 0.31	p< 0.15	**p< 0.05**
Mean number of concave profiles	Potentiated hemispheres	13.8 ± 2.29	33.6 ± 3.43	**25.00 ± 5.05**
	Control Hemispheres	10.00 ± 2.21	31.6 ± 8.52	**12.83 ± 3.73**
	Potentiated v control	p< 0.16	p< 0.43	**p< 0.02**
Mean number macular synapses	Potentiated hemispheres	89.4 ± 6.53	72.8 ± 5.24	84.67 ± 6.62
	Control Hemispheres	98.20 ± 7.05	66.8 ± 9.85	86.17 ± 6.62
	Potentiated v control	p< 0.16	p< 0.20	p< 0.23

Table 4.6 Classification of synaptic profiles in the inner molecular layer of the dentate gyrus, 24h after the induction of LTP.

Results (± S.E.M.) of the classification of synaptic profiles, in 350μm^2 of the inner molecular layer of the dentate gyrus, 24 h after the induction of LTP by theta-burst stimulation (TBS) or high frequency stimulation (HFS). The combined category represents the results from 3 animals, with the highest levels of potentiation, from each stimulation protocol (n=6).

Chapter Five General Discussion

It has been established that long-term potentiation is an enhancement of synaptic strength that can be produced by the pairing of presynaptic activity with postsynaptic depolarisation and can last for many days (Bliss and Collingridge, 1993). Many morphological changes have been shown to occur with LTP, but it is important to consider the extent to which the observed alterations could account for the increase in synaptic efficacy during LTP.

Morphological studies have affirmed some of the mechanisms believed to be involved in the induction phase of L-LTP i.e. the 2h post-tetanisation period that is mediated by the modification of kinases (Racine *et al.*, 1983). Studies of the dynamics of presynaptic vesicles have supported the concept that glutamate is released during the induction of LTP. One minute after tetanic stimulation in hippocampal area CA1, the proportion of presynaptic vesicles near to the presynaptic membrane, or attached to the membrane, increased although the total number of vesicles decreased (Applegate and Landfield, 1988). Early postsynaptic morphological changes are triggered by alterations in calcium homeostasis (Fifkova and Morales, 1992; Harris and Kater, 1994; Harris, 1999) after LTP induction. A rise in the postsynaptic calcium concentration, and consequent activation of various signalling cascades, leads to modification of the actin-dependent dynamics of the spine, transformation of receptor properties and insertion of new receptors into the PSD - mechanisms that are restricted to activated synapses.

These modifications may result in changes in the size and shape of synapses and such changes have been found associated with LTP (Fifkova and Anderson, 1981); Van Harreveld and Fifkova, 1975; Desmond and Levy, 1986b; Weeks *et al.*, 2000). In the research reported in this thesis any difference observed in the size of synapses between hemispheres was not significant however, when only activated synapses have been examined, increased area of spine head profiles and increased length of PSDs have been reported (Buchs and Muller, 1996).

Changes in the incidence of concave synapses have been reported after LTP and the concavity of a synapse may have a role in increasing synaptic efficacy by allowing for more efficient uptake of neurotransmitter (Chang and Greenough, 1984; Desmond and Levy, 1986b). Concave synapses tend to be larger (Desmond and Levy, 1986b) and presumably have more receptors (Nusser *et al.*, 1998) and this larger PSD area may mediate the enhanced synaptic function measured in LTP. Here, whether 45 min or 24h after the induction of LTP, the incidence of concave synapses did not change when TBS was used to induce potentiation. This could be due to differences in the mechanisms of induction and maintenance of L-LTP when different stimulating protocols are employed (Larkman and Jack, 1995). Alternatively, the absence of an increased incidence of concave synapses may explain why L-LTP induced by TBS is not always as robust as L-LTP induced by HFS.

In most studies L-LTP is produced by multiple trains of strong, artificial stimulation which probably does not occur in nature. cAMP mediated transcription is important for the development of L-LTP and tetani that generate L-LTP have been shown to provoke increased gene expression (Impey *et al.*, 1996) which can be instigated by activation of PKA and adenylyl cyclase. Unlike LTP induced by non-theta tetanisation regimes, little is known about the biochemical mechanisms underlying theta-burst LTP in the hippocampus (Nguyen and Kandel, 1997). Evidence suggests that synapses that undergo LTP can undergo a family of phenotypically similar but mechanistically quite different synaptic changes (Fields *et al.*, 1997).

Therefore, even NMDA receptor -dependent LTP does not necessarily imply a single mechanism and it is important that different protocols for eliciting LTP be employed when examining morphological changes (Winder *et al.*, 1999).

Endogenous neurotrophins may play a role in mediating L-LTP induction. The application of antibodies to the Trk receptors of hippocampal slices had no effect on LTP induced by several trains of tetanic stimulation; however, there were significant deficits in LTP induced by TBS. Slices exposed to the same number of inducing stimuli, delivered either as TBS or as a single 100 Hz tetanisation, only exhibited Trk-sensitive LTP when TBS was used. The late phase of LTP was also significantly impaired in slices pre-treated with these antibodies. TrkB ligands were required for up to 1 hr after induction to maintain L-LTP. These results indicate that both the temporal patterns of synaptic activity and the different temporal phases of synaptic enhancement are important in determining the neurotrophin dependence of plasticity in the hippocampus (Kang *et al.*, 1997).

Other studies have pointed toward a specific and unique role of endogenous BDNF but not of other neurotrophins in the process of TBS-induced hippocampal LTP (Chen *et al.*, 1999). After the application of BDNF antibodies, deficits in LTP were observed with TBS but not with tetanic stimulation. LTP was only reduced if BDNF was blocked before and during TBS stimulation, suggesting that endogenous BDNF is required for a limited time period around the time of LTP induction but not during the whole process of LTP.

Studies using protein kinase inhibitors have suggested functional roles for several kinases in the induction of LTP in the hippocampus e.g. inhibitors of PKA attenuate both the early and late components of L-LTP (Matthies and Reymann, 1993) (Frey *et al.*, 1993). The precise role of any given kinase has yet to be fully established but it has been observed that LTP produced by theta frequency stimulation is completely dependent on PKA (Thomas *et al.*, 1996).

There is some evidence that the molecular mechanisms may be similar regardless of the stimulation applied. Investigations in area CA1 of the mouse hippocampus have suggested that cAMP- mediated gene transcription may be a common mechanism responsible for the late phases of LTP induced by both theta and non-theta patterns of stimulation (Nguyen and Kandel, 1997). One of the targets of the cAMP/PKA pathway is the phosphorylation of transcription factors such as cAMP response-element-binding protein (CREB) which directly affects gene expression required for late LTP and after HFS there is a direct activation of CREB.

However, different patterns of stimulation may produce LTP by recruiting different molecular signalling pathways. Activation of the MAPK pathway is critical for the induction and maintenance of L-LTP (Impey *et al.*, 1998) but LTP produced by TBS differs from LTP produced by HFS by requiring activated ERK (Winder *et al.*, 1999). Activated ERK may regulate synaptic efficacy at the postsynaptic membrane and possibly play a role in targeting long-term changes to activated synapses (Thomas *et al.*, 1996).

Regardless of the stimulating protocol, morphological changes in the incidence of perforated synapses have been observed (Buchs and Muller, 1996; Toni *et al.*, 1999; Weeks *et al.*, 2000; Geinisman *et al.*, 1993). Activated synapses may develop separate presynaptic boutons and therefore strengthen synaptic transmission and eventually result in a duplication of spine synapses and an increase in synaptic efficacy by increasing the number of release sites between the individual synaptically coupled neurons.

Glutamatergic excitatory synapses contain both ionotropic and metabotropic glutamate receptors, NMDAR and AMPAR. The ratio of NMDAR and AMPAR is physiologically important as one extreme produces synapses that are silent at normal resting potentials (Issac *et al.*, 1995) while, at the other, synapses are formed that are incompatible with NMDA receptor-dependent synaptic plasticity (Madison *et al.*,

1991). These effectively non-functional synapses have been observed in various regions of the hippocampus (Liao *et al.*, 1995; Min *et al.*, 1998).

These silent synapses acquire AMPA-type responses following LTP induction and this modification could be caused by an increase in the number of receptors, their open probability, their kinetics, or their single-channel conductance. Elementary channel properties can be rapidly modified by synaptic activity such as the induction of LTP (Benke *et al.*, 1998) but tetanic stimulation has been shown to induce a rapid delivery of GluR1 AMPA receptors into dendritic spines (Shi *et al.*, 1999).

The GluR2 subunit is the most commonly expressed form of glutamate receptor and, in studies of dissociated cell culture, a punctate surface distribution of AMPA receptors, co-localised with synaptophysin, has been demonstrated (Noel *et al.*, 1999). Synaptic size may be an important factor in determining the ratio of AMPA to NMDA receptors at the synapse and the ratio may depend on the PSD diameter (Takumi *et al.*, 1999) and require synapses to grow in size after the insertion of AMPA receptors. Studies of immunoreactive AMPA receptor density have observed that the most densely labelled synapses tend to be on the largest spines, an average PSD diameter of 260nm, while many smaller spines remained unlabelled (< 160nm) (Nusser *et al.*, 1998; Takumi et al., 1999; Baude *et al.*, 1995).

It has been suggested that two regulatory mechanisms control the local insertion and removal of AMPA receptors from the synapse - a constructive pathway and a maintenance pathway (Malinow *et al.*, 2000). The constructive pathway is rapidly turned on by synaptic activity. It is driven by transient events localised at a few synapses e.g. the rise in Ca^{2+} concentration in spines, and results in a change, in the number of receptors, at those synapses. Receptors with the GluR1 subunit are delivered to the postsynaptic membrane this way and it has been demonstrated that GluR1 knockout mice do not demonstrate LTP. However these mice do not show a learning deficiency and it has been proposed that the GluR4 subunit, with a similar carboxy tail, is also trafficked by this pathway. The maintenance pathway is always

switched on and is responsible for the constant turnover in receptors. It replaces existing postsynaptic receptors with receptors from a reserve pool (either newly synthesised or recycled) and does not increase or decrease the number of receptors. This is the mechanism for trafficking of AMPA receptors with the GluR2 and GluR3 subunit, which have similar intracellular domains.

The trafficking and stabilisation of AMPA receptors in synapses may be controlled through interactions with the AMPA receptors intracellular carboxy tails and variety of cytosolic proteins that then interact with various transmembrane proteins and form a scaffolding complex. Presently, GluR1 is only known to interact with synapse associated protein 97 (SAP 97) (Leonard *et al.*, 1998). Interaction between NSF and GluR2 is involved in the recycling process that is necessary for the insertion and stabilisation of AMPA receptors at the PSD (Noel et al., 1999).

It is proposed that the delivery of receptors with GluR1 subunits depends on a retention signal that prevents the insertion of receptors into the synapse unless relieved by activity - it has been shown that GluR1 cannot enter spines unless there is postsynaptic activation of NMDA receptors (Shi et al., 1999). Once inserted in synapses, GluR1-containing receptors are renewed by the maintenance pathway and the availability of these receptors to this pathway may well depend on protein synthesis initiated by kinase activity (Malinow *et al.*, 2000).

Activation of mGluRs is also required for induction of LTP (Bashir *et al.*, 1993; Richter-Levin *et al.*, 1994) and while the ratio of AMPA to NMDA receptors is important, ionotropic and metabotropic receptors require segregation from each other within the PSD at individual synapses. The irregular outline of some synapses may result from a need to accommodate more perisynaptic mGluRs by increasing the circumference of the PSD. Therefore, perforated synapses may develop in order to increase the ratio of perisynaptic to synaptic membrane proteins and keep their relative distance from transmitter release sites constant (Lujan, 1996). (Figure 5.1) It has been demonstrated that in the MML of the dentate gyrus, perforated axospinous synapses

switched on and is responsible for the constant turnover in receptors. It replaces existing postsynaptic receptors with receptors from a reserve pool (either newly synthesised or recycled) and does not increase or decrease the number of receptors. This is the mechanism for trafficking of AMPA receptors with the GluR2 and GluR3 subunit, which have similar intracellular domains.

The trafficking and stabilisation of AMPA receptors in synapses may be controlled through interactions with the AMPA receptors intracellular carboxy tails and variety of cytosolic proteins that then interact with various transmembrane proteins and form a scaffolding complex. Presently, GluR1 is only known to interact with synapse associated protein 97 (SAP 97) (Leonard *et al.*, 1998). Interaction between NSF and GluR2 is involved in the recycling process that is necessary for the insertion and stabilisation of AMPA receptors at the PSD (Noel et al., 1999).

It is proposed that the delivery of receptors with GluR1 subunits depends on a retention signal that prevents the insertion of receptors into the synapse unless relieved by activity - it has been shown that GluR1 cannot enter spines unless there is postsynaptic activation of NMDA receptors (Shi et al., 1999). Once inserted in synapses, GluR1-containing receptors are renewed by the maintenance pathway and the availability of these receptors to this pathway may well depend on protein synthesis initiated by kinase activity (Malinow *et al.*, 2000).

Activation of mGluRs is also required for induction of LTP (Bashir *et al.*, 1993; Richter-Levin *et al.*, 1994) and while the ratio of AMPA to NMDA receptors is important, ionotropic and metabotropic receptors require segregation from each other within the PSD at individual synapses. The irregular outline of some synapses may result from a need to accommodate more perisynaptic mGluRs by increasing the circumference of the PSD. Therefore, perforated synapses may develop in order to increase the ratio of perisynaptic to synaptic membrane proteins and keep their relative distance from transmitter release sites constant (Lujan, 1996). (Figure 5.1) It has been demonstrated that in the MML of the dentate gyrus, perforated axospinous synapses

are twice as likely to express detectable levels of AMPA receptor subunits as their non-perforated counterparts (Desmond and Weinberg, 1998). Although this study could not establish if the AMPA receptors identified were actually functional, segmented synapses could therefore be perceived as more potent than non-perforated synapses or the vestiges of recent synaptic activity. The authors of this study believe it

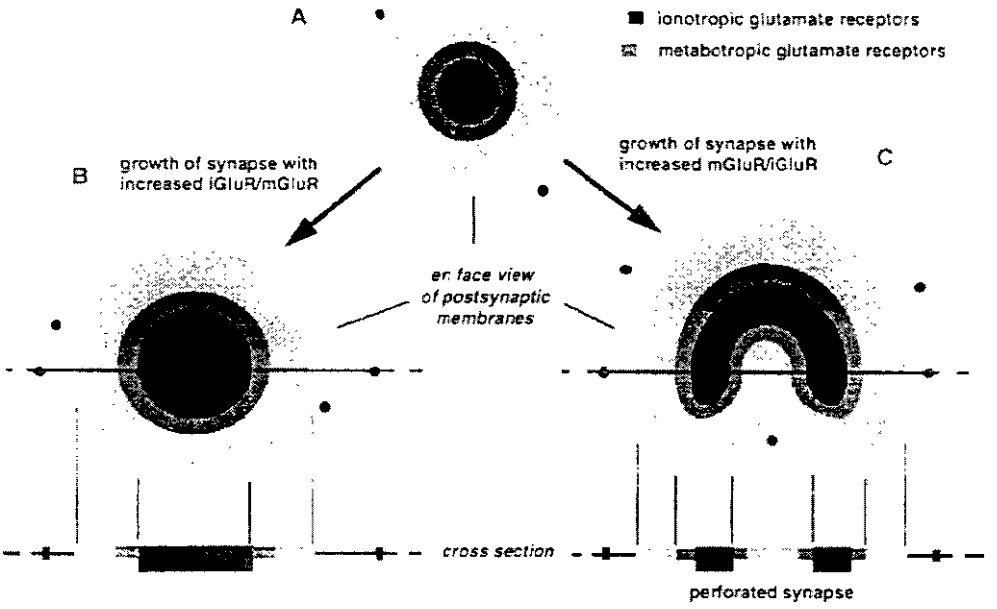

Figure 5.1 Schematic diagram of the distribution of glutamate receptors at glutamatergic synapses in the hippocampus.

(A) Summary of the distribution of postsynaptic ionotropic (black) and metabotropic (grey) glutamate receptors at glutamatergic synapses in the hippocampus. The AMPA-type receptors are concentrated in the membrane opposite the presynaptic bouton in an area concomitant with the PSD. The type 1 and 5 mGluRs are concentrated in a perisynaptic ring surrounding the ionotropic receptors, followed by a wider band of receptors decreasing in density. Both classes occur at a lower density further in the extrasynaptic membranes (dots). (B) A possible effect of the segregation of receptor classes is that when synapses increase in size, an expansion of the postsynaptic membrane occupied by ionotropic receptors may lead to an increase in the ionotropic to metabotropic receptor ratio, if the synaptic density maintains a regular edge. (C) If synapses increase in size by producing a PSD with an irregular edge, leading to the appearance of perforated synapses, this could increase the metabotropic to ionotropic receptor ratio and maintain the relative spatial relationship between the centre of the presynaptic bouton and the metabotropic receptors. After Lujan et al 1996

to be unlikely that the difference in the incidence of AMPA receptors is entirely due to their larger size. It has been demonstrated that changes in the postsynaptic structure of a synapse can invoke synchronous changes in the presynaptic membrane. Ca^{2+}

activated structural change may lead to an increase in the synaptic gap resistance that enhances positive synaptic electrical feedback and so augment release probability (Voronin *et al.*, 1995). The degree of perforation of a PSD may depend on the total number of vesicles released over a period of seconds to minutes. When massive vesicular release was stimulated in the presence of agents that blocked the recycling of presynaptic vesicles there was a rapid enlargement and perforation of PSDs (Shupliakov *et al.*, 1997). Therefore, an increased number of perforated synapses, immediately after LTP induction, may be a consequence of receptor insertion and maintenance of receptor ratios that promote the enlargement of activated synapses. This would support the theory that perforations are not permanent features of a synapse but occur transiently in response to activation.

The early maintenance of LTP requires the synthesis of new proteins from existing mRNAs (Krug *et al.*, 1984; Otani *et al.*, 1989; Fazeli *et al.*, 1993 and local dendritic protein synthesis may contribute to the persistence of late LTP. Immediately after the induction of LTP, it is hypothesised that a synaptic tag is set to identify the activated synapse for further modifications after the transcription of new mRNA and protein synthesis and tag candidates include anatomical changes (Frey and Morris, 1997). Activation of the cAMP/PKA pathway leads to gene activation and to the synthesis and distribution of plasticity-related proteins that reveal or stabilise new effector mechanisms (new receptors or ion channels) and additional changes in plasticity at activated synapses. Changes in synaptic number have been observed in the first few hours post induction (Lee, 1980) - although this was not an unbiased stereological study. However, when activated synapses were examined an increase in the incidence of multiple synapse boutons was reported (Toni *et al.*, 1999) and such changes effecting a small proportion of synapses would be difficult to determine in a study of all synapses. Although Toni and colleagues found that the spines, synapsing with multiple synapse boutons, shared the same postsynaptic neuron, a model has been proposed that suggests that such boutons could spread LTP between neurons.

If synapses are tagged for further modification then such modifications may be initiated by a retrograde signal that is restricted to the synaptic clefts of the potentiated neurons and may lead to enhanced release of neurotransmitter at the potentiated synapses. This change would affect all synapses that are located on the potentiated boutons, and lead to LTP at synapses on neighbouring neurons that share multiple-synapse boutons with the initially potentiated neurons (Harris, 1995). In this model, restricting the retrograde signal to the potentiated synaptic clefts ensures the axonal-input specificity of LTP, and the induction of the secondary LTP requires the same cellular mechanisms as those of induction of the primary LTP.

The results reported in this thesis, and increases in asymmetric, axospinous synapse number reported by Weeks *et al* (1998) suggest that, in the maintenance phase of LTP, the increase in the number of synapses is more widespread than during the induction phase of LTP. Changes in the number of synapses are believed to be the result of CREB activation and gene expression, as phosphorylation of CREB has been shown to result in an increase in dendritic spine density that is not restricted to a single dendrite (Murphy and Segal, 1996).

Among the effector proteins that are produced after gene expression are the neurotrophins that can have a retrograde effect on the presynaptic membrane and can trigger gene expression in the presynaptic cell. Therefore in protein synthesis transcription, presynaptic protein kinase activity may be implicated in LTP maintenance. Tetanic stimulation of the perforant path that induces LTP in the dentate gyrus has been shown to result in an increase in mRNAs encoding for synapsin I and syntaxin 2B in the granule cells (Hicks *et al.*, 1997). An increase in presynaptic proteins measured postsynaptically results in a corresponding increase in protein levels in the axonal terminals of these cells, i.e. in the mossy fibre terminal zone of CA3, 5h later. This trans-synaptic LTP is a potential molecular mechanism for the distribution of synaptic plasticity beyond a single synapse (Davis *et al.*, 1998).

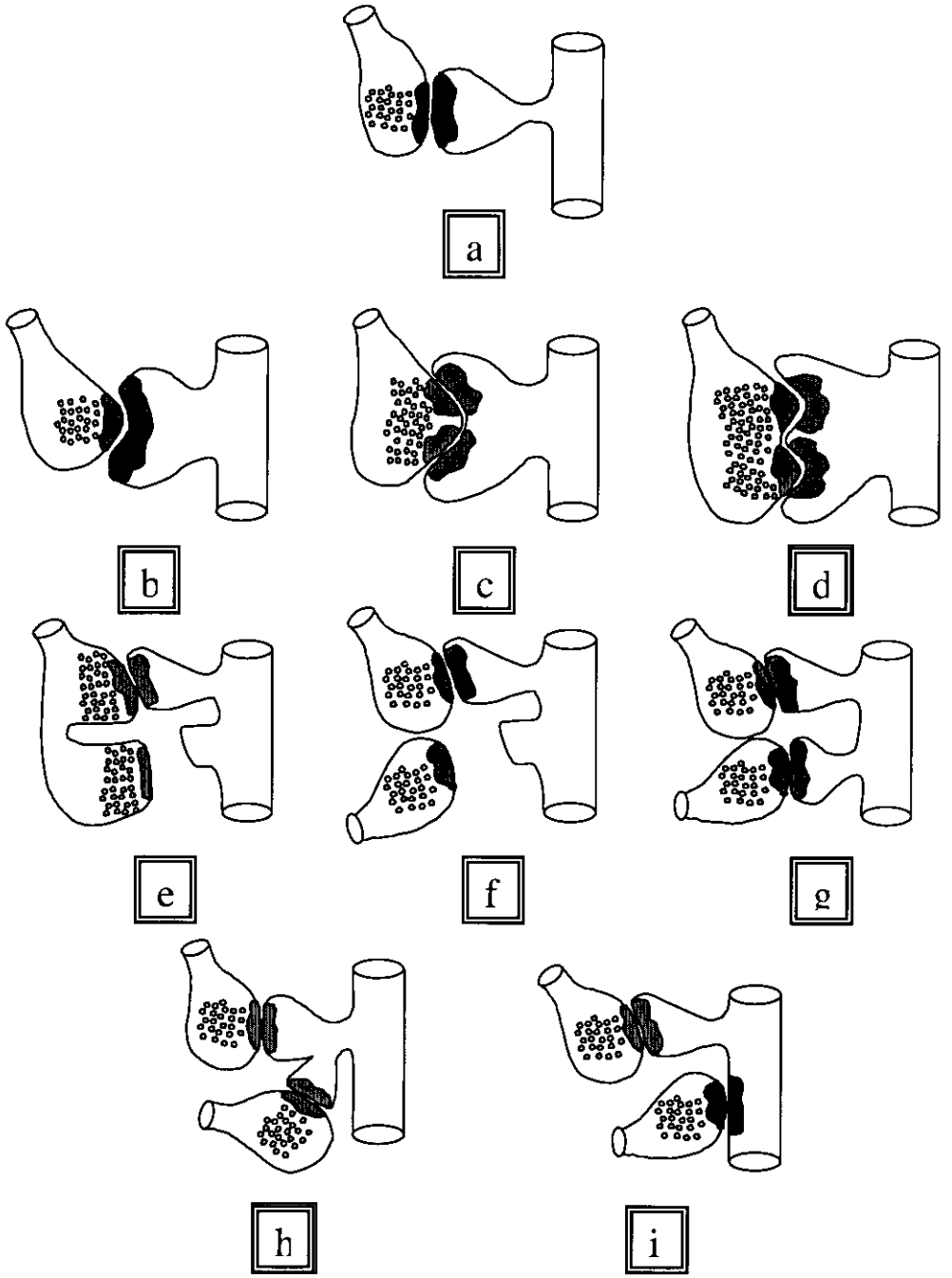

Figure 5.2 Morphological changes following the induction and maintenance of LTP.

Synaptic stimulation, NMDA activation, calcium entry, activation of metabotropic glutamate receptors and second messenger cascades (a). Short Term Stage of Synaptic Enhancement: Modifications of the internal cytoskeleton lead to insertion of receptors into the PSD and changes in synapse size and shape e.g. widening and shortening of spine neck, active zone curvature (b). Production of new synaptic proteins with further enlargement of synaptic active zones and the formation of synaptic perforations (c-d). Intermediate Stage of Synaptic Enhancement: Division of perforated synapses and /or formation of new synapses and dendritic spines (e-f). Increase in the number of asymmetric axospinous synapses (g). Fusion of spines as spine density decreases (h). Long Term Stage of Synaptic Enhancement: Retraction of spines to increase the incidence of axodendritic synapses (i).

As an increase in axodendritic synapses is observed 13 days after tetanisation, the increase in axospinous synapse density appears to be transient. This could be explained by retraction of some spines (Rusakov *et al.*, 1997b) to convert axospinous synapses to axodendritic ones and further consolidation of synaptic efficacy. (Figure 5.2)

Since initial interest in LTP was aroused by the possibility that this phenomenon may be the mechanism that underlies memory formation then similar morphological changes may be expected after learning. The search for cellular correlates of learning is a major challenge in neurobiology and structural reorganisation or remodelling appears to be associated with various learning paradigms. Immediately after training morphological modifications are apparent e.g. spatial re-arrangement of the vesicle apparatus in forebrain synapses of the chick has been observed after passive avoidance learning (Rusakov *et al.*, 1993).

Alterations in the size of synapses have been reported in studies of behavioural paradigms such as visual deprivation (Turner and Greenhough, 1985) and increases in the size of PSDs have been observed in rats trained or housed in complex environments (Wallace *et al.*, 1992). Alterations in the thickness of the postsynaptic density have been described during the maturation of young chicks (Rostas *et al.*, 1991). Interestingly, NMDA administration alone appears to be capable of rapidly inducing a transient increase in the length of PSDs and the formation of new synapses (Brooks *et al.*, 1991). Therefore, the NMDA receptor, that is crucial for the induction of LTP, appears to have an important role in synaptogenesis and synaptic structural plasticity.

Changes in the shape of dendritic spines have been demonstrated, in the molecular layer of the dentate gyrus, in rats subjected to a one-way active avoidance task. In trained animals the frequency of perforated concave synapses significantly increased as compared to untrained controls and the length of the postsynaptic density

in both perforated, and non-perforated synapses, significantly increased (Van Reempts *et al.*, 1992).

An increase in spine density, reflecting an increased number of excitatory synapses per neuron, has been observed after spatial learning (Moser *et al.*, 1994). This appears to be a transient increase as a reported increase in spine number 6 h post-training had returned to control levels by 72 h post-training (O'Malley *et al.*, 2000). This is supported by a further study that found no training-associated changes 6 days after spatial training, although there was a training-associated increase in the clustering of synaptic active zones in CA1, indicating alterations in local neural circuitry (Rusakov *et al.*, 1997a).

Studies of rats trained to acquire a passive avoidance response have also reported a similar transient increase in spine density in the dorsal dentate gyrus, 3 h - 6 h after training that returned to basal levels after 72 h (O'Malley *et al.*, 1998). Studies of the chick learning model, a one-trial passive avoidance learning task, have reported an increase in synaptic density, 60min post-training (Doubell and Stewart, 1993) in one area of the striatum and 24-48h after training in another region (Lowndes and Stewart, 1994).

The activity of the neural cell adhesion molecule has been implicated in the molecular processes associated with synaptic plasticity and stabilisation during memory formation (Doyle *et al.*, 1992a) (Doyle *et al.*, 1992b); (Scholey *et al.*, 1993). Performance of rats in the Morris mater maze, a spatial learning paradigm which requires the hippocampus, is impaired by either intraventricular injection of NCAM antibodies (Arami *et al.*, 1996) or the injection of an enzyme which removes polysialic acid residuals from extracellular NCAM domains (Becker *et al.*, 1996).

A time course of NCAM expression has been identified in both the chick and rat avoidance paradigms that involves a wave of glycoprotein synthesis 5.5-8h post-training ((Rose, 1995); (Murphy *et al.*, 1998); (Skibo *et al.*, 1998). In addition,

intraventricular injections of anti-NCAM antibodies 6-8 h post-training were shown to impair memory for a one-trial passive avoidance task (Doherty *et al.*, 1995); Scholey *et al.*, 1993) - a time window susceptible to the amnesic effects of protein synthesis inhibitors (Freeman *et al.*, 1995). This is associated with spatially clustered granule cells in the adult rat hippocampus that show a transient time-dependent increase in dendritic spine number 6-8 hr following training (Fox *et al.*, 1995).

It is proposed that NCAM antibodies may not block *de novo* synapse formation but that NCAMs are likely to contribute to selective stabilisation of synapses following formation (Schuster *et al.*, 1996) and the selection of synapses to be retained and / or eliminated may be dependent on cell adhesion molecule glycosylation events in the 10-12h post training period (Doyle et al., 1992a); (Murphy et al., 1998).

This cascade of events fulfils many of the requirements of LTP maintenance whereby L-LTP is dependent on protein synthesis, relies on intracellular transport mechanisms and occurs predominantly on dendritic spines to result in changed synaptic weight. It would be interesting to investigate morphological changes in perforant path-dentate gyrus synapses 3-8 hours post tetanisation, and the effects of the application of NCAM antibodies, at various time points, after the induction of LTP.

In conclusion, morphological investigations in the hippocampus following the acquisition of different learning paradigms do appear to show some similar results to morphological, post-stimulation studies of long-term potentiation induced by various stimulating protocols. In future, a more precise relationship, if any, between LTP and hippocampal-dependent learning may be found by combining both paradigms in the same animal (Moser *et al.*, 1998).

Future Experiments

While the experiments in this thesis have clarified some aspects of the changes in morphology after LTP induction with various stimulating protocols the results have suggested other areas of investigation.

As any early changes in morphology are likely to be restricted to activated synapses a study of the morphology of spines that are potentiated would be important. Confocal microscopy techniques could visualise the activation of individual spines that could then be serially reconstructed after electron microscopy. Similarly, electron microscopy and reconstruction of neurons from dissociated hippocampal cultures after chemical activation might prove useful.

It would be particularly interesting to examine morphological changes 3 to 6 hours after the induction of LTP with different stimulating protocols, a period of time when changes are seen in the dentate gyrus of the rat after passive avoidance learning. These morphological investigations would include an examination of new granule cell generation in the dentate gyrus to assess whether this contributes to the increase in synapse number observed after 24h. A study of morphological changes several weeks after LTP induction, but with TBS, would be an interesting comparison to Geinisman's study 13 days after tetanisation with HFS. Different stimulating protocols appear to utilise different signalling pathways and blockade of components of translation and transcription, while employing different stimulation paradigms, would perhaps indicate which are relevant.

As already mentioned, whether LTP is the mechanism underlying learning would be best investigated by studying LTP and learning success in the same animal. Since there appear to be similarities in the morphology reported in the dentate gyrus of rats both after LTP of the perforant path, and after passive avoidance learning, it would be interesting to saturate LTP in the rodent dentate gyrus and then subject those animals to passive avoidance learning.

References

Abel T, Nguyen PV, Barad M, Deuel TAS and Kandel ER. 1997. Genetic demonstration of a role for PKA in the late phase of LTP and in hippocampus-based long-term memory. Cell 88: 615-626.

Abeliovich A, Chen C, Goda Y, Silva AJ, Stevens CF and Tonegawa S. 1993. Modified hippocampal long-term potentiation in PKC-gamma-mutant mice. Cell 75: 1253-1262.

Abercrombie M. 1946. Estimation of nuclear population from microtome sections. Anat. Rec. 94: 239-247.

Agnihotri N, Lopez-Garcia JC, Hawkins RD and Arancio O. 1998. Morphological changes associated with long-term potentiation. Histol. and Histopath. 13: 1155-1162.

Akers RF, Lovinger DM, Colley PA, Linden DJ and Routtenberg A. 1986. Translocation of protein kinase C may mediate hippocampal LTP. Science 231: 587-589.

Akirav I, and Richter-Levin G. 1999. Behavioral stress and basolateral amygdala bi-phasic modulation of hippocampal synaptic plasticity in the rat. J. Neurosci. 19: 10530-10535.

Alford S and Collingridge GL. 1992. In: Excitatory amino acids and second messenger systems. (Teichbeck, Turski VI, eds). Berlin: Springer; 43-53.

Allison DW, Gelfand VI, Spector I and Craig AM. 1998. Role of actin in anchoring postsynaptic receptors in cultured hippocampal neurons: Differential attachment of NMDA versus AMPA receptors. J. Neurosci. 18: 2423-2436.

Amaral DG and Witter MP. 1989. The three-dimensional organisation of the hippocampal formation: A review of anatomical data. Neurosci. 31: 571-591.

Amaral DG. 1978. A golgi study of the cell types in the hilar region of the hippocampus in the rat. J. Comp. Neurol. 182: 851-914.

Amaral DG. 1993. Morphological analyses of the brains of behaviourally characterised aged non-human primates. Neurobiol. Aging 14: 671-672.

Andersen P, Bliss TPV and Skrede KK. 1971. Lamellar organisation of hippocampal excitatory pathways. Exp. Brain. Res. 13: 222-238.

Andersen P, Sundberg SH, Sveen O, Swann JW and Wigstrom H. 1977. Specific long-lasting potentiation of synaptic transmission in hippocampal slices. Nature 266: 736-737.

Andersen P and Soleng AF. 1998. Long-term potentiation and spatial training are both associated with the generation of new excitatory synapses. Brain Res. Rev. 26: 353-359.

Aoki C and Siekevitz P. 1985. Ontogenetic changes in the cyclic adenosine 3',5'- monophosphate-stimulatable phosphorylation of cat visual-cortex proteins, particulary of microtubule-sssociated protein-2 (Map2) - effects of normal and dark rearing and of the exposure to light. J. Neurosci. 5: 2465-2483.

Applegate MD, Kerr DS and Landfield PW. 1987. Redistribution of synaptic vesicles during long-term potentiation in the hippocampus. Brain Res. 401: 401-406.

Applegate MD and Landfield PW. 1988. Synaptic vesicle redistribution during hippocampal frequency potentiation and depression in young and aged rats. J. Neurosci. 8: 1096-1111.

Arai A and Lynch G. 1992. Factors regulating the magnitude of long-term potentiation induced by theta pattern stimulation. Brain Res. 598: 173-184.

Arami S, Jucker M, Schachner M and Welzl H. 1996. The effect of continuous intraventricular infusion of L1 and NCAM antibodies on spatial learning in rats. Behav. Brain Res. 81: 81-87.

Attwell D. 1994. Neurobiology - Glia and Neurons in Dialog. Nature 369: 707-708.

Balschun D, Manahan-Vaughan D, Wagner T, Behnisch T, Reymann KG and Wetzel W. 1999. A specific role for group I mGluRs in hippocampal LTP and hippocampus-dependent spatial learning. Learning & Memory 6: 138-152.

Barnes CA and McNaughton B.L. 1985. An age comparison of the rates of acquisition and forgetting of spatial information in relation to long-term enhancement of hippocampal synapses. Behav. Neurosci. 99: 1040-1048.

Barria A, Derkach V and Soderling T. 1997a. Identification of the Ca^{2+}/calmodulin-dependent protein kinase II regulatory phosphorylation site in the alpha-amino-3- hydroxyl-5-methyl-4-isoxazole-propionate-type glutamate receptor. J. Biol. Chem. 272: 32727-32730.

Barria A, Muller D, Derkach V, Griffith LC and Soderling TR. 1997b. Regulatory phosphorylation of AMPA-type glutamate receptors by CaMKII during long-term potentiation. Science 276: 2042-2045.

Bashir ZI, Bortolotto ZA, Davies CH, Beretta N, Irving AJ, Sea AJ, Henley JM, Jane DE, Watkins JC and Collingridge GL. 1993. Induction of LTP in the hippocampus needs synaptic activation of glutamate metabotropic receptors. Nature 363: 347-350.

Baude A, Nusser Z, Molnar E, McIlhinney RAJ and Somogyi P. 1995. High-resolution immunogold localization of AMPA type glutamate-receptor subunits at synaptic and non-synaptic sites in rat hippocampus. Neurosci. 69: 1031-1055.

Becker CG, Artola A, Gerardy-Schahn R, Decker T, Welzl H and Schachner M. 1996. The polysialic acid modification of the neural cell adhesion molecule is involved in spatial learning and hippocampal LTP. J. Neurosci. Res. 45: 143-152.

Benke TA, Luthi A, Isaac JTR and Collingridge GL. 1998. Modulation of AMPA receptor unitary conductance by synaptic activity. Nature 393: 793-797.

Bennett MK, Calakos N and Scheller RH. 1992. Syntaxin - a synaptic protein implicated in docking of synaptic vesicles at presynaptic active zones. Science 257: 255-259.

Bianchin M, Walz R, Ruschel AC, Zanatta MS, Dasilva RC, Silva MBE, Paczko N, Medina JH and Izquierdo I. 1993. Memory expression Is blocked by the infusion of CNQX into the hippocampus and or the amygdala up to 20 days after training. Behav. Neural Biol. 59: 83-86.

Blackstad TW. 1958. On the termination of some afferents to the hippocampus and fascia dentata. Acta Anat. 35: 202-214.

Blackstad TW, Brink K, Hem J and Jeune B. 1970. Distribution of hippocampal mossy fibres in the rat. An experimental study with silver impregnation methods. J. Comp. Neurol. 138: 433-450.

Bliss TVP and Collingridge GL. 1993. A synaptic model of memory: long-term potentiation in the hippocampus. Nature 361: 31-39.

Bliss TVP and Lomo T. 1973. Long-lasting potentiation of synaptic transmission in the dentate area of the anaesthetised rabbit following stimulation of the perforant path. J. Physiol. 232: 331-356.

Bolshakov VY, Golan H, Kandel ER and Siegelbaum SA. 1997. Recruitment of new sites of synaptic transmission during the cAMP-dependent late phase of LTP at CA3-CA1 synapses in the hippocampus. Neuron 19: 635-651.

Bortolotto ZA, Bashir ZI, Davies CH and Collingridge GL. 1994. A molecular switch activated by metabotropic glutamate receptors regulates induction of long-term potentiation. Nature 368: 740-743.

Boss BD, Peterson GM and Cowan WM. 1985. On the number of neurons in the dentate gyrus of the rat. Brain Res. 338: 144-150.

Braendgaar H and Gundersen HJG. 1986. The impact of recent stereological advances on quantitative studies of the nervous system. J. Neurosci. Meth. 18: 39-78.

Brakeman PR, Lanahan AA, O'Brien R, Roche K, Barnes CA, Huganir RL and Worley PF. 1997. Homer: a protein that selectively binds metabotropic glutamate receptors. Nature 386: 284-288.

Brooks WJ, Petit TL, Leboutillier JC and Lo R. 1991. Rapid alteration of synaptic number and postsynaptic thickening length by NMDA - an electron-microscopic study in the occipital cortex of postnatal rats. Synapse 8: 41-48.

Buchs PA and Muller D. 1996. Induction of long-term potentiation is associated with major ultrastructural changes of activated synapses. Proc. Nat. Acad. Sci. USA. 93: 8040-8045.

Carlin RK and Siekevitz P. 1983. Plasticity in the central nervous system: do synapses divide? Proc. Natl. Acad. Sci. USA. 80: 3517-3521.

Castro CA, Silbert LH, McNaughton BL and Barnes CA. 1989. Recovery of spatial-learning deficits after decay of electrically induced synaptic enhancement in the hippocampus. Nature 342: 545-548.

Chang F-LF and Greenough WT. 1984. Transient and enduring morphological correlates of synaptic activity and efficacy in the rat hippocampal slice. Brain Res. 309: 35-46.

Chen GQ, Kolbeck R, Barde YA, Bonhoeffer T and Kossel A. 1999. Relative contribution of endogenous neurotrophins in hippocampal long-term potentiation. J. Neurosci. 19: 7983-7990.

Chen SJ, Sweatt JD and Klann E. 1997. Enhanced phosphorylation of the postsynaptic protein kinase C substrate RC3/neurogranin during long-term potentiation. Brain Res. 749: 181-187.

Chen W, Wieraszko A, Hogan MV, Yang HA, Kornecki E and Ehrlich YH. 1996. Surface protein phosphorylation by ecto-protein kinase is required for the maintenance of hippocampal long-term potentiation. Proc. Nat. Acad. Sci. USA 93: 8688-8693.

Claiborne BJ, Amaral DG and Cowan WM. 1986. A light and electron-microscopic analysis of the mossy fibres of the rat dentate gyrus. J. Comp. Neurol. 246: 435-458.

Claiborne BJ, Amaral DG, and Cowan WM. 1990. Quantitative, three-dimensional analysis of granule cell dendrites in the rat dentate gyrus. J. Comp. Neurol. 302: 206-219.

Coan EJ, Saywood W and Collingridge GL. 1987. MK-801 blocks NMDA receptor-mediated synaptic transmission and long-term potentiation in rat hippocampal slices. Neurosci. Lett. 80: 111-114.

Coggeshall RE, Laforte R, and Klein CM. 1990. Calibration of methods for determining numbers of dorsal-root ganglion-cells. J. Neurosci. Meth. 35: 187-194.

Cohen NJ, Ryan J, Hunt C, Romine L, Wszalek T and Nash C. 1999 Hippocampal system and declarative (relational) memory: summarising the data from functional neuroimaging studies. Hippocampus 9: 83-98.

Cole A, Saffen D, Baraban J and Worley P. 1989. Rapid increase of an immediate early gene mRNA in hippocampal neurons by synaptic NMDA receptor activation. Nature 340: 474-476.

Colley P and Routtenberg A. 1993. Long-term potentiation as synaptic dialogue. Brain Res. Rev. 18: 115-122.

Collin C, Miyaguchi K and Segal M. 1997. Dendritic spine density and LTP induction in cultured hippocampal neurons. J. Neurophysiol. 77: 1614-1623.

Collingridge GL, Kehl SJ and McLennan H. 1983. The action of an N-methylaspartate antagonist on synaptic processes in the rat hippocampus. J. Physiol.-London 338: P27-P27.

Collingridge GL, Herron CE and Lester RAJ. 1988. Frequency-dependent N-methyl-D-aspartate receptor-mediated synaptic transmission in rat hippocampus. J. Physiol.-London 399: 301-312.

Collingridge GL and Bliss TVP. 1995. Memories of NMDA receptors and LTP. Trends Neurosci. 18: 54-56.

Collins DR and Davies SN. 1993. Co-administration of (1s,3r)-1-aminocyclopentane-1,3- dicarboxylic acid and arachidonic-acid potentiates synaptic transmission in rat hippocampal slices. Eur. J. Pharmacol. 240: 325-326.

Conn PJ and Pin J-P. 1997. Pharmacology and function of metabotropic glutamate receptors. Annu. Rev. Pharmacol.Toxicol 37: 205-237.

Connor JA, Miller LDP, Petrozzino J and Muller W. 1994. Calcium signalling in dendritic spines of hippocampal-neurons. J. Neurobiol. 25: 234-242.

Crain B, Cotman C, Taylor D and Lynch G. 1973. A quantitative electron microscopic study of the synaptogenesis in the dentate gyrus of the rat. Brain Res. 63: 195-204.

Crick F. 1982. Do dendritic spines twitch? Trends Neurosci. 5:44-46.

Cummings JA, Nicola SM and Malenka RC. 1994. Induction in the rat hippocampus of long-term potentiation (LTP) and long-term depression (LTD) in the presence of a nitric-oxide synthase inhibitor. Neuroscience Letts. 176: 110-114.

Dailey ME and Smith SJ. 1996. The dynamics of dendritic structure in developing hippocampal slices. J. Neurosci. 16: 2983-2994.

Davis S and Laroche S. 1998. A molecular biological approach to synaptic plasticity and learning. Comptes Rendus De L Academie Des Sciences Serie Iii-Sciences De La Vie-Life Sciences 321: 97-107.

Davis S, Rodger J, Stephan A, Hicks A, Mallet J and Laroche S. 1998. Increase in syntaxin 1B mRNA in hippocampal and cortical circuits during spatial learning reflects a mechanism of trans-synaptic plasticity involved in establishing a memory trace. Learning & Memory 5: 375-390.

De Groot DMG. 1988. Comparison of methods for the estimation of the thickness of ultrathin tissue sections. J. of Microscopy 151: 23-42.

Derkach V, Barria A and Soderling TR. 1999. Ca^{2+}/calmodulin-kinase II enhances channel conductance of alpha-amino-3-hydroxy-5-methyl-4-isoxazolepropionate type glutamate receptors. Proc. Nat. Acad. Sci. USA 96: 3269-3274.

Desmond NL, and Levy WB. 1982. A quantitative anatomical study of the granule cell dendritic fields of the rat dentate gyrus using a novel probabilistic method. J. Comp. Neurol. 212: 131-145.

Desmond NL and Levy WB. 1983. Synaptic correlates of associative potentiation/depression: an ultrastructural study in the hippocampus. Brain Res. 265: 21-30.

Desmond NL, and Levy WB. 1985. Granule cell dendritic spine density in the rat hippocampus varies with shape and location. Neuroscience Letts. 54: 219-224.

Desmond NL and Levy WB. 1986a. Changes in the numerical density of synaptic contacts with long-term potentiation in the hippocampal dentate gyrus. J. Comp. Neurol. 253: 466-475.

Desmond NL and Levy WB. 1986b. Changes in the postsynaptic density with long-term potentiation in the dentate gyrus. J. Comp. Neurol. 253:476-482.

Desmond NL and Levy WB. 1988. Anatomy of associative long-term synaptic modification. In: Long-term potentiation: From Biophysics to Behaviour (Landfield PW, Deadwyler SA, eds). New York: Alan R. Liss,; 265-305.

Desmond NL and Levy WB. 1990. Morphological correlates of long-term potentiation imply the modification of existing synapses, not synaptogenesis, in the hippocampal dentate gyrus. Synapse 5: 139-143.

Desmond NL and Weinberg RJ. 1998. Enhanced expression of AMPA receptor protein at perforated axospinous synapses. Neuroreport, 9: 857-860.

Doherty P, Fruns M, Seaton P, Dickson G, Barton CH, Sears TA and Walsh FS. 1990. A threshold effect of the major isoforms of NCAM on neurite outgrowth. Nature 343: 464-466.

Doherty P, Fazeli MS and Walsh FS. 1995. The neural cell-adhesion molecule and synaptic plasticity. J. Neurobiol. 26: 437-446.

Dolorfo CL and Amaral DG. 1998. Entorhinal cortex of the rat: organisation of intrinsic connections. J. Comp. Neurol. 398: 49-82.

Doubell TP and Stewart MG. 1993. Short-term changes in the numerical density of synapses in the intermediate and medial hyperstriatum-ventrale following one- trial passive-avoidance training in the chick. J. Neurosci. 13: 2230-2236.

Doyle E, Nolan P, Bell R and Regan CM. 1992a. Neurodevelopmental events underlying information acquisition and storage. Network-Computation in Neural Systems 3: 89-94.

Doyle E, Nolan PM, Bell R and Regan CM. 1992b. Hippocampal-NCAM180 transiently increases sialylation during the acquisition and consolidation of a passive-avoidance response in the adult-rat. J. Neurosci. Res. 31: 513-523.

Engert F and Bonhoeffer T. 1999. Dendritic spine changes associated with hippocampal long-term synaptic plasticity. Nature 399: 66-70.

Fazeli MS, Corbet J, Dunn MJ, Dolphin AC and Bliss TVP. 1993. Changes in protein-synthesis accompanying long-term potentiation in the dentate gyrus *in vivo*. J. Neurosci. 13: 1346-1353.

Fazeli MS, Breen K, Errington ML and Bliss TVP. 1994. Increase in extracellular NCAM and amyloid precursor protein following induction of long-term potentiation in the dentate gyrus of anaesthetised rats. Neurosci. Letts. 169: 77-80.

Ferreira A, Chin LS, Li L, Lanier LM, Kosik KS and Greengard P. 1998. Distinct roles of synapsin I and synapsin II during neuronal development. Mol. Med. 4: 228.

Fiala JC, Feinberg M, Popov V and Harris KM. 1998. Synaptogenesis via dendritic filopodia in developing hippocampal area CA1. J. Neurosci. 18: 8900-8911.

Fields RD, Eshete F, Stevens B and Itoh K. 1997. Action potential-dependent regulation of gene expression: Temporal specificity in Ca^{2+} cAMP-responsive element binding proteins, and mitogen-activated protein kinase signaling. J. Neurosci. 17: 7252-7266.

Fifkova E and Anderson CL. 1981. Stimulation-induced changes in dimensions of stalks of dendritic spines in the dentate molecular layer. Exp. Neurol. 74: 621-627.

Fifkova E and Anderson CL. 1982. Stimulation-induced changes in dimensions of stalks of dendritic spines in the dentate molecular layer. Anat. Rec. 202: A56-A57.

Fifkova E and Delay RJ. 1982. Cytoplasmic actin in neuronal processes as a possible mediator of synaptic plasticity. J. Cell Biol. 95: 345-350.

Fifkova E and Morales M. 1992. Actin matrix of dendritic spines synaptic plasticity and long-term potentiation. Int. Rev. Cytol. 139: 267-307.

Fifkova E. 1975. Two types of terminal degeneration in the molecular layer of the dentate fascia following lesions of the entorhinal cortex. Brain Res. 96: 169-175.

Figurov A, Pozzo-Miller LD, Olaffson P, Wang T and Lu B. 1996. Regulation of synaptic responses to high-frequency stimulation and LTP by neurotrophins in the hippocampus. Nature 381: 706-709.

Fischer M, Kaech S, Knutti D and Matus A. 1998. Rapid actin-based plasticity in dendritic spines. Neuron 20: 847-854.

Fox GB, Oconnell AW, Murphy KJ and Regan CM. 1995. Memory consolidation induces a transient and time-dependent increase in the frequency of neural cell-adhesion molecule polysialylated cells in the adult-rat hippocampus. J. Neurochem. 65: 2796-2799.

Freeman FM, Rose SPR and Scholey AB. 1995. 2 time windows of anisomycin-induced amnesia for passive- avoidance training in the day-old chick. Neurobiol.Learning and Memory 63: 291-295.

Frey U, Huang YY and Kandel ER. 1993. Effects of cAMP simulate a late-stage of LTP in hippocampal CA1 neurons. Science 260: 1661-1664.

Fukanaga K, Muller D and Miyamoto E. 1995. Increased phosphorylation of CaMKII and its endogenous substrates in the induction of LTP. J. Biol. Chem. 270: 6119-6124.

Fukanaga K, Stoppini L, Miyamoto E and Muller D. 1993. LTP is associated with an increased activity of CaMKII. J. Biol. Chem. 268: 7863-7867.

Fukunaga K and Miyamoto E. 1999. Current studies on a working model of CaM kinase II in hippocampal long-term potentiation and memory. Jap. J. Pharmacol. 79: 7-15.

Fukunaga K and Miyamoto E. 2000. A working model of CaM kinase II activity in hippocampal LTP and memory. Neurosci. Res. 38: 3-17.

Geinisman Y, deToledo-Morrell L and Morrell F. 1986. Loss of perforated synapses in the dentate gyrus: Morphological substrate of memory deficit in aged rats. Proc. Natl. Acad. Sci. USA 83: 3027-3031.

Geinisman Y, deToledo-Morrell L and Morrell F. 1991. Induction of long-term potentiation is associated with an increase in the number of axospinous synapses with segmented postsynaptic densities. Brain Res. 566: 77-88.

Geinisman Y, deToledo-Morrell L, Morrell F, Persina IS and Rossi M. 1992b. Structural synaptic plasticity associated with the induction of long-term potentiation is preserved in the dentate gyrus of aged rats. Hippocampus 2: 445-446.

Geinisman Y, deToledo-Morell L, Morell F, Heller RE, Rossi M and Parshall RF. 1993. Structural synaptic correlate of long-term potentiation - formation of axospinous synapses with multiple, completely partitioned transmission zones. Hippocampus 3: 435-446.

Geinisman Y, deToledoMorrell L, Morrell F, Persina IS and Beatty MA. 1996. Synapse restructuring associated with the maintenance phase of hippocampal long-term potentiation. J. Comp. Neurol. 368: 413-423.

Gerendasy DD, Herron SR, Watson JB and Sutcliffe JG. 1994. Mutational and biophysical studies suggest that RC3/neurogranin regulates calmodulin availability. J. Biol. Chem. 269: 22420-22426.

Gerendasy DD, Herron SR, Jennings PA and Sutcliffe JG. 1995. Calmodulin stabilises an amphilic a-helix within RC3 / neurogranin and GAP 43/ neuromodulin only when calcium is absent. J. Biol. Chem. 270: 6741-6750.

Gerst JE. 1999. SNAREs and SNARE regulators in membrane fusion and exocytosis. Cell. Mol. Life Sci. 55: 707-734.

Giese KP, Federov N, Filipkowski RK and Silva AJ. 1998. Autophosphorylation at Thr286 of the alpha calcium-calmodulin kinase II in learning and memory. Science 279: 870-873.

Gluck MA and Granger R. 1993. Computational models of the neural basis of learning and memory. Ann. Rev. Neurosci. 16: 667-706.

Gray EG. 1959. Electron microscopy of synaptic contacts on dendritic spines of the cerebral cortex. Nature 183: 1592-1593.

Greengard P, Jen J, Nairn AC and Stevens CF. 1991. Enhancement of the glutamate response by cAMP-dependent protein-kinase in hippocampal neurons. Science 253: 1135-1138.

Greenough WT, West RW and DeVoogd TJ. 1978. Subsynaptic plate perforations: changes with age and experience in the rat. Science 202: 1096-1098.

Gunderson HJG and Jensen EB. 1987. The efficiency of systematic sampling in stereology and its prediction. J. Microsc. 147: 229-263.

Guthrie PB, Segal M and Kater SB. 1991. Independent regulation of calcium revealed by imaging dendritic spines. Nature 354: 76-80.

Hall A. 1998. Rho GTPases and the actin cytoskeleton. Science 279: 509-514.

Halpain S, Hipolito A and Saffer L. 1998. Regulation of F-actin stability in dendritic spines by glutamate receptors and calcineurin. J. Neurosci. 18: 9835-9844.

Halpain S. 2000. Actin and the agile spine: how and why do dendritic spines dance? Trends Neurosci. 23:141-146.

Harris KM and Stevens, J.K. 1989. Dendritic spines of CA1 pyramidal cells in the rat hippocampus: serial electron microscopy with reference to their biophysical characteristics. J of Neuroscience 9: 2982-2997.

Harris KM and Kater SB. 1994. Dendritic spines: Cellular specializations imparting both stability and flexibility to synaptic function. Annu. Rev. Neurosci 17:341-371.

Harris KM. 1995. How multiple-synapse boutons could preserve input specificity during an interneuronal spread of LTP. Trends Neurosci. 18: 365-369.

Harris KM. 1999. Calcium from internal stores modifies dendritic spine shape. Proc. Nat. Acad. of Sci. USA 96: 12213-12215.

Hawkins RD. 1996. NO honey, I don't remember. Neuron 16: 465-467.

Hawkins RD, Son H and Arancio O. 1998. Nitric oxide as a retrograde messenger during long-term potentiation in hippocampus. In: Nitric Oxide in Brain Development, Plasticity and Disease: 155-172.

Hebb DO. 1949. The Organisation of Behaviour. New York: Wiley.

Helme-Guizon A, Davis S, Israel M, Lesbats B, Mallet J, Laroche S and Hicks A. 1998. Increase in syntaxin 1B and glutamate release in mossy fibre terminals following induction of LTP in the dentate gyrus: a candidate molecular mechanism underlying transsynaptic plasticity. Eur. J. Neurosci. 10: 2231-2237.

Hicks A, Davis S, Rodger J, HelmeGuizon A, Laroche S and Mallet J. 1997. Synapsin I and syntaxin 1B: Key elements in the control of neurotransmitter release are regulated by neuronal activation and long-term potentiation in vivo. Neurosci. 79: 329-340.

Hjorth-Simonsen A. 1972. Projection of the lateral part of the entorhinal area to the hippocampus and fascia dentata. J. Comp. Neurol. 146: 219-232.

Hjorth-Simonsen A and Jeune B. 1972. Origin and termination of the hippocampal perforant path in the rat studied by silver impregnation. J. Comp. Neurol. 144: 215-232.

Hoff SF and Cotman CW. 1982. A continuous conversion disassembly for synapse turnover: A quantitative serial section study. Soc. Neurosci. Abstr. 8: 745.

Hosokawa T, Rusakov DA, Bliss TVP and Fine A. 1995. Repeated confocal imaging of individual dendritic spines in the living hippocampal slice: evidence for changes in length and orientation associated with chemically induced LTP. J. Neurosci. 15: 5560-5573.

Impey S, Mark M, Villacres EC, Poser S, Chavkin C and Storm DR. 1996. Induction of CRE-mediated gene expression by stimuli that generate long-lasting LTP in area CA1 of the hippocampus. Neuron 16: 973-982.

Impey S, Obrietan K, Wong ST, Poser S, Yano S, Wayman G, Deloulme JC, Chan G and Storm DR. 1998. Cross talk between ERK and PKA is required for Ca^{2+} stimulation of CREB-dependent transcription and ERK nuclear translocation. Neuron 21: 869-883.

Insausti R, Amaral DG and Cowan WM. 1987. The entorhinal cortex of the monkey: II Cortical afferents. J.Comp. Neurol. 264: 356-395.

Isaac JTR, Hjelmstad GO, Nicoll RA and Malenka RC. 1996. Long-term potentiation at single fibre inputs to hippocampal CA1 pyramidal cells. Proc. Nat. Acad. Sci. USA 93: 8710-8715.

Isokawa M, Levesque MF, Babb TL and Engel J. 1993. Single mossy fibre axonal systems of human granule cells studied in hippocampal slices from patients with temporal lobe epilepsy. J. Neurosci. 13: 1511-1522.

Issac JT, Nicholl RA and Malenka RC. 1995. Evidence for silent synapses: implications for the expression of LTP. Neuron 15: 427-434.

Izquierdo I. 1973. Regulation of hippocampal information processing by K^+ release and (K^+) accumulation: Possible role in learning. In: Neurohumoral coding of brain function. (Myers RD and Drucker-Colin RR. Ed.) New York: Plenum Press: 151-166.

Izquierdo I, Quillfeldt JA, Zanatta MS, Quevedo J, Schaeffer E, Schmitz PK and Medina JH. 1997. Sequential role of hippocampus and amygdala, entorhinal cortex and parietal cortex in formation and retrieval of memory for inhibitory avoidance in rats. Eur. J. Neurosci. 9: 786-793.

Jeffrey KJ and Morris RGM. 1993 Cumulative long-term potentiation in the rat dentate gyrus correlates with, but does not modify, performance in the water-maze. Hippocampus 3: 133-140.

Jones DG. 1993. Synaptic plasticity and perforated synapses - their relevance fror an understanding of abnormal synaptic organisation. APMIS Suppl. 40 101: 25-34.

Jung MW, Larson J and Lynch G. 1991. Evidence that changes in spine neck resistance are not responsible for expression of LTP. Synapse 7: 216-220.

Jung MW, Wiener SI and McNaughton BL. 1994. Comparison of spatial firing characteristics of units in dorsal and ventral hippocampus of the rat. J. Neurosci. 14: 7347-7356.

Kaech S, Fischer M, Doll T and Matus A. 1997. Isoform specificity in the relationship of actin to dendritic spines. J. Neurosci. 17: 9565-9572.

Kandel ER, Schwartz JH and Jessell TM (Eds) 2000. Principles of neural science. 4th Edition. McGraw-Hill, New York.

Kang H and Schuman EM. 1995. Long-lasting neurotrophin-induced enhancement of synaptic transmission in the adult hippocampus. Science 267: 1658-1662.

Kang HJ, Welcher AA, Shelton D and Schuman EM. 1997. Neurotrophins and time: Different roles for TrkB signalling in hippocampal long-term potentiation. Neuron 19: 653-664.

Kato A, Ozawa F, Saitoh Y, Fukazawa Y, Sugiyama H and Inokuchi K. 1998. Novel members of the Vesl/Homer family of PDZ proteins that bind metabotropic glutamate receptors. J. Biol. Chem. 273: 23969-23975.

Kempermann, G, Kuhn, HG, and Gage, FH. 1997 Genetic influence on neurogenesis in the dentate gyrus of adult mice. Proc. Natl. Acad. Sci. USA 94: 10409-10414.

Kennedy MB. 1997. The postsynaptic density at glutamatergic synapses. Trends Neurosci. 20: 264-268.

Kennedy MB. 1998. Signal transduction molecules at the glutamatergic postsynaptic membrane. Brain Res. Rev. 26: 243-257.

Kim CH and Lisman JE. 1999. A role of actin filament in synaptic transmission and long-term potentiation. J. Neurosci. 19: 4314-4324.

Klann E, Chen S-J and Sweatt JD. 1991. Persistant protein kinase activation in the maintainance phase of LTP. J. Biol. Chem. 266: 24253-24256.

Klann E, Chen S-J and Sweatt JD. 1993. Mechanisms of protein kinase C activation during the induction and maintenance of LTP probed using a novel peptide substrate. Proc. Natl. Acad. Sci. USA 90: 8337-8341.

Korkotian E and Segal M. 1998. Fast confocal imaging of calcium released from stores in dendritic spines. Eur. J. Neurosci. 10: 2076-2084.

Korkotian E and Segal M. 1999. Release of calcium from stores alters the morphology of dendritic spines in cultured hippocampal neurons. Proc. Nat. Acad. Sci. USA 96: 12068-12072.

Korol DL, Abel TW, Church LT, Barnes CA and McNaughton BL. 1993. Hippocampal synaptic enhancement and spatial learning in the Morris swim task. Hippocampus 3: 127-132.

Korte M, Griesbeck O, Grand C, Carroll P, Staiger V, Thoenen H and Bonhoffer T. 1996. Virus-mediated gene transfer into hippocampal CA1 region restores long-term potentiation in brain-derived neurotropic factor mutant mice. Proc. Natl. Acad. Sci. USA. 93: 12547-12552.

Kramer I, Hall H, Bleistein U and Schachner M. 1997. Developmentally regulated masking of an intracellular epitope of the 180 kDa isoform of the neural cell adhesion molecule NCAM. J. Neurosci. Res. 49: 161-175.

Krettek JE and Price JL. 1977. Projections from the amygdaloid complex and adjacent, olfactory structures to the entorhinal cortex and to the subiculum in the rat and the cat. J. Comp. Neurol. 172: 723-752.

Krug M, Lossner B and Ott T. 1984. Anisomycin blocks the phase of LTP in the dentate gyrus of freely moving rats. Brain Res. Bull. 13: 39-42.

Lambert JDC and Jones RSG. 1990. A re-evaluation of excitatory amino acid-mediated synaptic transmission in rat dentate gyrus. J. Neurophys. 64: 119-132.

Lanahan A and Worley P. 1998. Immediate early genes and synaptic function. Neurobiol. of Learning and Memory 70: 37-43.

Larkman AU and Jack JJB. 1995. Synaptic plasticity: hippocampal LTP. Curr. Opin. Neurobiol. 5: 324-334.

Larson J and Lynch G. 1986. Induction of synaptic potentiation in hippocampus by patterned stimulation involves two events. Science 232: 985-988.

Larson JA and Lynch, G. 1988. Role of N-methyl-D aspartate receptors in the induction of synaptic potentiation patterned after the hippocampal theta rhythm. Brain Res. 441: 111-118.

Larson J and Lynch G. 1991. A test of the spine resistance hypothesis for LTP expression. Brain Res. 538: 347-350.

Lee KS, Schottler F, Oliver M and Lynch G. 1980. Brief bursts of high-frequency stimulation produce two types of structural change in rat hippocampus. J. Neurophysiol. 44: 247-258.

Leonard AS, Davare MA, Horne MC, Garner CC and Hell JW. 1998. SAP97 is associated with the AMPA receptor GluR1 subunit. J. Biol. Chem. 273: 19518-19524.

Leonard AS, Lim IA, Hemsworth DE, Horne MC and Hell JW. 1999. Calcium/calmodulin-dependent protein kinase II is associated with the N-methyl-D-aspartate receptor. Proc. Nat. Acad. Sci. USA 96: 3239-3244.

Levy WB and Steward O.1979. Synapses as associative memory elements in the hippocampal formation. Brain Res. 175: 233-245.

Liao DZ, Hessler NA and Malinow R. 1995. Activation of postsynaptically silent synapses during pairing-induced LTP in CA1 region of hippocampal slice. Nature 375: 400-404.

Lisman JE and Harris KM. 1993. Quantal analysis and synaptic anatomy - integrating two views of hippocampal plasticity. Trends Neurosci. 16: 141-147.

Littlefield R and Fowler VM. 1998. Defining actin filament length in striated muscle: rulers and caps or dynamic stability. Annu. Rev. Cell Dev. Biol. 14: 487-525.

Liu J, Fukunaga K, Yamamoto H, Nishi K and Miyamoto E. 1999. Differential roles of Ca^{2+}/calmodulin-dependent protein kinase II and mitogen-activated protein kinase activation in hippocampal long-term potentiation. J. Neurosci. 19: 8292-8299.

Lledo PM, Zhang XY, Sudhof TC, Malenka RC and Nicoll RA. 1998. Postsynaptic membrane fusion and long-term potentiation. Science 279: 399-403.

Lovinger DM, Akers AF, Nelson RF, Barnes CA, McNaughton BL and Routtenberg A. 1985. A selective increase in phosphorylation of protein F1, a protein kinase C substrate,directly related to three day growth of synaptic long term enhancement. Brain Res. 343: 137-143.

Lovinger DM, Colley PA, Akers AF, Nelson R and Routtenberg A. 1986. Direct relation of long term synaptic potentiation to phosphorylation of membrane protein F1, a substrate for membrane protein kinase C. Brain Res. 399: 205-211.

Lowndes M and Stewart MG. 1994. Dendritic spine density in the lobus parolfactorius of the domestic chick is increased 24h after one-trial passive avoidance training. Brain Res. 654: 129-136.

Lujan R, Nusser Z, Roberts J.D.B, Shigemoto R and Somogyi P. 1996. Perisynaptic location of metabotropic glutamate receptors mGluR1 and mGluR5 on dendrites and dendritic spines in the rat hippocampus. Eur. J. Neurosci. 8: 1488-1500.

Luthi A, Laurent JP, Figurov A, Muller D and Schachner M. 1994. Hippocampal long-term potentiation and neural cell-adhesion molecules L1 and NCAM. Nature 372: 777-779.

Lyford GL, Yamagata K, Kaufmann WE, Barnes CA, Sanders LK, Copeland NG, Gilbert DJ, Jenkins NA, Lanahan AA and Worley PF. 1995. Arc, a growth factor and activity-regulated gene, encodes a novel cytoskeleton-associated protein that is enriched in neuronal dendrites. Neuron 14: 433-445.

Lynch G, Dunwiddie T and Gribkoff V. 1977. Heterosynaptic depression: A postsynaptic correlate of LTP. Nature 266: 737-739.

Lynch G, Larson J, Kelso S, Barrioneuvo G and Schottler F. 1983. Intracellular injections of EGTA block induction of hippocampal LTP. Nature 305: 719-721.

Lynch G and Baudry M. 1984. The biochemistry of memory - a new and specific hypothesis. Science 224: 1057-1063.

Lynch G and Baudry M. 1987. Brain spectrin, calpain and long-term changes in synaptic efficacy. Brain Res. Bull. 18: 809-815.

Lynch G, Muller D, Seubert P and Larson J. 1988. Long-term potentiation: persisting problems and recent results. Brain Res. Bull. 21: 363-372.

Lynch G, Kessler M, Arai A and Larson J. 1990. The nature and causes of hippocampal long-term potentiation. In: Progress in Brain Research. (Storm-Mathisen J, Zimmer J. and Ottersen O.P., eds): Elsevier Science Publishers B.V.: 233-250.

Lynch G and Granger R. 1992. Variations in synaptic plasticity and types of memory in corticohippocampal networks. J.Cogn. Neurosci. 4: 189-199.

Mackler SA, Brooks BP and Eberwine JH. 1992. Stimulus-induced co-ordinate changes in messenger-RNA abundance in single postsynaptic hippocampal CA1 Neurons. Neuron 9: 539-548.

Madison DV, Malenka R and Nicholl RA. 1991. Mechanisms underlying LTP of synaptic transmission. Annu. Rev. Neurosci. 14: 379-197.

Maletic-Savatic M, Malinow R and Svoboda K. 1999. Rapid dendritic morphogenesis in CA1 hippocampal dendrites induced by synaptic activity. Science 283: 1912-1926.

Malinow R, Madison DV and Tsien RW. 1988. Persistent protein kinase activity underlying LTP. Nature 335: 820-824.

Malinow R, Mainen ZF and Hayashi Y. 2000. LTP mechanisms: from silence to four-lane traffic. Curr. Opin. Neurobiol. 10: 352-357.

Mammen AL, Kameyame K, Roche KW and Huganir RL. 1997. Phosphorylation of the AMPA receptor Glu1 subunit by CaMKII. J. Biol. Chem. 272: 32528-32533.

Manahan-Vaughan D and Reymann KG. 1996. Metabotropic glutamate receptor subtype agonists facilitate long-term potentiation within a distinct time window in the dentate gyrus in vivo. Neuroscience 74: 723-731.

Mansuy IM, Mayford M, Jacob B, Kandel ER and Bach ME. 1998. Restricted and regulated over-expression reveals calcineurin as a key component in the transition from short-term to long-term memory. Cell 92: 39-49.

Manzoni OJ, Weisskopf MG and Nicoll RA. 1994. MCPG antagonises metabotropic glutamate receptors but not long-term potentiation in the hippocampus. Eur. J. Neurosci. 6: 1050-1054.

Martin KC, Michael D, Rose JC, Barad M, Casadio A, Zhu HX and Kandel ER. 1997. MAP kinase translocates into the nucleus of the presynaptic cell and is required for long-term facilitation in Aplysia. Neuron 18: 899-912.

Martin SJ and Morris R.G.M. 1997. (R,S)- alpha-methyl-4 - carboxyphenylglycine (MCPG) fails to block long-term potentiation under urethane anaesthesia *in vivo*. Neuropharmacol. 36:1339-1354.

Matthews DA, Cotman C and Lynch G. 1976. An electron microscopic study of lesion-induced synaptogenesis in the dentate gyrus of the adult rat. I. Magnitude and time course of degeneration. Brain Res. 115: 1-21.

Matthews DA, Salvaterra PM, Crawford GD, Houser CR and Vaughn JE. 1987. An immunocytochemical study of acetyltransferase-containing neurons and axon terminals in normal and partially deafferented hippocampal formation. Brain Res. 402: 30-43.

Matthies H. 1989. In search of the cellular mechanisms of memory. Prog. Neurobiol. 32: 277-349.

Matthies H and Reymann KG. 1993. Protein kinase A inhibitors prevent the maintenance of hippocampal long-term potentiation. Neuroreport 4: 712-714.

McGahon B and Lynch MA. 1994. A study of the synergism between metabotropic glutamate-receptor activation and arachidonic acid in the rat hippocampus. Neuroreport 5: 2353-2357.

McGuinness N, Anwyl R and Rowan M. 1991. Trans-ACPD enhances long-term potentiation in the hippocampus. Eur. J. Pharmacol. 197: 231-232.

McNaughton BL and Barnes C.A. 1978. Physiological identification and analysis of dentate granule cell responses to stimulation of the medial and lateral perforant pathways in the rat. J. Comp. Neurol. 175: 439-454.

McNaughton BL, Douglas RM and Goddard GV. 1978. Synaptic enhancement in fascia dentata: Cooperativity among coactive afferents. Brain Res. 157: 277-294.

McNaughton BL, Barnes CA, Rao G, Baldwin J and Rasmussen M. 1986. Long-term enhancement of hippocampal synaptic transmission and the acquisition of spatial information. J. Neurosci. 6: 563-571.

McNaughton BL. 1993. The mechanism of expression of long-term enhancement of hippocampal synapses: current issues and theoretical implications. Annu. Rev. Physiol. 55: 375-396.

Min MY, Asztely F, Kokaia M and Kullmann DM. 1998. Long-term potentiation and dual-component quantal signalling in the dentate gyrus. Proc. Nat. Acad. Sci. USA 95: 4702-4707.

Morales M and Fifkova E. 1989. Distribution of MAP2 in dendritic spines and its co-localisation with actin - an immunogold electron-microscope study. Cell and Tissue Res. 256: 447-456.

Morimoto K, Sato K, Sato S, Yamada N and Hayabara T. 1998. Time-dependent changes in rat hippocampal synapsin I mRNA expression during LTP. Brain Res. 783: 57-62.

Moser E, Moser MB and Andersen P. 1993. Spatial-learning impairment parallels the magnitude of dorsal hippocampal lesions, but is hardly present following ventral lesions. J. Neurosci. 13: 3916-3925.

Moser MB, Trommald M and Andersen P. 1994. An increase in dendritic spine density on hippocampal CA1 pyramidal cells following spatial learning in adult rats suggests the formation of new synapses. Proc. Nat. Acad. Sci. USA 91: 12673-12675.

Moser EI, Krobert KA, Moser M-B and Morris RGM. 1998. Impaired spatial learning after saturation of long-term potentiation. Science 281: 2038-2042.

Muller D, Joly M and Lynch G. 1988. Contributions of quisqualate and NMDA receptors to the induction and expression of LTP. Science 242: 1694-1697.

Muller D and Lynch G. 1988a. Long-term potentiation differentially affects two components of synaptic responses in hippocampus. Proc. Nat. Acad. Sci. USA 85: 9346-9350.

Muller D, Arai A and Lynch G. 1992. Factors governing the potentiation of NMDA-receptor mediated responses in hippocampus. Hippocampus 2: 29-38.

Muller D, Wang C, Skibo G, Toni N, Cremer H, Calaora V, Rougon G and Kiss JZ. 1996. PSA-NCAM is required for activity-induced synaptic plasticity. Neuron 17: 413-422.

Murphy DD and Segal M. 1996. Regulation of dendritic spine density in cultured rat hippocampal neurons by steroid hormones. J. Neurosci. 16: 4059-4068.

Murphy KJ, O'Connell A, O'Connell C, O'Malley A and Regan C. 1998. Contributions of the neural cell adhesion molecule to synaptic plasticity associated with memory consolidation. J.Neurochem. 71: S26-S26.

Nafstad PHJ. 1967. An electron microscope study on the termination of the perforant path fibres in the hippocampus and the fascia dentata. Zeitschrift fur Zellforschung 76: 532-542.

Nakanishi S, 1994. Metabotropic glutamate receptors: Synaptic transmission, modulation and plasticity. Neuron 13: 1031-1037.

Neuhoff H, Roeper J and Schwezer M. 1999. Activity-dependent formation of perforated synapses in cultured hippocampal neurons. Eur. J. Neurosci. 11: 4241-4250.

Nguyen PV and Kandel ER. 1996. A macromolecular synthesis-dependent late phase of long-term potentiation requiring cAMP in the medial perforant pathway of rat hippocampal slices. J. Neurosci. 16: 3189-3198.

Nguyen PV and Kandel ER. 1997. Brief theta-burst stimulation induces a transcription-dependent late phase of LTP requiring cAMP in area CA1 of the mouse hippocampus. Learning & Memory 4: 230-243.

Nicholls DG. 1994. Proteins, transmitters and synapses. Oxford: Blackwell Science Ltd.

Nicoll RA and Malenka RC. 1995. Contrasting properties of two forms of long-term potentiation in the hippocampus. Nature 377: 115-118.

Nieto-Sampedro N, Hoff, S.F. and Cotman, C.W., 1982. Perforated postsynaptic densities: probable intermediates on synapse turnover. Proc. Natl. Acac. Sci. USA 79: 5718-5722.

Noel J, Ralph GS, Pickard L, Williams J, Molnar E, Uney JB, Collingridge GL and Henley JM. 1999. Surface expression of AMPA receptors in hippocampal neurons is regulated by an NSF-dependent mechanism. Neuron 23: 365-376.

Nowak L, Bregestovski P, Ascher P, Herbet A and Prochiantz A. 1984. Magnesium gates glutamate-activated channels in mouse central neurones. Nature 307: 462-465.

Nusser Z, Lujan, R, Laube, G, Roberts, J.D.B, Molnar, E and Somogyi, P. 1998. Cell type and pathway dependence of synaptic AMPA receptor number and variability in the hippocampus. Neuron 21: 545-559

Oddie SD and Bland BH. 1998. Hippocampal formation theta activity and movement selection. Neurosci. Behav. Rev. 22: 221-231.

O'Dell TJ, Hawkins RD, Kandel ER and Arancio O. 1991. Tests of the roles of two diffusible substances in long-term potentiation: Evidence for nitric oxide as a possible early retrograde messenger. Proc. Natl. Acad. Sci. USA 88: 11285-11289.

O'Dell TJ, Huang PL, Dawson TM, Dinerman JL, Snyder SH, Kandel ER and Fishman MC. 1994. Endothelial NOS and blockade of LTP by NOS inhibitors in mice lacking neuronal NOS. Science 265: 542-546.

O'Malley A, O'Connell C and Regan CM. 1998. Ultrastructural analysis reveals avoidance conditioning to induce a transient increase in hippocampal

dentate spine density in the 6 hour post-training period of consolidation. Neurosci. 87: 607-613.

O'Malley A, O'Connell C, Murphy KJ and Regan CM. 2000. Transient spine density increases in the mid-molecular layer of hippocampal dentate gyrus accompany consolidation of a spatial learning task in the rodent. Neurosci. 99: 229-232.

Otani S and Abraham WC. 1989. Inhibition of protein synthesis in the dentate gyrus, but not the entorhinal cortex, blocks maintenance of LTP in rats. Neurosci. Letts. 106: 175-180.

Otani S, Marshall CJ, Tate WP, Goddard GV and Abraham WC. 1989. Maintenance of LTP in rat dentate gyrus requires protein synthesis but not messenger RNA synthesis immediate post-tetanisation. Neurosci. 28: 519-526.

Paoletti P and Ascher P. 1994. Mechanosensitivity of NMDA receptors in cultured mouse neurons. Neuron 13: 645-655.

Patel SN, Stewart MG and Rose SPR. 1988a. Training-induced spine density changes are specifically related to memory formation processes in the chick, *Gallus domesticus.* Brain Res. 463: 168-173.

Patel SN, Stewart MG and Rose SPR. 1988b. Changes in the number and structure of dedritic spines, 25h after passive avoidance training in the domestic chick, *Gallus domesticus.* Brain Res. 449: 34-46.

Patton PE and McNaughton B. 1995. Connection matrix of the hippocampal formation: I. The dentate gyrus. Hippocampus 5: 245-286.

Persohn E, Pollerberg GE and Schachner M. 1989. Immunoelectron microscopic localisation of the 180 KD component of the neural cell adhesion molecule N-CAM in postsynaptic membranes. J. Comp. Neurol. 288: 92-100.

Peters A and Palay SL. 1996. The morphology of synapses. J. Neurocytol. 25: 687-700.

Pozzo-Miller LD, Gottschalk W, Zhang L, McDermott K, Du J, Gopalakrishnan R, Oho C, Sheng ZH and Lu B. 1999. Impairments in high-frequency transmission, synaptic vesicle docking, and synaptic protein distribution in the hippocampus of BDNF knockout mice. J. Neurosci. 19: 4972-4983.

Purves D, Augustine GJ, Fitzpatrick D, Katz LC, LaMantia A-S and McNamara JO (Eds). 1997. Neuroscience: Sinauer Associates Inc., Sunderland, Massachusetts.

Racine RJ, Milgram NW and Hafner S. 1983. LTP in the rat limbic forebrain. Brain Res. 260: 217-231.

Ramakers GMJ, De Graan PNE, Urban IJA, Kraay D, Tang T, Pasinelli P, Oestreicher AB and Gispen WH. 1995. Temporal differences in the phosphorylation state of pre- and postsynaptic kinase C substrates B50/GAP 43 and neurogranin during LTP. J. Biol. Chem. 270: 13892-13898.

Ramakers GMJ, Pasinelli P, Hens JJH, Gispen WH and DeGraan PNE. 1997. Protein kinase C in synaptic plasticity: Changes in the *in situ* phosphorylation state of identified pre- and postsynaptic substrates. Prog. Neuro-Psychopharmacol. Biol. Psychiatry 21: 455-486.

Raymond CR, Thompson VL, Tate WP and Abraham WC. 2000. Metabotropic glutamate receptors trigger homosynaptic protein synthesis to prolong long-term potentiation. J. Neurosci. 20: 969-976.

Raymond LA, Blackstone CD and Huganir RL. 1993. Phosphorylation of amino acid neurotransmitter receptors in synaptic plasticity. Trends Neurosci. 16: 147-153.

Reymann KG, Brodemann R, Kase H and Matthies H. 1988. Inhibitors of calmodulin and protein kinase C block different phases of hippocampal long-term potentiation. Brain Res. 440: 305-314.

Richter-Levin G, Errington ML, Maegawa H and Bliss TVP. 1994. Activation of metabotropic glutamate receptors is necessary for long-term potentiation in the dentate gyrus and for spatial learning. Neuropharmacol. 33: 853-857.

Richter-Levin G, Canevari L. and Bliss TVP. 1998. Spatial training and high-frequency stimulation engage a common pathway to enhance glutamate release in the hippocampus. Learning and Memory 4: 445-450.

Roberts LA, Higgins MJ, O'Shaughnessy CT, Stone TW and Morris BJ. 1996. Changes in hippocampal gene expression associated with the induction of long-term potentiation. Mol. Brain Res. 42: 123-127.

Roberts LA, Large CH, Higgins MJ, Stone TW, O'Shaughnessy CT and Morris BJ. 1998a. Increased expression of dendritic mRNA following the induction of long-term potentiation. Mol. Brain Res. 56: 38-44.

Roberts LA, Morris BJ and O'Shaughnessy CT. 1998b. Involvement of two isoforms of SNAP-25 in the expression of long-term potentiation in the rat hippocampus. Neuroreport 9: 33-36.

Roche KW, O'Brien OJ, Mammen AL, Bernhardt J and Huganir RL. 1996. Characterisation of multiple phosphorylation sites on the AMPA receptor GluR1 subunit. Neuron 16: 1179-1188.

Rosahl TW, Spillane D, Missler M, Herz J, Selig DK, Wolff JR, Hammer RE, Malenka RC and Sudhof TC. 1995. Essential functions of synapsin I and II in synaptic vesicle regulation. Nature 375: 488-493.

Rose SPR. 1995. Cell-adhesion molecules, glucocorticoids and long-term-memory formation. Trends Neurosci. 18: 502-506.

Rostas JAP, Kavanagh JM, Dodd PR, Heath JW and Powis DA. 1991. Mechanisms of synaptic plasticity: changes in postsynaptic densities and glutamate receptors in chicken forebrain during maturation. Mol. Neurobiol. 5: 203-215.

Routtenberg A, Lovinger DM and Steward O. 1985. Selective increase in phosphorylation of a 47-kDa protein (F1) directly related to LTP. Behav. Neural Biol. 43: 3-11.

Rusakov DA, Stewart MG, Davies HA and Harrison E. 1993. Spatial re-arrangement of the vesicle apparatus in forebrain synapses of chicks 30min after passive avoidance learning. Neurosci.Letts 154: 13-16.

Rusakov DA and Stewart MG. 1995. Quantification of dendritic spine populations using image analysis and a tilting disector. J. Neurosci. Meth. 60: 11-21.

Rusakov DA, Stewart MG and Korogod SM. 1996. Branching of active dendritic spines as a mechanism for controlling synaptic efficacy. Neurosci. 75: 315-323.

Rusakov DA, Davies HA, Harrison E, Diana G, Richter-Levin G, Bliss TVP and Stewart MG. 1997a. Ultrastructural synaptic correlates of spatial learning in rat hippocampus. Neurosci. 80: 69-77.

Rusakov DA, Richter-Levin G, Stewart MG and Bliss TVP. 1997b. Reduction in spine density associated with long-term potentiation in the dentate gyrus suggests a spine fusion and branching model of potentiation. Hippocampus 7: 489-500.

Rusakov DA, Harrison E and Stewart MG. 1998. Synapses in hippocampus occupy only 1-2% of cell membranes and are spaced less than half-micron apart: a quantitative ultrastructural analysis with discussion of physiological implications. Neuropharmacol. 37: 513-521.

Ruth RE, Collier TJ and Routtenberg A. 1982. Topography between the entorhinal cortex and the dentate septotemporal axis in rats: I. Medial and intermediate entorhinal projecting cells. J. Comp. Neurol. 209: 69-78.

Sato K, Morimoto K, Suemaru S, Sato T and Yamada N. 2000. Increased synapsin I immunoreactivity during LTP in the rat hippocampus. Brain Res. 872: 219-222.

Scharfman HE, Kunkel DD and Schwartzkroin PA. 1990. Synaptic connections of dentate granule cells and hilar neurons - results of paired intracellular-recordings and intracellular horseradish-peroxidase injections. Neurosci. 37: 693-707.

Scholey AB, Rose SPR, Zamani MR, Bock E and Schachner M. 1993. A role for the neural cell adhesion molecule in a late, consolidating phase of glycoprotein synthesis six hours following passive avoidance training of the young chick. Neurosci. 55: 499-509.

Schulz S, Siemer H, Krug M and Hollt V. 1999. Direct evidence for biphasic cAMP responsive element-binding protein phosphorylation during long-term potentiation in the rat dentate gyrus *in vivo*. J. Neurosci. 19: 5683-5692.

Schuster CM, Davis GW, Fetter RD and Goodman CS. 1996. Genetic dissection of structural and functional components of synaptic plasticity. II Fasciclin II controls presynaptic structural plasticity. Neuron 17: 655-667.

Schuster T, Krug M and Wenzel J. 1990. Spinules in axospinous synapses of the rat dentate gyrus: changes in density following long-term potentiation. Brain Res. 523: 171-174.

Schuster T, Krug M, Hassan H and Schachner M. 1998. Increase in proportion of hippocampal spine synapses expressing neural cell adhesion molecule NCAM180 following long-term potentiation. J. Neurobiol. 37: 359-372.

Scoville W and Milner B. 1957. Loss of recent memory after bilateral hippocampal lesions. J. Neurol. Neurosurg. Psychiatry. 20: 11-21.

Segal M. 1995. Imaging of calcium variations in living dendritic spines of cultured rat hippocampal neurons. J. Physiol.-London 486: 283-295.

Segal M. 1995. Morphological alterations in dendritic spines of rat hippocampal neurons exposed to N-methyl-D-aspartate. Neurosci. Lett. 193: 73-76.

Segal M, Korkotian E and Murphy DD. 2000. Dendritic spine formation and pruning: common cellular mechanisms. Trends Neurosci. 23: 53-57.

Seki T and Arai Y. 1993. Highly polysialylated neural cell-adhesion molecule (NCAM-H) is expressed by newly generated granule cells in the dentate gyrus of the adult rat. J. Neurosci. 13: 2351-2358.

Selig DK, Lee HK, Bear MF and Malenka RC. 1995. Re-examination of the effects of MCPG on hippocampal LTP, LTD and depotentiation. J. Neurophysiol. 74: 1075-1082.

Shen K, Teruel MN, Subramanian K and Meyer T. 1998. CaMKII beta functions as an F-actin targeting module that localises CaMKII alpha/beta heterooligomers to dendritic spines. Neuron 21: 593-606.

Shi SH, Hayashi Y, Petralia RS, Zaman SH, Wenthold RJ, Svoboda K and Malinow R. 1999. Rapid spine delivery and redistribution of AMPA receptors after synaptic NMDA receptor activation. Science 284: 1811-1816.

Shupliakov O, Low P, Grabs D, Gad H, Chen C, Takei DK, De CP and Brodin L. 1997. Synaptic vesicle endocytosis impaired by disruption of dynamin-SH3 domain interactions. Science 276: 259-263.

Siekevitz P. 1985. The postsynaptic density - a possible role in long-lasting effects in the central nervous-system. Proc. Nat. Acad. Sci. USA 82: 3494-3498.

Skaggs WE and McNaughton BL. 1996. Replay of neuronal firing sequences in rat hippocampus during sleep following spatial experience. Science 271: 1870-1873.

Skibo GG, Davies HA, Rusakov DA, Stewart MG and Schachner M. 1998. Increased immunogold labelling of neural cell adhesion molecule isoforms in synaptic active zones of the chick striatum 5-6 hours after one-trial passive avoidance training. Neurosci. 82: 1-5.

Sorra KE and Harris KM. 1998. Stability in synapse number and size at 2 h after long-term potentiation in hippocampal area CA1. J. Neurosci. 18: 658-671.

Sorra KE, Fiala, J.C. and Harris, K.M. 1998. Critical assessment of the involvement of perforations, spinules, and spine branching in hippocampal synapse formation. J. Comp. Neurol. 398: 225-240.

Spacek J and Harris KM. 1997. Three-dimensional organisation of smooth endoplasmic reticulum in hippocampal CA1 dendrites and dendritic spines of the immature and mature rat. J. Neurosci. 17: 190-203.

Staubli U, Rogers G and Lynch G. 1994. Facilitation of glutamate receptors enhances memory. Proc. Natl. Acad. Sci. USA 91: 777-781.

Stevens CF. 1993. Quantal release of neurotransmitter and long-term potentiation. Cell 72: 55-63.

Steward O, 1976. Topographic organisation of the projections from the entorhinal area to the hippocampal formation of the rat. J. Comp. Neurol. 167: 285-314.

Steward O and Vinsant SL. 1983. The process of re-innervation in the dentate gyrus of the adult rat: A quantitative electron microscopic analysis of terminal proliferation and reactive synaptogenesis. J. Comp. Neurol. 214: 370-386.

Steward O and Falk PM. 1986. Protein-synthetic machinery at postsynaptic sites during synaptogenesis - a quantitative study of the association between polyribosomes and developing synapses. J. Neurosci. 6: 412-423.

Steward O and Ribak CE. 1986. Polyribosomes associated with synaptic specialisations on axon initial segments - localisation of protein-synthetic machinery at inhibitory synapses. J. Neurosci. 6: 3079-3085.

Steward O, Falk PM and Torre ER. 1996. Ultrastructural basis for gene expression at the synapse: Synapse-associated polyribosome complexes. J. Neurocytol. 25: 717-734.

Steward O, Wallace CS, Lyford GL and Worley PF. 1998. Synaptic activation causes the mRNA for the IEG *Arc* to localise selectively near postsynaptic sites on dendrites. Neuron 21: 741-751.

Stewart MG, Rose SPR, King TS, Gabbot PLA and Bourne RC. 1984. Hemispheric asymmetry of synapses in chick medial hyperstriatum ventrale following passive avoidance training: A stereological investigation. Dev. Brain. Res. 12: 261-269.

Stewart MG, Rose SPR and Csillag A. 1987. Alterations in synaptic structure in the paleostriatal complex of the domestic chick, *Galus domesticus*, following passive avoidance training. Brain Res. 426: 69-81.

Storm-Matheson J, Leknes AK, Bore AT, Vaaland JL, Edminson P, Haug F-MS and Ottersen OP. 1983. First visualisation of glutamate and GABA in neurones by immunocytochemistry. Nature 301: 517-520.

Strack S, Barban MA, Wadzinski BE and Colbran RJ. 1997. Differential inactivation of postsynaptic density - associated and soluble calcium/ calmodulin-dependent protein kinase II by protein phosphatase 1 and 2A. J. Neurochem. 68: 2119-2128.

Sudhof TC. 1995. The synaptic vesicle cycle: a cascade of protein-protein interactions. Nature 375: 645-653.

Sugimori M, Tong CK, Fukuda M, Moreira JE, Kojima T, Mikoshiba K and Llinas R. 1998. Presynaptic injection of syntaxin-specific antibodies blocks transmission in the squid giant synapse. Neurosci. 86: 39-51.

Swanson LW, Kohler C and Bjorklund A. 1987. The limbic region. I. The septohippocampal system. In: Handbook of Chemical Neuroanatomy. Integrated

systems of the CNS, Part 1 (Bjorklund A, Hokfelt T, Swanson LW, eds). Amsterdam: Elsevier Science Publishers: 125-277.

Sweatt JD, Atkins CM, Johnson J, English JD, Robertson ED, Chen SJ, Newton A and Klann E. 1998. Protected-site phosphorylation of protein kinase C in hippocampal long-term potentiation. J. Neurochem. 71: 1075-1085.

Takumi Y, Ramirez-Leon V, Laake P, Rinvik E and Otterson OP. 1999. Different modes of expression of AMPA and NMDA receptors in hippocampal synapses. Nature Neurosci. 2: 618-624.

Tang LX, Hung CP and Schuman EM. 1998. A role for the cadherin family of cell adhesion molecules in hippocampal long term potentiation. Neuron 20: 1165-1175.

Tarrant SB and Routtenberg A. 1977. The synaptic spinule in the dendritic spine: electron microscopic study of the hippocampal dentate gyrus. Tissue Cell 9: 461-473.

Thomas KL, Laroche S, Errington ML, Bliss TVP and Hunt SP. 1994. Spatial and temporal changes in signal-transduction pathways during LTP. Neuron 13: 737-745.

Thomas MJ, Moody TD, Makhinson M and O'Dell TJ. 1996. Activity-dependent beta- adrenergic modulation of low frequency stimulation induced LTP in the hippocampal CA1 region. Neuron 17: 475-482.

Toni N, Buchs PA, Nikonenko I, Bron CR and Muller D. 1999. LTP promotes formation of multiple spine synapses between a single axon terminal and a dendrite. Nature 402: 421-425.

Trommald M, Vaaland JL, Blackstad TW and Andersen P. 1990 Dendritic spine changes in rat dentate granule cells associated with long-term potentiation.

In: Neurotoxicity of Excitatory Amino Acids (A Guidotti A, ed), New York: Raven: 163-174.

Trommald M and Hulleberg G. 1997. Dimensions and density of dendritic spines from rat dentate granule cells based on reconstructions from serial electron micrographs. J. Comp. Neurol. 377: 15-28.

Turner AM and Greenhough WT. 1985. Differential rearing effects on rat visual cortex synapses. I Synaptic and neuronal density and synapses per neuron. Brain Res. 329: 195-203.

Van Harreveld A and Fifkova E. 1975. Swelling of dendritic spines in the fascia dentata after stimulation of the perforant fibres as a mechanism of post-tetanic potentiation. Exp. Neurobiol. 49: 736-749.

Van Reempts J, Dikova M, Werbrouck L, Clincke G and Borgers M. 1992. Synaptic plasticity in rat hippocampus associated with learning. Behav. Brain Res. 51: 179-183.

van Rossum D and Hanisch UK. 1999. Cytoskeletal dynamics in dendritic spines: direct modulation by glutamate receptors? Trends Neurosci. 22: 290-295.

Volfovsky N, Parnas H, Segal M and Korkotian E. 1999. Geometry of dendritic spines affects calcium dynamics in hippocampal neurons: Theory and experiments. J. Neurophysiol. 82: 450-462.

Voronin L, Byzov A, Kleschevnikov A, Kozhemyakin M, Kuhnt U and Volgushev M. 1995. Neurophysiological analysis of long-term potentiation in mammalian brain. Behav. Brain Res. 66: 45-52.

Wallace CS, Kilman VL, Withers GS and Greenough WT. 1992. Increases in dendritic length in occipital cortex after four days of differential housing in weanling rats. Behav. Neurol. Biol. 58: 64-68.

Wallace CS, Lyford GL, Worley PF and Steward O. 1998. Differential intracellular sorting of immediate early gene mRNAs depends on signals in the mRNA sequence. J. Neurosci. 18: 26-35.

Wang J-H and Feng D-P. 1992. Postsynaptic protein kinase C essential to induction and maintenance of LTP in the hippocampal CA1 region. Proc. Natl. Acad. Sci. USA. 89: 2576-2580.

Weeks ACW, Ivanco TL, LeBoutillier JC, Racine RJ and Petit TL. 1998. The degree of potentiation is associated with synaptic number during the maintenance of long-term potentiation in the rat dentate gyrus. Brain Res. 798: 211-216.

Weeks ACW, Ivanco TL, Leboutillier JC, Racine RJ and Petit TL. 1999. Sequential changes in the synaptic structural profile following long-term potentiation in the rat dentate gyrus: I. The intermediate maintenance phase. Synapse 31: 97-107.

Weeks ACW, Ivanco TL, Leboutillier JC, Racine RJ and Petit TL. 2000. Sequential changes in the synaptic structural profile following long-term potentiation in the rat dentate gyrus. II. Induction/early maintenance phase. Synapse 36: 286-296.

Wenzel J, Kammerer E, Kirsche W, Matthies H and Wenzel M. 1980. Electron microscopic and morphological studies on synaptic plasticity in the hippocampus of the rat following conditioning. J. Hirnforsch. 21: 647-654.

Wheal HV, Chen Y, Mitchell J, Schachner M, Maerz W, Wieland H, Van Rossum D and Kirsch J. 1998. Molecular mechanisms that underlie structural and functional changes at the postsynaptic membrane during synaptic plasticity. Prog. Neurobiol. 55: 611-640.

Wieraszko A, Li G, Kornecki E, Hogan MV and Ehrlich YH. 1993. Long-term potentiation in the hippocampus by platelet- activating factor. Neuron 10: 553-557.

Williams JH and Bliss TVP. 1988. Induction but not maintenance of calcium-induced long-term potentiation in dentate gyrus and area CA1 of the hippocampal slice is blocked by nordihydroguaiaretic acid. Neurosci. Letts 88: 81-85.

Williams JH and Bliss TVP. 1989. An *in vitro* study of the effect of lipoxygenase and cyclooxygenase inhibitors of arachidonic-acid on the induction and maintenance of long-term potentiation in the hippocampus. Neurosci. Letts 107: 301-306.

Williams JH. 1996. Retrograde messengers and long-term potentiation: A progress report. J. Lipid Med. Cell Sig. 14: 331-339.

Winder DG, Martin KC, Muzzio IA, Rohrer D, Chruscinski A, Kobilka B and Kandel ER. 1999. ERK plays a regulatory role in induction of LTP by theta frequency stimulation and its modulation by beta-adrenergic receptors. Neuron 24: 715-726.

Witter MP, van Hoesen GW and Amaral DG. 1989. Topographical organisation of the entorhinal projection to the dentate gyrus of the monkey. J. Neurosci 9: 216-228.

Wyss JM. 1981. An autoradiological study of the efferent connections of the entorhinal cortex in the rat. J. Comp. Neurol. 199: 495-512.

Xaio P, Bahr BA, Staubli U, Vanderklish PW and Lynch G. 1991. Evidence that matrix recognition contributes to the stabilisation but not the induction of LTP. Neuroreport 2: 461-464.

Yamagata K, Sanders LK, Kaufmann WE, Yee W, Barnes CA, Nathans D and Worley PF. 1994. Rheb, a growth factor-regulated and synaptic activity-regulated gene, encodes a novel Ras-related protein. J. Biol. Chem. 269: 16333-16339.

Yee WM and Worley PF. 1997. Rheb interacts with Raf-1 kinase and may function to integrate growth factor- and protein kinase A-dependent signals. Mol. Cell. Biol. 17: 921-933.

Zamanillo D, Sprengel R, Hvalby O, Jensen V, Burnashev N, Rozov A, Kaiser KMM, Koster HJ, Borchardt T, Worley P, Lubke J, Frotscher M, Kelly PH, Sommer B, Andersen P, Seeburg PH and Sakmann B. 1999. Importance of AMPA receptors for hippocampal synaptic plasticity but not for spatial learning. Science 284: 1805-1811.

Zhuo M, Small SA, Kandel ER and Hawkins RD. 1993. Nitric oxide and carbon monoxide produce activity-dependent long-term synaptic enhancement in hippocampus. Science 260: 1946-1950.

Zhuo M, Hu Y, Schultz C, Kandel ER and Hawkins RD. 1994. Role of guanylyl cyclase and cGMP-dependent protein kinase in long-term potentiation. Nature 368: 635-639.

Zhuo M, Laitinen JT, Li X-C and Hawkins, RD. 1999. On the respective roles of nitric oxide and carbon monoxide in long-term potentiation in the hippocampus. Learning and Memory. 5: 63-76.

Ziv NE, Smith SJ, 1996. Evidence for a role of dendritic filopodia in synaptogenesis and spine formation. Neuron 17: 91-102.

Appendix

Preparation of stock solutions.

0.2M Sodium cacodylate buffer.

Consult relevant CoSHH assessments.

For each 1000ml:

- Dissolve 42.8g sodium cacodylate in 500 ml distilled water.
- Add approx. 8ml 1M hydrochloric acid to yield a pH 7.4.
- Make up to 1000ml with distilled water.

Fixative

2% paraformaldehyde and 2% glutaraldehyde in 0.1M sodium cacodylate buffer.

Consult relevant CoSHH assessments.

For each 1000ml:

- Weigh 20g paraformaldehyde.
- Add approximately 350ml distilled water and 5.0ml 1M sodium hydroxide (made fresh each time).
- Heat the paraformaldehyde solution in a fume cupboard to 60°C when the paraformaldehyde dissolves.
- Cool and add 80ml of EM grade 25% glutaraldehyde.
- Make up to 500ml with distilled water.
- Make up to 1000ml with 0.2M sodium cacodylate buffer pH 7.4.
- Filter before use.

Fixative must be used within 12h and stored at 4°C.

Epon 812 embedding resin

Consult relevant CoSHH assessments.

Epon 812 (Agar Scientific Ltd, England)

DDSA - Dodecenyl succinic anhydride (Agar Scientific Ltd, England)

MNA - Methyl nadic anhydride (Agar Scientific Ltd, England)

BDMA – N- benzyldimethylamine (Agar Scientific Ltd, England)

Stock bottles of Epon, DDSA and MNA, as well as mixing bottles and a graduated cylinder are warmed for approx. 20min to 60°C. 20ml of Epon, 16ml of DDSA and 8ml MNA are added to the mixing bottle and placed on a rotating mixer until well mixed.1.3ml BDMA is finally added and the bottle replaced on the mixer until the resin is a uniform colour.

The tissue to be embedded must be completely infiltrated with resin. This is achieved by initially soaking the tissue in a mixture of Epon and acetone i.e.:

1. Add 1:1 Epon/acetone overnight, on a rotating mixer, with the bottle caps off to allow the evaporation of the acetone.
2. Replace with fresh Epon and mix for 3h with the bottle caps off.
3. Replace with fresh Epon and mix for 2h on a rotating mixer with the bottle caps on.

Sections are then placed in flat bottomed beem capsules, filled with fresh Epon and polymerised overnight at 60°C.